Radioimmunotherapy using ^{186}Re-labeled humanized monoclonal antibodies

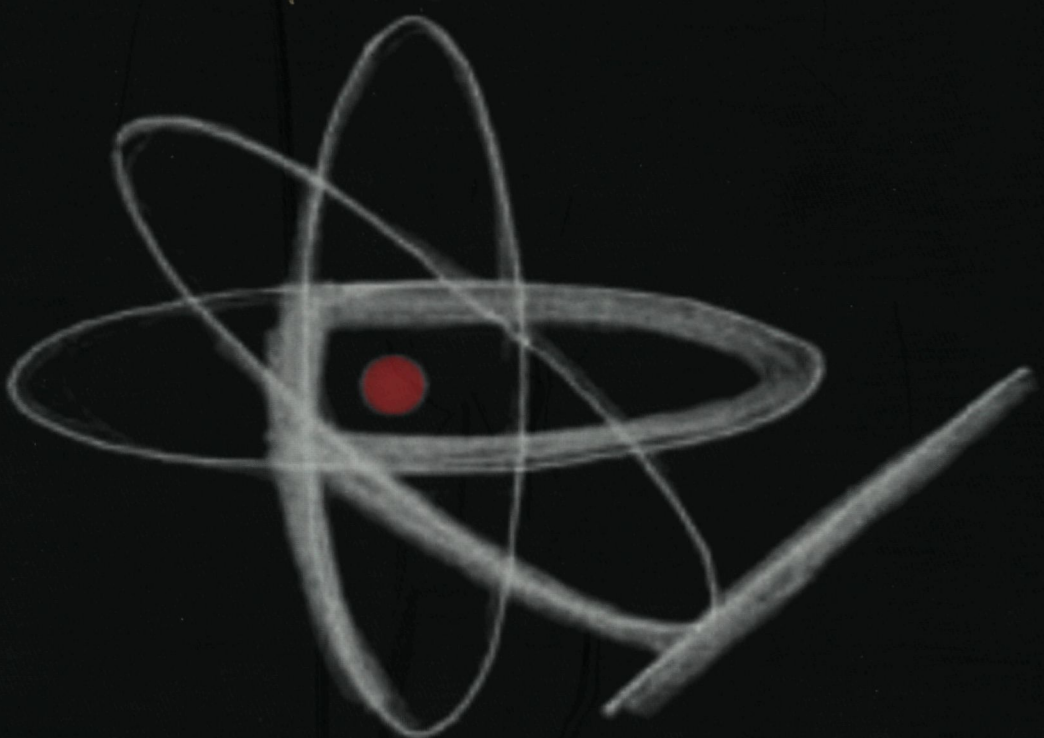

E.J. Postema

Radioimmunotherapy

using ^{186}Re-labeled humanized monoclonal antibodies

This research project was supported by The Netherlands Organization for Health Research and Development (ZonMw), project # 920-03-073.

Printing of this thesis was supported by
Boehringer Ingelheim bv, Alkmaar
Boehringer Ingelheim Pharma GmbH & Co KG, Biberach an der Riss
ZonMw, Den Haag

ISBN 90-9017813-9

Layout: Michiel Postema
Style-file: Jeroen Goudswaard
Typesetting: LaTeX 2ε
Cover design: Rik Jagtenberg
Printed by: Drukkerij "QUICKPRINT" B.V., Nijmegen

Radioimmunotherapy
using ^{186}Re-labeled humanized monoclonal antibodies

een wetenschappelijke proeve
op het gebied van de Medische Wetenschappen

PROEFSCHRIFT

ter verkrijging van de graad van doctor
aan de Katholieke Universiteit Nijmegen,
op gezag van de Rector Magnificus Prof. Dr. C.W.P.M. Blom,
volgens besluit van het College van Decanen
in het openbaar te verdedigen
op dinsdag 23 maart 2004
des namiddags op 1.30 uur precies

door

Ernst Jeroen Postema

geboren op 13 augustus 1971 te Blokzijl

Promotores:	Prof. Dr. F.H.M. Corstens Prof. Dr. W.J.G. Oyen
Copromotores:	Dr. O.C. Boerman Dr. J.M.M. Raemaekers
Manuscriptcommissie:	Prof. Dr. B.E. de Pauw (voorzitter) Prof. Dr. A.J. van der Kogel Prof. Dr. P.H.M. De Mulder

Contents

Outline of this thesis

Radioimmunotherapy (RIT) can be defined as irradiation of cancer cells by radionuclides attached to monoclonal antibodies to guide the radionuclide to the tumor selectively. Theoretically, the doses absorbed by the tumor should be as high as possible, whereas the radiation doses absorbed by normal tissues should be low This approach differs from conventional chemotherapy, leading to toxicity in many tissues containing dividing cells, and from external beam radiation, in which the surrounding tissue of the tumor will absorb high doses, by the fact that the toxic agent is guided specifically to the tumor cells, as "magic bullets".

B-cell non-Hodgkin's lymphoma in advanced stages can have an indolent course, but has a bad prognosis *quoad vitam* One of the new treatment modalities is the use of monoclonal antibodies like rituximab, which can induce responses in about half of the treated patients. Studies with radiolabeled monoclonal antibodies in the same group of patients with relapsed or refractory indolent lymphoma, however, revealed higher response rates when compared to unlabeled antibody treatment. Chapter 1 of this thesis describes the current status of antibody treatment and radioimmunotherapy of patients with non-Hodgkin's lymphoma.

In Chapter 2, the development of a mouse lymphoma model for preclinical RIT studies is described. In this animal model, biodistribution studies with radiolabeled anti-CD22 antibodies were performed in order to select the optimal radionuclide for RIT, as described in Chapter 3.

Finally, a phase I clinical study with the selected radiopharmaceutical ^{186}Re-epratuzumab was conducted The aims of the study were to determine the safety and the maximum tolerated dose of this radiolabeled antibody preparation in patients with relapsed or refractory B-cell NHL, and to obtain preliminary data on efficacy of this treatment. The results of this study are described in Chapter 4, whereas the dosimetric analysis is described in Chapter 5.

Squamous cell carcinoma of the head and neck (HNSCC) is a common

malignancy with a good prognosis for patients diagnosed in an early stage. However, two thirds of the patients present with advanced stages of the disease. In this group of patients, a significant proportion will have locoregional recurrence or distant metastases after first-line treatment, consisting of surgery and/or external beam radiation therapy. Since HNSCC is a relatively radiosensitive tumor, RIT could play a role in an adjuvant setting. Chapter 6 gives an overview of current treatment and the role of RIT in the treatment of HNSCC.

In Chapter 7, the results of a phase I clinical study with ^{186}Re-bivatuzumab are discussed. The primary aim of the study was to determine the maximum tolerated dose in patients with recurrent HNSCC or metastases, for whom no other curative treatment was available. Therapeutic effects of this therapy were monitored as well. The results of dosimetric analysis are described in Chapter 8, in relation with toxicity that was observed.

In Chapter 9 a general discussion and future perspectives are provided.

Chapter 1

Radioimmunotherapy of B-cell non-Hodgkin's lymphoma

Ernst J. Postema
Otto C. Boerman
Wim J.G. Oyen
John M.M. Raemaekers
Frans H.M. Corstens

European Journal of Nuclear Medicine 2001; 28: 1725–1735
Updated October 2003

Abstract

In the past decade, several new antibody-based therapies — using either radiolabeled or unlabeled monoclonal antibodies — have become available for the treatment of patients with refractory or recurrent non-Hodgkin's lymphoma (NHL). Unlabeled monoclonal antibodies (mAbs) kill lymphoma cells by activating host immune effector mechanisms, or by inducing apoptosis. These mAbs can also be used to guide radionuclides to the lymphoma. This radioimmunotherapy (RIT) has been studied with various nuclides (^{131}I, ^{90}Y, ^{67}Cu, and ^{186}Re) and with various mAbs In this review the radionuclides, methods of dosing, and recent RIT studies in patients with B-cell NHL are reviewed. Most of these studies demonstrate that RIT is an effective new treatment modality for NHL.

Introduction

The diagnosis and treatment of patients with malignant lymphomas originated in 1832, the year that Thomas Hodgkin described a disease that is still known as Hodgkin's disease [1]. Hodgkin's disease is just one circumscribed entity of malignant lymphoma (characterized by the growth of Reed-Sternberg and Hodgkin cells), and all other types of malignant lymphoma are known as non-Hodgkin's lymphoma (NHL) Therefore, the recognition and description of NHL, being a very heterogeneous group of lymphoma types, took quite a long time. In the twentieth century, various schemes of classification were introduced. In 1942, a lymphoma classification based on clinical and histological criteria was introduced by Gall and Mallory. In 1956, Rappaport presented a lymphoma classification which used two criteria to differentiate lymphoma subtypes: architecture and cell size (small, intermediate, and large). In 1978, Lennert was the first to recognize the follicle center cell, which became the basis of Lennert's Kiel classification. The "Revised European American Lymphoid neoplasms" (REAL) classification was introduced in 1994 (Table 1.1). Nowadays the REAL classification is widely used in Europe and North America and has recently been adopted in the new WHO classification [2]. For staging of the disease the Ann Arbor classification is still used, which is summarized in Table 1 2.

I	Precursor B-cell neoplasms	Precursor B-lymphoblastic leukemia/lymphoma	
II	Peripheral B-cell neoplasms	1	B-cell chronic lymphocytic leukemia/prolymphocytic leukemia/small lymphocytic lymphoma
		2	Lymphoplasmacytoid lymphoma/immunocytoma
		3	Mantle cell lymphoma
		4	Follicle center lymphoma, follicular Provisional cytological grades I (small cell), II (mixed small and large cell), III (large cell) Provisional subtype diffuse, predominantly small cell type
		5	Marginal zone B-cell lymphoma Extranodal MALT type Provisional subtype nodal
		6	Provisional entity splenic marginal zone lymphoma
		7	Hairy cell leukemia
		8	Plasmacytoma/plasma cell myeloma
		9	Diffuse large B cell lymphoma Subtype primary mediastinal (thymic) B-cell lymphoma
		10	Burkitt's lymphoma
		11	Provisional entity diffuse large B-cell lymphoma, Burkitt like

Table 1 1 REAL classification of B cell neoplasms

Stage I	Involvement of a single lymph node region, a single organ or a site other than the lymph nodes
Stage II	Involvement of two or more lymph node areas above or below the diaphragm; disease is found in only one organ or area outside the lymph nodes and in lymph nodes around it
Stage III	Involvement of lymph node areas on both sides of the diaphragm; disease may have spread to an area or organ near lymph nodes or to the spleen
Stage IV	Widespread involvement of one or more sites other than lymph nodes with or without lymph node involvement; disease has spread to only one organ outside the lymph node area, but the lymph node area is far away from the organ site

Table 1.2: Ann Arbor staging system

Standard treatment for NHL

The incidence of NHL in the USA is 20.1 new cases per 100,000 inhabitants per year. Treatment of NHL depends on tumor type, grade and stage of the disease. Patients with stage I NHL of an indolent type are treated with local external radiotherapy, with a cure rate of 80%–90%. Patients with stage II NHL of an indolent type are also treated with local radiotherapy, but the chance for long-time disease-free survival is reduced to 40%–50% at best. Patients with more advanced stages of indolent types of NHL are considered to be incurable. They can be treated with chlorambucil or COP (cyclophosphamide, vincristine, and prednisone), generally resulting in temporary remissions. After several relapses the lymphoma will become therapy resistant or it will histologically dedifferentiate to an NHL of higher malignancy grade. Patients with intermediate- or high-grade NHL are treated with anthracyclin-containing combination chemotherapy (three to four cycles for patients with stage I, eight cycles for patients with stage II, III, or IV), followed by radiotherapy if necessary in stage I disease, and on indication in the more advanced stages.

Up to now only myeloablative therapy followed by allogeneic stem cell transplantation can potentially cure patients with relapsed low-grade NHL [3]. An initial "wait-and-see" policy in patients with advanced stages of low-grade NHL without symptoms is accepted, as it does not influence overall survival.

New treatment modalities for NHL are based on the use of monoclonal antibodies (mAbs). In this paper the developments in mAb-based therapies are reviewed.

Immunotherapy with monoclonal antibodies

In 1980, the first use of an idiotypic monoclonal antibody against malignant lymphoma cells in a patient was described [4]. In this particular case antibody 89 ("Ab 89") was used to treat patient "N.B." without a clinical response. More immunotherapies were conducted, using mAbs against the immunoglobulin variable region (idiotype) of B-cell malignancies. With these anti-idiotype mAbs, responses were seen [5]. However, developing antibodies for each individual patient is very impracticable. These difficulties can be avoided by using mAbs that recognize antigens more universally expressed on the surface of the B cells, such as HLA-DR, CD19, CD20, CD21, CD22, CD37, and CD52. These antigens are expressed on B cells in different stages of development. The earliest pre-B cells are defined by the expression of the cell surface antigens HLA-DR, CD34, and CD19. Later in

their development stage, the pre-B cells express the pan-B-cell restricted antigen CD20, which functions as an ion channel. After maturation of the pre-B cells, the cells are exported to the peripheral blood and to lymphoid tissues. Mature B cells express, amongst others, HLA-DR, CD19, CD20, CD21, CD24, and CD22. CD22 is a pan-B-cell adhesion molecule, and CD21 is an Epstein-Barr virus receptor. During development, B cells acquire several other antigens (CD37, CD39, CDw75, CD76) which are present until the conversion to plasma cells. CD52 is not restricted to B cells. It is also present on other leukocyte subspecies.

Each of the B cell-associated antigens has been used as a target antigen to design an antibody-based immunotherapy. The success of such a therapy partly depends on many characteristics of the B cell-associated antigen. The ideal target antigen has the following characteristics [6]:

1. It should be expressed only on the malignant cell, and not on normal cells, to prevent elimination of the latter.

2. The density of expression of the antigen on the B-cell surface should be high.

3. The antigen should not be expressed in various variants.

4. The antigen should not be secreted or shed by the malignant B cell, as mAbs could interact with these circulating antigens.

5. The antigen-antibody complex should not be internalized by the cell, to allow recognition of this cell by the immune system as a cell to be removed. (However, internalization of the antigen-antibody complex is not always an unwanted characteristic. When using the mAb as a carrier of immunotoxins, internalization is needed to bring the toxin into the cell. Similarly, internalization could also be exploited to bring a radionuclide into a cell, as will be discussed later.)

There are several mechanisms by which mAbs can kill lymphoma cells. Killer cells, being non-phagocytic mononuclear T cells, can recognize the Fc part of the bound mAb and subsequently kill the cell [7]. This is called antibody-dependent cellular cytotoxicity (ADCC). Furthermore, the mAb can activate the complement system. In complement-dependent cytotoxicity (CDC), the conformational change in the Fc region of the IgG mAb with the antigen on the cell surface initiates the classical complement pathway, resulting in lysis of the target cell [7]. Induction of apoptosis, or programmed cell death, is the goal of many anti-cancer therapies. Cross-linked antibodies can induce apoptosis in lymphoma cells [8]. Finally, an-

tibodies can interfere with a vital function of the target antigens on cells [9].

The first immunotherapy studies with mAbs against B cell-associated antigens revealed that large quantities of murine antibody can repeatedly be infused into patients provided that the infusion rate is low. A rapid drop in circulating cells that bear the target antigen can be observed after a single mAb injection. Such a response usually lasts only a few hours. When antibody is infused every 3–4 days for several weeks, a sustained decrement may be achieved [9].

One of the problems to overcome when using murine mAbs is the development of human anti-murine antibodies (HAMAs). HAMAs are endogenous human antibodies directed against mouse antibodies. These antibodies can be non-specific anti-isotypic, directed against constant regions in murine antibodies, or anti-idiotypic, directed against specific idiotypes of an injected mAb [10]. Both types of HAMA can limit effective mAb therapy by:

1. Induction of immune complex formation, leading to serum sickness or renal toxicity
2. Inhibition of binding of the mAb to tumor cells
3. Increased removal of mAbs by the reticulo-endothelial system [11]

Usually, HAMA formation is clinically silent. However, anaphylaxis has been reported in a patient treated with murine mAbs in the presence of HAMAs, even after plasmapheresis [12]. Not all patients treated with murine mAbs develop HAMAs. It has been suggested that patients with lymphoid malignancies develop HAMA less frequently than patients treated with murine mAbs for other diseases, possibly because of the immunosuppressive nature of the disease and as a result of prior immunosuppressive therapy [13]. Especially the latter seems quite important, since HAMA formation occurred in 65% of previously untreated patients after treatment with a radiolabeled mAb [14], while none of 14 patients treated with the combination of fludarabine and the same radiolabeled mAb developed HAMAs [15]. HAMAs are not necessarily associated with decreased effectiviness of mAb therapy. It has been reported that the presence of HAMAs may even be associated with improved survival [16]. This association may represent the effect of a functioning immune system. The presence of anti-idiotypic HAMAs might facilitate host recognition of tumor, as these antibodies mimic tumor cell antigen [16].

To overcome the development of HAMAs, human/murine chimeric constructs were developed. In a chimeric antibody, constant regions of the

heavy and light chains of the murine mAb are substituted by human regions using molecular biological technology. Chimeric antibodies can generally be infused for a longer period of time without inducing HAMAs. Formation of human anti-chimeric antibodies is reported in a minority of patients with solid tumors treated with chimeric mAbs [17,18].

An even more sophisticated method to reduce the immunogenicity of murine antibodies is humanization of the antibodies. In a humanized antibody, the murine hypervariable regions of the heavy and light chains (CDRs) are grafted into a human antibody framework. Theoretically, these mAbs should not be more immunogenic than regular human antibodies, although anti-idiotypic human anti-human antibodies (HAHAs) could still be induced against the hypervariable regions of these mAbs.

By now a series of antibodies has become available for mAb treatment of NHL. Table 1.3 summarizes the mAbs that were clinically used. Only chimeric and humanized antibodies are still being used for unlabeled antibody therapy.

Code name	Target antigen	Type of antibody	Generic name
Lym-1	HLA-DR10	Murine IgG2a	
Hu1D10	HLA-DR	Humanized IgG1	Apolizumab
Anti-B4	CD19	Murine IgG1	
Anti-B1	CD20	Murine IgG2a	Tositumomab
1F5	CD20	Murine IgG2a	
2B8	CD20	Murine IgG1	Ibritumomab
C2B8	CD20	Chimeric IgG1	Rituximab
OKB7	CD21	Murine IgG2b	
LL2	CD22	Murine IgG2a	
hLL2	CD22	Humanized IgG1	Epratuzumab
MB-1	CD37	Murine IgG1	
Campath-1G	CD52	Rat IgG2b	
Campath-1H	CD52	Humanized IgG1	Alemtuzumab

Table 1.3: Monoclonal antibodies used for therapy of NHL

Rituximab

The most widely used antibody for unlabeled antibody therapy is C2B8, also known as rituximab (Rituxan, MabThera). This mAb, directed against CD20, can induce both CDC and ADCC [5], and — probably most importantly — apoptosis [8]. It is a chimeric human IgG1 kappa antibody with

murine variable regions isolated from a murine anti-CD20 origin antibody (2B8) [19]. In a phase I single-dose escalation study, relevant anti-tumor responses were seen in 6 out of 15 patients [20]. In the subsequent multiple-dose trial, 20 patients with relapsed NHL were treated with four weekly doses of rituximab [21]. Six out of 18 patients had a partial remission. The treatment was well tolerated. Based on the data from this trial, a weekly dose of 375 mg/m^2 was selected for a phase II trial, in which 34 evaluable patients were treated weekly for 4 weeks [22]. Complete remissions (CRs) were seen in three patients, and partial remissions (PRs) in 14. In the following phase III single-agent trial in 151 evaluable patients, CRs and PRs were recorded in 6% and 44% of patients, respectively [19]. To date, rituximab is the only commercially available mAb for the treatment of NHL.

Alemtuzumab

Campath-1H (alemtuzumab, Campath, MabCampath) is a humanized IgG1 mAb against the panlymphoid cell antigen CD52, registered for the treatment of patients with chronic lymphocytic leukemia. It was also studied for the treatment of patients with NHL. Initially two patients with NHL were treated with alemtuzumab [23]. In both patients, lymphoma cells were cleared from the blood and bone marrow and splenomegaly resolved. One patient had lymphadenopathy which also resolved. Of the first seven patients treated in a phase II multicenter trial, three showed complete or partial responses [24]. In this study, patients with recurrent or progressive low-grade NHL were treated with three weekly intravenous infusions of alemtuzumab. The study was prematurely stopped due to unacceptable toxicity. The most significant toxicity was profound lymphopenia and associated infection, usually of viral origin. Six of seven patients had culture or serologically documented infections and four patients had two or more of such episodes. All infections responded to temporary discontinuation of antibody therapy and appropriate antiviral or antibiotic treatment. It was concluded that alemtuzumab has therapeutic activity against low-grade NHL. However, application is limited by marked lymphopenia and an unacceptably high frequency of serious infections.

In 1998, the European Study Group of Campath-1H Treatment in Low-Grade NHL came to similar conclusions based on the results of a multicenter phase II trial of alemtuzumab in 50 patients with advanced, low-grade NHL [25]. In this study six patients (14%) with B-cell lymphomas achieved a PR. Lymphopenia ($< 0.5 \times 10^9$/l) occurred in all patients. Grade 4 neutropenia was observed in 14 patients (28%). Opportunistic infections were diagnosed in seven patients and nine patients had bacterial septicemia.

Three patients died of infectious complications. Phase II studies with alemtuzumab are still being conducted in NHL patients.

Epratuzumab

hLL2 (epratuzumab, LymphoCide) is a humanized IgG1 antibody against CD22. A phase I/II study, treating patients with indolent NHL with doses of epratuzumab ranging from 120-1000 mg/m^2 per week for 4 consecutive weeks, revealed no dose-limiting toxicity [26]. However, 84% of these patients experienced one or more adverse events, the vast majority being grade 1 toxicity, like nausea, fatigue, chills, and fever. There was no evidence of any HAHA response. Reduction of circulating B cells occurred in several patients.

No responses were seen at the lowest dose levels of 120 mg/m^2 per week and 240 mg/m^2 per week. Six of 14 patients treated at a dose level of 360 mg/m^2 per week responded (2 CR, 4 PR), as well as 3 of 11 patients at the dose level of 480 mg/m^2 per week (1 CR, 2 PR). No objective responses were seen on the two highest dose levels of 600 and 1000 mg/m^2. Therefore, future trials will use a dose of 360 mg/m^2 for 4 consecutive weeks.

Epratuzumab is also studied for the treatment of diffuse large B-cell lymphoma. Preliminary data show that objective responses were seen in 5 out of 22 patients (3 CR, 2 PR) [27]. Finally, epratuzumab is also studied in combination with rituximab in patients with follicular lymphoma (n = 16) and diffuse large B-cell lymphoma (n = 3), leading to a response rate of 53% (10/19) [28].

Radioimmunotherapy

Radionuclides

Monoclonal antibodies can be used to guide radionuclides to malignant cells. Radiolabeled antibody treatment could in particular be effective for NHL, since it is a relatively radiosensitive and immunogenic malignancy. This treatment modality — radioimmunotherapy (RIT) — is fundamentally different from external beam radiation. The latter is based on relatively high dose rates for short periods of time. Between the treatment sessions there are periods of hours to days that no radiation is administered. Using RIT, the radiation is continuously delivered with a lower peak rate [29].

Radionuclides suited for RIT usually emit β-radiation for irradiation of the tumor (cells). It is preferable for the radionuclide also to emit low-energy γ-radiation in a low abundancy in order to allow scintigraphic imag-

ing while avoiding the need for extensive safety measures to prevent high doses for family members and medical staff. The radionuclide should have a half-life of several days to ensure the delivery of a sufficiently high dose to the tumor for a prolonged period of time.

As long ago as in the late 1940s it was possible to label proteins with iodine-131 (^{131}I) [30] For decades, ^{131}I was the main radionuclide used for RIT. However, the physical properties of ^{131}I are not ideal for RIT It has relatively low-energy β-emissions (mean 192 keV) and relatively high-energy γ-rays (362 keV). The latter lead to high radiation doses for relatives and medical staff. Nevertheless, from the beginning the results of RIT in patients with NHL with ^{131}I-labeled antibodies have been very promising. To avoid hypothyroidism caused by free radioiodine, adequate blockage of the thyroid gland with potassium chloride and potassium iodine is necessary.

More recent RIT studies used yttrium-90 (^{90}Y) instead of ^{131}I. ^{90}Y decays by pure β-emission. The β-particles of ^{90}Y have a longer range than the β-particles of ^{131}I because of the higher mean energy of the former. As ^{90}Y does not emit γ-rays, the *in vivo* distribution of the ^{90}Y-labeled antibodies can not be visualized. As discussed earlier, some target antigens are internalized by the cell after binding to an antibody (*e.g.* CD22). ^{90}Y is a radiometal that is retained intracellularly, whereas ^{131}I is released from the cell after dehalogenation [31,32]. When targeting internalizing antigens, the use of ^{90}Y is preferred. To facilitate labeling of an antibody with ^{90}Y, a chelating agent has to be conjugated to the mAb Once released from the chelate, ^{90}Y is incorporated in the mineral bone, which could result in high radiation doses to the normal bone marrow. Chelators used to label antibodies with ^{90}Y are mainly derivatives of diethylene triamine penta-acetic acid (DTPA). Nowadays the most widely used chelators are macrocyclic chelators like 1,4,7,10-tetraazacyclododecane-N,N′,N″,N‴-tetra-acetic acid (DOTA), 1,4,7,11-tetraazacyclotetradecane-N,N′,N″,N‴-tetra-acetic acid (TETA), or 6-[*p*-(bromoacetamido)benzyl]-TETA (BAT). These are chelating agents that form the most stable complexes with Y(III).

Rhenium-186 (^{186}Re) is another metallic radionuclide suitable for RIT. It emits both β- and γ-radiation. The γ-rays (emitted in only 9% of the disintegrations) are of low energy (137 keV) whereas the β-emissions are of medium energy (mean 362 keV). The low-energy and low-abundancy γ is ideal for imaging and will not lead to high doses for medical staff and relatives of the patient. Although doses that are allowed for out-patient treatment may vary considerably depending on local legislation, in several countries there is no requirement to hospitalize patients after therapy with

^{186}Re. The N_2S_2 chelate mercaptoacetyltriglycine (MAG3) can be used to attach ^{186}Re to the mAb [33]. These radioimmunoconjugates are stable *in vitro* and *in vivo*, and radioimmunoconjugates with relatively high specific activities can be prepared. Another method of labeling antibodies with Re exploits sulphhydryl groups of the antibody to complex the rhenium species [34]. Although it was thought that rhenium would be retained in cells like other metalic radiolabels, some studies suggested the opposite [35].

Copper-67 (^{67}Cu) can also be chosen for RIT. It has low-energy β-emissions (average 141 keV) and medium-energy γ-rays (185 keV) suitable for imaging. It has been used for RIT since the early 1980s. ^{67}Cu can be linked to a mAb using the macrocyclic chelator TETA. Unlike some other radiometals, ^{67}Cu is not deposited in the skeleton or bone marrow [36]. However, it is not widely used owing to its limited availability.

The most relevant properties of these β-emitting radionuclides are summarized in Table 1.4.

Radionuclide	Half-life	$\beta_{average}$ (keV)	γ (keV)	Max. range in tissue (mm)	Advantages	Disadvantages
^{131}I	8.0 days	192	362	2.9	Easy labelling	High radiation burden to medical staff and relatives
					Inexpensive	In-patient treatment
						Thyroid blockage required
^{90}Y	64.0 h	935	—	11	Higher β-energy	Higher bone marrow dose in case of unbound yttrium
					Out-patient treatment possible	No imaging possible
^{186}Re	90.7 h	362	137	5.1	Out-patient treatment possible	Laborious labeling
					Ideal γ for imaging	
^{67}Cu	61.9 h	141	185	1.8	Out-patient treatment possible	Laborious labeling
					Ideal γ for imaging	Limited availability of nuclide
						Low β-energy

Table 1.4: Radionuclides used for RIT

Another approach is the use of radionuclides emitting α-radiation. Alpha particles have a very limited range in tissue (micrometers instead of millimeters) and a high linear energy transfer. At present, bismuth-213 (^{213}Bi) is used for RIT in patients with acute myelogenous leukemia by the group of Scheinberg at Memorial Sloan-Kettering Cancer Center, New York [37] The half-life of this α-emitting nuclide is short (45.6 min); this has the consequence that it is not feasible to use ^{213}Bi in combination with mAbs that need hours or even days to target tumor sites which are not immediately accesible, as is the case in NHL. Because of the very short range of the α-particles, using α-emitters is not very suitable for treatment of bulky disease (as in NHL), but they could be attractive for use in micrometastatic diseases or minimal residual disease [38].

Dosimetry

Radiation dose calculations, dosing schedules, and doses delivered to tumors and normal organs are subject to intensive discussion There are various ways to determine the radioactivity dose to be administered:

- Fixed doses
- Body weight-based doses
- Body surface area-based doses
- Doses based on the estimated whole body dose
- Doses based on the estimated red marrow dose

For all radiolabeled mAbs, phase I studies have been conducted to determine the maximum tolerated dose (MTD). Without exception, dose-limiting toxicity consists of leuko- and thrombocytopenia. In general, dosimetric calculations cannot forecast the outcome of therapy, nor can they predict the grade of toxicity following RIT. The need for patient-specific dosimetry is a matter of debate. Some research groups advocate individual dosing based on a diagnostic study for dosimetric purposes. Others have shown that RIT can safely be based on the body weight of the patient only, without the need for dosimetric calculations before treatment, provided that platelet counts are normal and bone marrow involvement is less than 25% [39].

Radiolabeled antibodies

An overview of clinical studies with various mAbs and various radionuclides is presented in Table 1 5

Study	Radiopharmaceutical	*n*	Myeloablative RIT	Dosing schedule	Responses
DeNardo *et al.* 1990 [40]	^{131}I-Lym-1	18	-	Multiple	2 CR, 8 PR, 3 SD, 1 PD, 4 NE
Goldenberg *et al.* 1991 [41]	^{131}I-LL2	7	-	Double	2 PR, 3 SD, 2 NE
Czuczman *et al.* 1993 [42]	^{131}I-OKB7	18	-	Quadruple	1 PR, 12 SD
Press *et al.* 1993 [43]	^{131}I-MB-1	6	3/6	RID/RIT	6 CR
	^{131}I-1F5	1	1/1	RID/RIT	1 PR
	^{131}I-anti-B1	12	11/12	RID/RIT	10 CR, 1 PD, 1 SD
Juweid *et al.* 1995 [44]	^{131}I-LL2	7	-	Multiple	1 CR, 1 PR, 5 unk
	^{131}I-LL2 F(ab')$_2$	13	-	Multiple	1 CR, 1 PR, 11 unk
	^{131}I-cLL2	1	-	Multiple	1 unk
	^{131}I-LL2	3	3/3	Multiple	2 PR, 1 NE
White *et al.* 1996 [45]	^{90}Y-anti-Id	9	-	Multiple	2 CR, 1 PR, 3 SD, 3 PD
DeNardo *et al.* 1998 [46]	^{131}I-Lym-1	21	-	RID/RIT 1-4	7 CR, 4 PR, 9 SD, 1 PD
Behr *et al.* 1999 [47]	^{131}I-hLL2	5	2/5	Single	2 CR, 1 PR, 1 PD, 1 unk
	^{131}I-C2B8	5	5/5	RID/RIT	3 CR, 1 PR, 1 unk
Juweid *et al.* 1999 [31]	^{131}I-hLL2	13	-	RID/RIT	1 CR, 1 PR, 5 SD, 6 PD
	^{90}Y-hLL2	7	-	RID/RIT	2 PR, 5 PD
Lindén *et al.* 1999 [48]	^{131}I-LL2	8	-	RID/RIT 1-3	3 PR, 1 SD, 4 PD
O'Donnell *et al.* 1999 [36]	^{67}Cu-Lym-1	12	-	Multiple	1 CR, 6 PR
Witzig *et al.* 1999 [49]	^{90}Y-2B8	50	-	Rituximab/RIT	13 CR, 21 PR
Vose *et al.* 2000 [50]	^{131}I-anti-B1	45	-	RID/RIT	15 CR, 12 PR
Davis *et al.* 2001 [51]	^{131}I-anti-B1	42	-	RID/RIT	14 CR, 9 PR
Witzig *et al.* 2002 [52]	^{90}Y-2B8	73	-	Rituximab/RIT	22 CR, 36 PR
Behr *et al.* 2002 [53]	^{131}I-C2B8	7	7/7	RID/RIT	6 CR, 1 PR
Postema *et al.* 2003 [54]	^{186}Re-hLL2	15	-	RID/RIT	1 CR, 4 PR, 4 SD, 6 PD
Turner *et al.* 2003 [55]	^{131}I-C2B8	35	-	Rituximab/RIT	19 CR, 6 PR
Scheidhauer *et al.* 2003 [56]	^{131}I-C2B8	26	-	RID/RIT	9 CR, 5 PR
	^{131}I-C2B8	25	25/25	RID/RIT	12 CR, 7 PR

RID, Radioimmunodetection, tracer dose; CR, complete response; PR, partial response; SD, stable disease; PD, progressive disease; NE, not evaluable; unk, unknown

Table 1.5: RIT of patients with NHL

Lym-1

In 1987, DeNardo *et al.* at UC Davis Medical Center, Sacramento, CA, treated a patient with Richter's syndrome — a malignant lymphomatous histological transformation of chronic lymphocytic leukemia — with a series of injections of ^{131}I-Lym-1, currently also known as Oncolym, with a good clinical response and reduction of tumor volume [57]. After this success, 18 patients with B-cell NHL were treated with ^{131}I-Lym-1 at doses of 1.11–2.22 GBq at 2–6 week intervals until a cumulative dose of 11.1 GBq had been administered or until HAMA responses were observed [40]. The rationale for fractionated doses of RIT was based on evidence that the radiation dose to the tumor can be increased and that the dose tolerated by normal tissues is higher when the dose is fractionated [46]. Two patients had a CR following treatment, eight had a PR, three had SD, and one had disease progression. Four patients received only one treatment dose of ^{131}I-Lym-1, without any response: these patients died or developed HAMA, so further treatment could not be given [40].

More recently, the same group determined the non-myeloablative MTD of the first two doses of ^{131}I-Lym-1 in 21 patients [46]. A maximum of four doses of ^{131}I-Lym-1 was allowed. The MTD of the first two doses of ^{131}I-Lym-1 appeared to be 3.7 GBq/m^2. In this study, only three patients were repeatedly treated at this highest dose level. All three had CRs following treatment. Among all 21 patients, seven CRs and four PRs were reported.

The DeNardo group also used Lym-1 labeled with ^{67}Cu. Twelve patients were included in a phase I/II study using ^{67}Cu-2IT-BAT-Lym-1 for RIT of patients with progressive NHL after anthracycline-based chemotherapy [36]. A total of four courses of RIT was planned. Only one of 12 patients actually received all four doses. Three different dose levels were chosen. If grade 4 hematological toxicity occurred, the next dose was reduced by 50%. One CR and six PRs were seen. The authors concluded that doses of ^{67}Cu greater than 1.85 GBq/m^2 resulted in serious hematological toxicity.

anti-B1

The group of Kaminski and Wahl at the University of Michigan Medical Center in Ann Arbor, MI, focussed on the treatment of NHL with ^{131}I-labeled antibodies against CD20. They used the murine IgG2a anti-B1 antibody, known as tositumomab. Nine patients were treated in a phase I dose-escalating study with one (n = 5) or two (n = 4) doses of ^{131}I-anti-B1 (Bexxar), preceded by a tracer dose and by variable amounts of unlabeled antibody to determine whether presaturation of non-specific binding sites or reservoirs of non-malignant B cells would allow better access

to tumor sites [58]. Optimal tumor targeting was obtained when administering 685 mg unlabeled anti-B1 prior to administration of the radioiodinated antibody. In some cases, pretreatment with unlabeled mAbs helped radiolabeled mAbs bypass an antigenic sink. Doses were calculated using increasing whole-body radiation doses as derived from a tracer dose study. Myelotoxicity occurred when whole-body radiation doses exceeded 0.75 Gy, which was thus defined as the MTD [59]. In this non-myeloablative dose-escalating study in 28 patients, 14 patients had a CR and eight had a PR.

In the following multicenter phase II trial, all patients received a dosimetric dose of 185 MBq ^{131}I labeled to 35 mg anti-B1, preceded by an infusion of 450 mg unlabeled antibody [50]. After 1–2 weeks, 450 mg unlabeled antibody was again adminstered, followed by a therapeutic dose of ^{131}I-anti-B1 that led to an estimated whole-body dose of 0.75 Gy, if platelet counts were above 150×10^9/l. If platelet counts were between 100 and 150×10^9/l, the whole-body dose was lowered to 0.65 Gy. Of 47 patients, six experienced a CR and 16 a PR.

Finally, a randomized open-label multicenter study was conducted, comparing the efficacy and safety of ^{131}I-labeled tositumomab to unlabeled tositumomab in patients with relapsed or refractory CD20-positive NHL [51]. Seventy-eight patients were enrolled. The original NHL type was follicular lymphoma in 97% of patients, with 17% having experienced transformation to an aggressive histology. Patients receiving ^{131}I-tositumomab therapy were dosed as aforementioned. The patients randomized to unlabeled tositumomab treatment received two doses of 485 mg, *i.e.* the same total antibody dose that is administered to patients treated with ^{131}I-tositumomab. Confirmed responses were documented in 23 of 42 (55%) patients who received tositumomab RIT (33% CR, 21% PR), and 6 of 36 (17%) patients who received tositumomab (8% CR, 8% PR), respectively. The median duration of confirmed responses for Bexxar-treated patients has not been reached yet, and for unlabeled tositumomab treated patients it was 18 months. This study documents that the radioiodine component of RIT using ^{131}I-tositumomab provides significant therapeutic effect over and above that provided by unlabeled tositumomab with an acceptable toxicity profile [51]. In June 2003, the FDA approved Bexxar for the treatment of patients with CD20-positive follicular NHL, with and without transformation, whose disease is refractory to rituximab and has relapsed following chemotherapy.

At present, the group in Ann Arbor is also using RIT as first-line treatment, employing the same dosimetric and therapeutic procedures and doses as described above. In a phase II trial with ^{131}I-anti-B1 in 76 pre-

viously untreated patients with advanced stage follicular NHL, 48 patients achieved a CR and 26 a PR [14]. The 3-year progression-free survival was 68.2% in this study.

At the University of Washington in Seattle, WA, the group of Press *et al.* used the same ^{131}I-labeled anti-B1 mAb for the treatment of refractory NHL. Their approach is different from that at Ann Arbor, as they re-infuse stem cells to enable administration of high, myeloablative doses of radiolabeled anti-B1. In aiming at myeloablation, toxicity to organs other than the bone marrow will limit the radiation dose that can be tolerated. Therefore a dose escalation study was designed in which the dose to tumor and critical normal organs was calculated using dosimetry and biopsy specimens after a diagnostic procedure with ^{131}I-labeled mAbs. Doses were escalated based on the radiation dose absorbed by normal organs, ranging from 10 to 30.75 Gy. This study showed that doses less than 27.25 Gy to normal organs did not cause serious, irreversible non-hematological toxicity [43]. In a subsequent trial, doses of ^{131}I-anti-B1 estimated to deliver 27 Gy to the dose-limiting organ, generally the lungs, were administered [60]. Recently, Johnson and Press updated the results of this myeloablative RIT with ^{131}I-labeled mAbs [61]. Complete responses were reported in 30 of 36 patients. A long-term follow-up study of the 29 patients treated with myeloablative doses of ^{131}I-anti-B1 antibody has documented estimated overall and progression-free survival rates of 68% and 42%, respectively, with a median follow-up time of 42 months. To optimize the durability of responses, this group is currently conducting a phase I/II trial studying the toxicity and efficacy of ^{131}I-anti-B1 antibody given in combination with high-dose etoposide and cyclophosphamide, followed by autologous hematopoietic stem cell rescue. The role of RIT as reported here differs from other forms of RIT. In these cases RIT replaces total body irradiation. The duration of response achieved by this highly effective approach should especially be compared with the duration of response after chemotherapy followed by total body irradiation and stem cell support. In the aforementioned trial, the overall survival and the progression-free survival of the group treated with myeloablative RIT appear to be better than in the conventionally treated group [62].

2B8

The anti-CD20 antibody 2B8 was the basis of the chimeric antibody rituximab. This murine IgG1 mAb labeled with ^{90}Y is also applied in RIT. In an initial study both anti-B1 (n = 4) and 2B8 (n = 14) were labeled with ^{90}Y [63]. RIT was preceded by various amounts of unlabeled 2B8,

resulting in improved biodistribution of the radiolabeled antibody and decreased doses to the spleen and spine. In a subsequent multicenter trial, patients were pretreated with unlabeled rituximab (C2B8), followed by ^{90}Y-labeled ibritumomab (Y2B8, Zevalin). Fifty patients were treated in the phase I/II study [49]. Fifteen patients were treated with either 7.4 or 11.1 or 14.8 MBq/kg ^{90}Y-2B8. In the next 35 patients a dose of 14.8 MBq/kg was chosen if platelet counts were above 150×10^9/l, and a dose of 11.1 MBq/kg if platelet counts ranged between 100 and 150×10^9/l. RIT in this group of 35 patients was preceded by infusion of 250 mg/m^2 rituximab. The overall response rate in both groups was 68% (13 CRs and 21 PRs). As hematological toxicity correlated best with the amount of ^{90}Y per kg body weight [64], doses of 14.8 MBq/kg and 11.1 MBq/kg, respectively, are used as described above.

In a subsequent phase III trial, RIT with ^{90}Y-ibritumomab was compared with control immunotherapy with rituximab in 143 patients with relapsed or refractory low-grade follicular or transformed CD20-positive NHL [52]. Patients received either a single intravenous dose of 14.8 MBq/kg of ^{90}Y-ibritumomab (n = 73) or four weekly doses of 375 mg/m^2 of rituximab (n = 70). The RIT group was pretreated with two rituximab doses (250 mg/m^2) to improve biodistribution and one dose of indium-111 (^{111}In) ibritumomab for imaging and dosimetry. The overall response rate was 80% for the ^{90}Y-ibritumomab group *versus* 56% for the rituximab group. CR rates were 30% and 16% in the RIT and rituximab groups, respectively. Median duration of response did not differ between the two groups. Neither did the time to progression. Reversible myelosuppression was the primary toxicity noted with ^{90}Y-ibritumomab. Zevalin was approved by the FDA in February 2002 [65].

C2B8

In an increasing number of studies, the chimeric version of the 2B8 mAb is used for radiolabeling and RIT. Behr *et al.* reported on the myeloablative use of ^{131}I-labeled rituximab instead of ibritumomab. In a study of five patients — two with high-grade and three with low-grade NHL — who received myeloablative RIT followed by autologous stem cell support, a CR was achieved in three [47]. When this approach was used in seven patients with mantle cell lymphoma, an aggressive and prognostically unfavorable type of NHL, it even achieved a CR in six cases and a PR in one [53]. Another German group presented data on both myeloablative and non-myeloablative RIT using ^{131}I-rituximab [56]. With the latter procedure in 26 patients, an overall response rate of 54% was achieved. Myeloablative

RIT of 25 patients led to a CR in 48%, and a PR in 28% of treated patients.

In Australia, a phase II trial in 42 patients with relapsed or refractory NHL was conducted, using their own dosing regimen [55]. First, an infusion of 375 mg/m^2 unlabeled rituximab was administered, followed by a tracer dose of 200 MBq ^{131}I-rituximab. Dosimetric analysis was used to determine the amount of radioiodine needed to deliver a whole body dose of 0.75 Gy, comparable to the dosing scheme of ^{131}I-tositumomab. This calculated amount of ^{131}I-rituximab was administered a week after the tracer dose, again preceded by an infusion of 375 mg/m^2 unlabeled rituximab. This approach led to grade 4 hematological toxicity in 2 of 42 patients. Nineteen patients of 35 evaluable patients (54%) showed CRs, 6 patients (17%) showed a PR to RIT. Nowadays, iodinated rituximab is used in German, Australian and UK RIT trials.

LL2

At the Garden State Cancer Center, Belleville, NJ, a mAb against CD22 was developed. The murine IgG2a mAb or the F(ab')$_2$ fragment was labeled with ^{131}I and administered to 16 patients with NHL for radioimmunodetection. Seven patients were treated with ^{131}I-LL2, consisting of a first injection of 1.11 GBq, followed 1 week later by an injection of 0.74 GBq [41]. In this study two PRs were seen. An update of this study, using variable doses of ^{131}I-labeled murine IgG, F(ab')$_2$, and in one case chimeric IgG, showed 1 CR and 2 PRs in 17 patients treated with non-myeloablative doses of LL2 [44]. Three other patients were treated with myeloablative doses of ^{131}I-LL2 followed by re-infusion of previously harvested bone marrow, two of whom achieved a PR.

As described earlier, a humanized version of LL2 (hLL2, epratuzumab) was produced in order to reduce the immunogenicity. This antibody was used for RIT with both ^{131}I and ^{90}Y. The pharmacokinetics, dosimetry, and initial therapeutic results with ^{131}I- and ^{111}In-/^{90}Y-labeled hLL2 were compared [31]. Doses were calculated applying an estimated red marrow dose of 1 Gy, or 0.5 Gy in case of prior high-dose chemotherapy, as determined after administration of a tracer dose of 222 MBq ^{131}I- or ^{111}In-hLL2. Protein dose in all infusions was 0.75 mg hLL2 per kg body weight. In the ^{131}I-hLL2 treatment group (n = 13), one CR and one PR were observed. In the ^{90}Y-hLL2 group (n = 7), two PRs were seen. Treatment with both radiolabels was equally safe, and pharmacokinetics and dosimetry were similar, but the tumor dosimetry of ^{90}Y-hLL2 appeared to be more favorable than that of ^{131}I-hLL2. As CD22 is an antigen that is internalized by the B cell, the use of ^{131}I is thought to result in release of the radioiodine after process-

ing of the labeled mAb in the cell. In contrast, radiometals are retained by the cell after internalization of the radioimmunoconjugate, which may contribute to the more successful use of ^{90}Y attached to hLL2. Even at low doses of ^{90}Y-hLL2, objective responses were seen. A group at the University Hospital in Lund, Sweden, gave patients two or three injections of only 185 MBq ^{90}Y-hLL2/m^2. Patients with prior high-dose chemotherapy and stem cell rescue received only 92.5 MBq ^{90}Y-hLL2/m^2. In five of eight patients, partial or complete responses were observed [66].

Currently the MTDs of non-myeloablative RIT with ^{90}Y-hLL2 and myeloablative RIT with ^{90}Y-hLL2 followed by stem cell re-infusion are being determined in two multicenter trials.

At the University Medical Center Nijmegen, The Netherlands, we have been studying the use of ^{186}Re-labeled hLL2 in a dose escalation study. The results of this study are discussed in Chapter 4 of this thesis [54].

Other mAbs used for RIT

The antibodies and radionuclides described above are those that are currently of major interest. Other combinations have been used for RIT. MB-1 is a mAb that targets CD37. The use of ^{131}I-MB-1 in six patients, three of whom received a myeloablative dose level, led to CR in all six patients [43]. In later studies this group switched to anti-B1.

OKB7 is a mAb directed against CD21. Czuczman *et al.* described the use of ^{131}I-OKB7 in 18 patients [42], in a phase I dose escalation trial. The MTD appeared to be 7.4 GBq ^{131}I-OKB7 in four doses of 1.85 GBq. In one patient a PR and in 12 patients a mixed response were reported. No further studies of OKB7 in NHL patients have been published.

White *et al.* described good clinical results using RIT with ^{90}Y-labeled anti-idiotype antibodies: two CRs and one PR in nine patients [45]. Nevertheless, development of anti-idiotype mAbs is very laborious.

Future role of RIT

The promising results of RIT for the treatment of NHL justify further trials with radiolabeled mAbs. The response rates in future trials may increase if patient selection is not limited to those who have been heavily pretreated and have recurrent or refractory NHL. If patients are treated earlier after diagnosis and RIT is given before or in combination with conventional therapy, higher doses and more cycles of RIT could probably be given, as these patients have a better bone marrow reserve than those who have had multiple cycles of chemotherapy. Both approaches are currently being

persued. As mentioned above, first-line treatment of 76 patients with follicular lymphomas using ^{131}I-tositumomab showed a response rate of 97% [14]. At present more trials are being conducted with the same radiopharmaceutical, *e.g.* in previously untreated patients with low-grade NHL after treatment with COP, and in patients with follicular NHL after treatment with CHOP (cyclophosphamide, doxorubicin, vincristine, and prednisone).

RIT could also be used in patients who are free of disease after conventional therapy in order to establish a longer lasting disease-free interval. ^{90}Y-ibritumomab has been used in this group of patients in a pan-European trial

Conclusion

RIT is a new and apparently successful treatment modality for refractory or relapsed NHL. Various combinations of mAbs and radionuclides have been studied. Future randomized, prospective trials must determine the role of RIT in NHL management, as well as the most suitable mAbs and radionuclides.

References

1. Aisenberg AC. Historical review of lymphomas. *Br J Haematol* 2000; 109: 466-476.

2. Harris NL, Jaffe ES, Diebold J, Flandrin G, Muller-Hermelink HK, Vardiman J, Lister TA, Bloomfield CD. World Health Organization classification of neoplastic diseases of the hematopoietic and lymphoid tissues: report of the Clinical Advisory Committee Meeting — Airlie House, Virginia, November 1997. *J Clin Oncol* 1999; 17: 3835-3849.

3. Mandigers CMPW, Raemaekers JMM, Schattenberg AVMB, Roovers EA, Bogman MJJT, van der Maazen RWM, de Pauw BE, de Witte T. Allogeneic bone marrow transplantation with T-cell-depleted marrow grafts for patients with poor-risk relapsed low-grade non-Hodgkin's lymphoma. *Br J Haematol* 1998; 100: 198-206.

4. Nadler LM, Stashenko P, Hardy R, Kaplan WD, Button LN, Kufe DW, Antman KH, Schlossman SF. Serotherapy of a patient with a monoclonal antibody directed against a human lymphoma-associated antigen. *Cancer Res* 1980; 40: 3147-3154.

5. Vose JM. Antibody-targeted therapy for low-grade lymphoma. *Semin Hematol* 1999; 36: 15-20.

6. Maloney DG. Monoclonal antibodies in lymphoid neoplasia: principles for optimal combined therapy. *Semin Hematol* 2000; 37: 17-26.

7. Chapel H, Haeney M. *Essentials of clinical immunology.* Blackwell Scientific Publications, Oxford 1988.

8. Mathas S, Rickers A, Bommert K, Dörken B, Mapara Y. Anti-CD20- and B-cell receptor-mediated apoptosis: evidence for shared intracellular signaling pathways. *Cancer Res* 2000; 60: 7170-7176.

9. Kwak LW, Longo DL. Monoclonal antibody therapy. In: Magrath IT (ed.). *The non-Hodgkin's lymphomas.* Arnold, London 1997: 703-705.

10. Klee GG. Human anti-mouse antibodies. *Arch Pathol Lab Med* 2000; 124: 921-923.

11. Schroff RW, Foon KA, Beatty SM, Oldham RK, Morgan AC. Human anti-murine immunoglobulin responses in patients receiving monoclonal antibody therapy. *Cancer Res* 1985; 45: 879-885.

12. Verhaar-Langereis MJ, Eagle KF, Keep PA, Casey JL, Begent RH. Anaphylactic reaction to radioimmunotherapy despite plasmapheresis to remove anti-mouse antibodies. *J R Soc Med* 2000; 93: 75-76.

13. Shawler DL, Bartholomew RM, Smith LM, Dillman RO. Human immune response to multiple injections of murine monoclonal IgG. *J Immunol* 1985; 135: 1530-1535.

14. Kaminski MS, Estes J, Tuck M, Mann J, Fisher S, Kison P, Regan D, Stagg R, Kroll SM, Magnuson DE, Wahl RL. Iodine I 131 tositumomab therapy for previously untreated follicular lymphoma. *Proc Am Soc Clin Oncol* 2000; 19: abstract 11.

15. Leonard JP, Coleman M, Kostakoglu L, Chadburn A, Cesarman E, Bhatnagar A, Tidmarsh GF, Kroll SM, Goldsmith SJ. Fludarabine monophosphate followed by iodine I 131 tositumomab for untreated low-grade and follicular non-Hodgkin's lymphoma (NHL). *Blood* 1999; 94: 90a.

16. Lamborn KR, DeNardo GL, DeNardo SJ, Goldstein DS, Shen S, Larkin EC, Kroger LA. Treatment-related parameters predicting efficacy of Lym-1 radioimmunotherapy in patients with B-lymphocytic malignancies. *Clin Cancer Res* 1997; 3: 1253-1260.

17. Steffens MG, Boerman OC, Oosterwijk-Wakka JC, Oosterhof GO, Witjes JA, Koenders EB, Oyen WJG, Buijs WCAM, Debruyne FM, Corstens FHM, Oosterwijk E. Targeting of renal cell carcinoma with iodine-131-labeled chimeric monoclonal antibody G250. *J Clin Oncol* 1997; 15: 1529-1537.

18. Wong JY, Williams LE, Yamauchi DM, Odom-Maryon T, Esteban JM, Neumaier M, Wu AM, Johnson DK, Primus FJ, Shively JE. Initial experience evaluating ^{90}yttrium-radiolabeled anti-carcinoembryonic antigen chimeric T84.66 in a phase I radioimmunotherapy trial. *Cancer Res* 1995; 55: 5929s-5934s.

19. Grillo-López AJ, White CA, Varns C, Shen D, Wei A, McClure A, Dallaire BK. Overview of the clinical development of rituximab: first monoclonal antibody approved for the treatment of lymphoma. *Semin Oncol* 1999; 26: 66-73.

20. Maloney DG, Liles TM, Czerwinski DK, Waldichuk C, Rosenberg J, Grillo-López AJ, Levy R. Phase I clinical trial using escalating single-dose infusion of chimeric anti-CD20 monoclonal antibody (IDEC-C2B8) in patients with recurrent B-cell lymphoma. *Blood* 1994; 84: 2457-2466.

21. Maloney DG, Grillo-López AJ, Bodkin DJ, White CA, Liles TM, Royston I, Varns C, Rosenberg J, Levy R. IDEC-C2B8: results of a phase I multiple-dose trial in patients with relapsed non-Hodgkin's lymphoma. *J Clin Oncol* 1997; 15: 3266-3274.

22. Maloney DG, Grillo-López AJ, White CA, Bodkin DJ, Schilder RJ, Neidhart JA, Janakiraman N, Foon KA, Liles TM, Dallaire BK, Wey K, Royston I, Davis T, Levy R. IDEC-C2B8 (rituximab) anti-CD20 monoclonal antibody therapy in patients with relapsed low-grade non-Hodgkin's lymphoma. *Blood* 1997; 90: 2188-2195.

23. Hale G, Dyer MJ, Clark MR, Phillips JM, Marcus R, Riechmann L, Winter G, Waldmann H. Remission induction in non-Hodgkin's lymphoma with reshaped human monoclonal antibody CAMPATH-1H. *Lancet* 1988; 2: 1394-1399.

24. Tang SC, Hewitt K, Reis MD, Berinstein NL. Immunosuppressive toxicity of CAMPATH1H monoclonal antibody in the treatment of patients with recurrent low grade lymphoma. *Leuk Lymphoma* 1996; 24: 93-101.

25. Lundin J, Osterborg A, Brittinger G, Crowther D, Dombret H, Engert A, Epenetos A, Gisselbrecht C, Huhn D, Jaeger U, Thomas J, Marcus R, Nissen N, Poynton C, Rankin E, Stahel R, Uppenkamp M, Willemze R, Mellstedt H. CAMPATH-1H monoclonal antibody in therapy for previously treated low-grade non-Hodgkin's lymphomas: a phase II multicenter study. *J Clin Oncol* 1998; 16: 3257-3263.

26. Leonard JP, Coleman M, Ketas JC, Chadburn A, Ely S, Furman RR, Wegener WA, Hansen HJ, Ziccardi H, Eschenberg M, Gayko U, Cesano A, Goldenberg DM. Phase I/II trial of epratuzumab (humanized anti-CD22 antibody) in indolent non-Hodgkin's lymphoma. *J Clin Oncol* 2003; 21: 3051-3059.

27. Press OW, Leonard JP, Coiffier B, Levy R, Timmerman J. Immunotherapy of non-Hodgkin's lymphomas. *Hematology (Am Soc Hematol Educ Program)* 2001; 221-240.

28. Leonard JP, Coleman M, Matthews JC, Fiore JM, Dosik A, Shore T, Kapushoc H, Macri M, Wegener WA, Cesano A, Goldenberg DM. Epratuzumab (anti-CD22) and rituximab (anti-CD20) combination immunotherapy for non-Hodgkin's lymphoma: preliminary response data. *Proc Am Soc Clin Oncol* 2002; 21: 266a.

29. Press OW. Physics for practitioners: the use of radiolabeled monoclonal antibodies in B-cell non-Hodgkin's lymphoma. *Semin Hematol* 2000; 37: 2-8.

30. Wilder RB, DeNardo GL, DeNardo SJ. Radioimmunotherapy: recent results and future directions. *J Clin Oncol* 1996; 14: 1383-1400.

31. Juweid ME, Stadtmauer E, Hajjar G, Sharkey RM, Suleiman S, Luger S, Swayne LC, Alavi A, Goldenberg DM. Pharmacokinetics, dosimetry, and initial therapeutic results with ^{131}I- and ^{111}In-/^{90}Y-labeled humanized LL2 anti-CD22 monoclonal antibody in patients with relapsed, refractory non-Hodgkin's lymphoma. *Clin Cancer Res* 1999; 5: 3292s-3303s.

32. Sharkey RM, Behr TM, Mattes MJ, Stein R, Griffiths GL, Shih LB, Hansen HJ, Blumenthal RD, Dunn RM, Juweid ME, Goldenberg DM. Advantage of residualizing radiolabels for an internalizing antibody against the B-cell lymphoma antigen, CD22. *Cancer Immunol Immunother* 1997; 44: 179-188.

33. Visser GWM, Gerretsen M, Herscheid JDM, Snow GB, van Dongen GAMS. Labeling of monoclonal antibodies with rhenium-186 using the MAG3 chelate for radioimmunotherapy of cancer: a technical protocol. *J Nucl Med* 1993; 34: 1953-1963.

34. Griffiths GL, Goldenberg DM, Diril H, Hansen HJ. Technetium-99m, rhenium-186, and rhenium-188 direct-labeled antibodies. *Cancer* 1994; 73: 761-768.

35. Steffens MG, Kranenborg MHGC, Boerman OC, Zegwaart-Hagemeier NEM, Debruyne FMJ, Corstens FHM, Oosterwijk E. Tumor retention of ^{186}Re-MAG3, ^{111}In-DTPA and ^{125}I labeled monoclonal antibody G250 in nude mice with renal cell carcinoma xenografts. *Cancer Biother Radiopharm* 1998; 13: 133-139.

36. O'Donnell RT, DeNardo GL, Kukis DL, Lamborn KR, Shen S, Yuan A, Goldstein DS, Mirick GR, DeNardo SJ. ^{67}Copper-2-iminothiolane-6-[*p*-(bromoacetamido)benzyl]-TETA-Lym-1 for radioimmunotherapy of non-Hodgkin's lymphoma. *Clin Cancer Res* 1999; 5: 3330s-3336s.

37. McDevitt MR, Sgouros G, Finn RD, Humm JL, Jurcic JG, Larson SM, Scheinberg DA. Radioimmunotherapy with alpha-emitting nuclides. *Eur J Nucl Med* 1998; 25: 1341-1351.

38. Jurcic JG. Antibody therapy of acute myelogenous leukemia. *Cancer Biother Radiopharm* 2000; 15: 319-326.

39. Wiseman GA, Witzig TE, Flinn I, Gordon LI, Emmanouilides C, Czuczman MS, Saleh M, Cripe L, Multani PS, Grillo-López AJ, White CA. Zevalin radioimmunotherapy (RIT) is effective and safe withput imaging and biodistribution dosimetry in patients with rituximab-refractory follicular lymphoma (F-NHL). *Cancer Biother Radiopharm* 2000; 15: 408.

40. DeNardo GL, DeNardo SJ, O'Grady LF, Levy NB, Adams GP, Mills SL. Fractionated radioimmunotherapy of B-cell malignancies with 131I-Lym-1. *Cancer Res* 1990; 50: 1014s-1016s.

41. Goldenberg DM, Horowitz JA, Sharkey RM, Hall TC, Murthy S, Goldenberg H, Lee RE, Stein R, Siegel JA, Izon DO, Burger K, Swayne LC, Belisle E, Hansen HJ, Pinsky CM. Targeting, dosimetry, and radioimmunotherapy of B-cell lymphomas with Iodine-131-labeled LL2 monoclonal antibody. *J Clin Oncol* 1991; 9: 548-564.

42. Czuczman MS, Straus DJ, Divgi CR, Graham M, Garin-Chesa P, Finn R, Myers J, Old LJ, Larson SM, Scheinberg DA. Phase I dose-escalation trial of iodine 131-labeled monoclonal antibody OKB7 in patients with non-Hodgkin's lymphoma. *J Clin Oncol* 1993; 11: 2021-2029.

43. Press OW, Eary JF, Appelbaum FR, Martin PJ, Badger CC, Nelp WB, Glenn SD, Butchko G, Fisher D, Porter B, Matthews DC, Fisher LD, Bernstein ID. Radiolabeled-antibody therapy of B-cell lymphoma with autologous bone marrow support. *N Engl J Med* 1993; 329: 1219-1224.

44. Juweid ME, Sharkey RM, Markowitz A, Behr TM, Swayne LC, Dunn RM, Hansen HJ, Shevitz J, Leung SO, Rubin AD, Herskovic T, Hanley D, Goldenberg DM. Treatment of non-Hodgkin's lymphoma with radiolabeled murine, chimeric, or humanized LL2, an anti-CD22 monoclonal antibody. *Cancer Res* 1995; 55: 5899s-5907s.

45. White CA, Halpern SE, Parker BA, Miller RA, Hupf HB, Shawler DL, Collins HA, Royston I. Radioimmunotherapy of relapsed B-cell lymphoma with yttrium 90 anti-idiotype monoclonal antibodies. *Blood* 1996; 87: 3640-3649.

46. DeNardo GL, DeNardo SJ, Goldstein DS, Kroger LA, Lamborn KR, Levy NB, McGahan JP, Salako Q, Shen S, Lewis JP. Maximum-tolerated dose, toxicity, and efficacy of ^{131}I-Lym-1 antibody for fractionated radioimmunotherapy of non-Hodgkin's lymphoma. *J Clin Oncol* 1998; 16: 3246-3256.

47. Behr TM, Wörmann B, Gramatzki M, Riggert J, Gratz S, Béhé M, Griesinger F, Sharkey RM, Kolb H-J, Hiddemann W, Goldenberg DM, Becker W. Low- *versus* high-dose radioimmunotherapy with humanized anti-CD22 or chimeric anti-CD20 antibodies in a broad spectrum of B cell-associated malignancies. *Clin Cancer Res* 1999; 5: 3304s-3314s.

48. Lindén O, Tennvall J, Cavallin-Ståhl E, Darte L, Garkavij M, Lindner KJ, Ljungberg M, Ohlsson T, Sjögreen K, Wingårdh K, Strand SE. Radioimmunotherapy using ^{131}I-labeled anti-CD22 monoclonal antibody (LL2) in patients with previously treated B-cell lymphomas. *Clin Cancer Res* 1999; 5: 3287s-3291s.

49. Witzig TE, White CA, Wiseman GA, Gordon LI, Emmanouilides C, Raubitschek A, Janakiraman N, Gutheil J, Schilder RJ, Spies S, Silverman DHS, Parker E, Grillo-López AJ. Phase I/II trial of IDEC-Y2B8

radioimmunotherapy for treatment of relapsed or refractory CD20+ B-cell non-Hodgkin's lymphoma. *J Clin Oncol* 1999; 17: 3793-3803.

50. Vose JM, Wahl RL, Saleh M, Rohatiner AZ, Knox SJ, Radford JA, Zelenetz AD, Tidmarsh GF, Stagg RJ, Kaminski MS. Multicenter phase II study of iodine-131 tositumomab for chemotherapy-relapsed/refractory low-grade and transformed low-grade B-cell non-Hodgkin's lymphomas. *J Clin Oncol* 2000; 18: 1316-1323.

51. Davis TA, Kaminski MS, Leonard JP, Gregory SA, Wahl RL, Hsu FJ, Wilkinson M, Frankel SR, Serafini A, Zelenetz AD, Kroll S, Coleman M, Levy R, Knox SJ. Results of a randomized study of Bexxar™ (tositumomab and iodine I 131 tositumomab) vs. unlabeled tositumomab in patients with relapsed or refractory low-grade or transformed non-Hodgkin's lymphoma (NHL). *Proc Am Soc Hematol* 2001; 3503.

52. Witzig TE, Gordon LI, Cabanillas F, Czuczman MS, Emmanouilides C, Joyce R, Bartlett NL, Wiseman GA, Grillo-López AJ, Multani P, White CA. Randomized controlled trial of yttrium-90-labeled ibritumomab tiuxetan radioimmunotherapy versus rituximab immunotherapy for patients with relapsed or refractory low-grade, follicular, or transformed B-cell non-Hodgkin's lymphoma. *J Clin Oncol* 2002; 20: 2453-2463.

53. Behr TM, Griesinger F, Riggert J, Gratz S, Behe M, Kaufmann CC, Wormann B, Brittinger G, Becker W. High-dose myeloablative radioimmunotherapy of mantle cell non-Hodgkin lymphoma with the iodine-131-labeled chimeric anti-CD20 antibody C2B8 and autologous stem cell support. Results of a pilot study. *Cancer* 2002; 94: 1363-1372.

54. Postema EJ, Raemaekers JMM, Oyen WJG, Boerman OC, Mandigers CMPW, Goldenberg DM, van Dongen GAMS, Corstens FHM. Final results of a phase I radioimmunotherapy trial using ^{186}Re-epratuzumab for the treatment of patients with non-Hodgkin's lymphoma. *Clin Cancer Res* 2003; 9: 3995s-4002s.

55. Turner JH, Martindale AA, Boucek J, Claringbold PG, Leahy MF. ^{131}I-anti CD20 radioimmunotherapy of relapsed or refractory non-Hodgkins lymphoma: A phase II clinical trial of a nonmyeloablative dose regimen of chimeric rituximab radiolabeled in a hospital. *Cancer Biother Radiopharm* 2003; 18: 513-524.

56. Scheidhauer K, Schwarz K, von Schilling C, Schmidt B, Wolf I, Peschel C, Schwaiger M. Prädiktion von Remission und ereignis-

freiem Uberleben nach Radioimmuntherapie (RIT) von Non-Hodgkin-Lymphomen. *41. Jahrestagung DGN* 2003: abstract V152.

57. DeNardo SJ, DeNardo GL, O'Grady LF, Macey DJ, Mills SL, Epstein AL, Peng JS, McGahan JP. Treatment of a patient with B cell lymphoma by I-131 LYM-1 monoclonal antibodies. *Int J Biol Markers* 1987; 2: 49-53.

58. Kaminski MS, Zasadny KR, Francis IR, Milik AW, Ross CW, Moon SD, Crawford SM, Burgess JM, Petry NA, Butchko GM, Glenn SD, Wahl RL. Radioimmunotherapy of B-cell lymphoma with [^{131}I] anti-B1 (anti-CD20) antibody. *N Engl J Med* 1993; 329: 459-465.

59. Kaminski MS, Zasadny KR, Francis IR, Fenner MC, Ross CW, Milik AW, Estes J, Tuck M, Regan D, Fisher S, Glenn SD, Wahl RL. Iodine-131-anti-B1 radioimmunotherapy for B-cell lymphoma *J Clin Oncol* 1996, 14: 1974-1981.

60. Press OW. Radiolabeled antibody therapy of B-cell lymphomas. *Semin Oncol* 1999; 26: 58-65.

61. Johnson TA, Press OW. Therapy of B-cell lymphomas with monoclonal antibodies and radioimmunoconjugates: the Seattle experience. *Ann Hematol* 2000; 79: 175-182.

62. Press OW, Eary JF, Gooley T, Gopal AK, Liu S, Rajendran JG, Maloney DG, Petersdorf S, Bush SA, Durack LD, Martin PJ, Fisher DR, Wood B, Borrow JW, Porter B, Smith JP, Matthews DC, Appelbaum FR, Bernstein ID. A phase I/II trial of iodine-131-tositumomab (anti-CD20), etoposide, cyclophosphamide, and autologous stem cell transplantation for relapsed B-cell lymphomas. *Blood* 2000; 96: 2934-2942.

63. Knox SJ, Goris ML, Trisler K, Negrin R, Davis T, Liles TM, Grillo-López AJ, Chinn P, Varns C, Ning SC, Fowler S, Deb N, Becker M, Marquez C, Levy R. Yttrium-90-labeled anti-CD20 monoclonal antibody therapy of recurrent B-cell lymphoma. *Clin Cancer Res* 1996; 2: 457-470.

64. Wiseman GA, White CA, Witzig TE, Gordon LI, Emmanouilides C, Raubitschek A, Janakiraman N, Gutheil J, Schilder RJ, Spies S, Silverman DHS, Grillo-Lopez AJ. Radioimmunotherapy of relapsed non-Hodgkin's lymphoma with Zevalin, a ^{90}Y-labeled anti-CD20 monoclonal antibody. *Clin Cancer Res* 1999; 5. 3281s-3286s.

65. Wagner HN, Jr, Wiseman GA, Marcus CS, Nabi HA, Nagle CE, Fink-Bennett DM, Lamonica DM, Conti PS. Administration guidelines for

radioimmunotherapy of non-Hodgkin's lymphoma with ^{90}Y-labeled anti-CD20 monoclonal antibody. *J Nucl Med* 2002; 43: 267-272.

66. Lindén O, Tennvall J, Cavallin-Ståhl E, Lindner KJ, Darte L, Ohlsson T, Hindorf C, Wingårdh K, Strand SE. A phase I/II trial with ^{90}Y hLL2 in recurrent B-cell lymphomas. Preliminary results. *Cancer Biother Radiopharm* 2000; 15: 413.

Chapter 2

Enhancing tumor implantation and growth rate of Ramos B-cell lymphoma in nude mice

Jeroen M.B. Manders
Ernst J. Postema
Frans H.M. Corstens
Otto C. Boerman

Comparative Medicine 2002; 52: 36-38

Abstract

The ability of a human B-cell lymphoma cell line to grow subcutaneously as tumors in nude mice was investigated. The effect of pretreating mice with cyclophosphamide or whole-body irradiation (WBI) was compared with no pretreatment of the mice. Both methods of pretreatment resulted in a higher tumor implantation rate, compared with that for non-pretreated controls. In mice that underwent WBI-pretreatment, a tumor implantation rate of 100% was observed, whereas mice pretreated with cyclophosphamide had a tumor implantation rate of 80%. In nonpretreated control mice, an implantation rate of only 50% was observed. Three weeks after injection, tumor size was significantly larger in mice of the pretreated groups, compared with that in mice of the group that did not receive pretreatment. Furthermore, particularly in the group pretreated with WBI, the tumors grew more synchronously, compared with tumors in the control group. Results of this study indicate that pretreatment with cyclophosphamide or WBI improves the tumor implantation rate of Ramos cells in nude mice, providing a workable animal model for studying human B-cell lymphoma.

Introduction

Immunotherapy with monoclonal antibodies (mAbs) and radioimmunotherapy with radiolabeled mAbs are new treatment modalities for patients with recurrent or widespread malignancies. Patients with malignant B-cell lymphomas may respond especially well to this kind of treatment [1]. Mice with human tumors are used as models to optimize this kind of treatment (*e.g.*, to determine which monoclonal antibody and which radionuclide would be the best choice for this kind of treatment). Malignant lymphomas are usually disseminated *in vivo*, as represented by mouse models using severe combined immune deficient (SCID) mice [2–5]. For evaluation of radioimmunotherapy, only one circumscribed, subcutaneous tumor lesion that allows evaluation of tumor growth, is preferable. For this purpose, athymic BALB/c mice bearing a subcutaneous lymphoma xenograft are used in most animal studies [6–12]. Transplantation of human lymphoma cells in nude mice is difficult [6]. Vuist *et al.* reported failure of several Burkitt's lymphoma cell lines (BJAB, EB3, Ramos, Jiyoye, and Namalwa) to grow subcutaneously. Only the Daudi cells eventually grew in BALB/c nude mice younger than eight weeks [6]. Leonard *et al.* observed that, after subcutaneous injection of Namalwa cells, none of the inoculated BALB/c nude mice developed a tumor [7]. In nude mice, num-

bers of B cells, natural killer (NK) cells, and macrophages are at least similar to those in immunocompetent mice [13]. This residual immunologic defense is considered to prevent growth of some human tumors in nude mice [13–15].

To enhance induction and growth rates of tumor xenografts in nude mice, the following immunosuppressive strategies can be used: pretreatment with cyclophosphamide [13,14], and pretreatment with whole-body irradiation (WBI) [7,13,15]. In the study reported here, the effect of both methods on tumor implantation and growth rate of Ramos cells in nude mice was investigated.

Materials and methods

Animals and husbandry

Female, home-bred mice of the seventh generation BALB/c-nu inbred strain were studied. The mice were serologically screened for known rodent viruses according to recommendations of the Federation of European Laboratory Animal Science Associations (FELASA) and were found negative for these viruses. The mice were housed behind strict barriers to maintain the specific-pathogen-free status. At the start of the experiment, the mice were six to eight weeks old and weighed 20.6 ± 1.0 g. The mice were housed in wire- and filter-topped Macrolon type-II cages (375 cm^2, Techniplast, Utrecht, The Netherlands), five mice per cage, with autoclaved sawdust bedding (Woodyclean 3/4, BMI, Helmond, The Netherlands). Cages were cleaned once a week. Food pellets (RMH-GS, Hope Farms, Woerden, The Netherlands) and acidified tap water (HCl, pH 2.5 to 3) were provided *ad libitum*. The animal room had a controlled photoperiod (7 a.m. to 7 p.m., lights on; 7 p.m. to 7 a.m., lights out), temperature (21 °C), relative humidity (±55%), and ventilation (15 air changes/h).

Animals were treated and used humanely, according to the requirements of Dutch legislation. This experiment was approved by the internal review board for the use of laboratory animals.

Cell culture

Ramos cells (CRL-1596, American Type Culture Collection, Manassas, VA) were cultured in RPMI 1640 medium supplemented with 10% fetal bovine serum, penicillin (100 U/ml), streptomycin (100 μg/ml), and 100 m*M* L-glutamine. Cell cultures were kept in logarithmic growth phase and were maintained in a humidified 5% CO_2 atmosphere at 37 °C. On the day of

tumor cell inoculation, cell suspensions were centrifuged in 50-ml tubes at $500 \times g$ during 5 min, washed once in RPMI 1640 medium, and resuspended in RPMI 1640 medium (10^8 cells/ml), then were injected into mice within 1 h.

Experimental procedure

Mice were randomly divided into three groups of 10 mice/group. One group served as a control group and did not receive any pretreatment. The second group received cyclophosphamide (100 mg/kg of body weight) intraperitoneally [14]. Cyclophosphamide (Endoxan-Asta, Dagra Pharma B.V., Diemen, The Netherlands) was obtained from the Department of Clinical Pharmacy. The third group received WBI by use of external beam radiation with 15 MeV electrons at a dose of 6 Gy, using a linear accelerator (Saturne 42F, GE Medical Systems, Buc, France) [2,15]. During the WBI procedure, mice were kept in plexiglass boxes. Twenty-four hours after pretreatment, 10^7 Ramos tumor cells in 0.1 ml were injected subcutaneously into the right flank of the mice.

Tumor growth was monitored by use of caliper measurements in three dimensions, and was performed by the same investigator (JM). Tumor growth was classified as negative, positive (but not yet measurable), or measurable. As soon as tumors were measurable, measurements were carried out three times a week. Tumor volume of measurable tumors was calculated by assuming that tumors were ellipsoids [16], and the mathematical formula for calculating the volume of an ellipsoid ($1/6\pi \times$ length $\times$ width $\times$ height) was used. Minimal detectable tumor volume was 50 mm^3. Mice were considered suitable for further experiments when tumor volume was between 50 and 1,000 mm^3.

Analysis of data

Tumor volumes measured three weeks after inoculation were compared statistically using Wilcoxon tests

Results

Figure 2.1 depicts mean tumor size in each group during three weeks after inoculation with tumor cells. Three weeks after injection, tumor sizes were significantly larger in both groups, compared with that for the control group ($P = 0.01$ for pretreatment with cyclophosphamide, $P < 0.01$ for pretreatment with WBI). There were no significant differences between the

group pretreated with cyclophosphamide and the WBI pretreated group. Tumor behavior and tumor implantation rate markedly varied among the three groups. Therefore, the three groups are discussed separately.

Control group

In the control group, tumor growth was observed macroscopically 19 days after tumor induction in three mice (mean ± SD, 50 ± 10 mm^3). Tumor growth in these mice was relatively slow. On day 31 after tumor cell inoculation, all mice had a tumor with mean volume of 310 ± 322 mm^3. Mean time from inoculation to first appearance of a tumor was 22 days. In five of these mice, tumors regressed. Thus, the tumor implantation rate in this group was 50%.

Pretreatment with cyclophosphamide

Macroscopic tumor growth in the mice that received pretreatment with cyclophosphamide, started 14 days after tumor cell inoculation, when four tumors appeared. On day 19 after tumor cell inoculation, all mice had a tumor, with mean volume of 213 ± 230 mm^3. Two tumors regressed; thus, the tumor implantation rate in this group was 80%.

Pretreatment with WBI

In the group of mice that were irradiated prior to tumor inoculation, tumor growth became apparent 14 days after inoculation in nine mice, with mean volume of 100 ± 111 mm^3. On day 19, all mice had a tumor, with mean volume of 257 ± 132 mm^3. Regression of tumors was not observed; thus, the tumor implantation rate in this group was 100%.

Discussion

Tumor growth profiles of the groups indicate that both pretreatment methods enhanced tumor survival and growth rate. Tumor survival rate increased from 50% to 80% in association with cyclophosphamide, and to 100% in association with WBI. To allow evaluation of various therapeutic strategies, it is essential that tumors do not spontaneously regress. In addition, in both pretreated groups, therapeutic experiments could be started within three weeks after tumor induction. Considering that tumors measuring between 50 and 1,000 mm^3 could be used for further experiments, 50% of the mice pretreated with cyclophosphamide were suitable

for actual experiments between days 18 and 21 after tumor cell inoculation. For mice of the WBI-pretreated group, 100% were suitable for further experiments between days 14 and 21. In a subsequent experiment in 20 mice, each pretreated with cyclophosphamide, 80% of the mice (16/20) had developed tumors with suitable size 14 days after inoculation.

In the study reported here, we used athymic BALB/c mice. In most preclinical studies with (radiolabeled) mAbs, athymic BALB/c mice were used [6–12]. Athymic BALB/c mice lack functional T cells. The SCID mice have even less residual immunity than do athymic mice; the former lack functional T and B cells. However, both mouse strains still have some NK-cell activity. Since SCID mice are even more immunodeficient than are BALB/c mice, these mice are also used in models of disseminated hematologic malignancies [2–5]. In those experiments, the lymphoma cells are injected intravenously, not leading to uniformly comparable tumors. Induction of subcutaneous, human Hodgkin lymphoma xenografts in SCID and athymic mice were described by Kapp *et al.* [17]. After subcutaneous injection of three Hodgkin lymphoma cell lines in three groups of five athymic mice, tumor growth was not seen in athymic mice. In three groups of five SCID mice, tumors were seen in three of five, three of five, and one of five of these mice. A fourth Hodgkin cell line induced subcutaneous tumors in three of five nude mice and five of five SCID mice. Finally, a fifth cell line did not grow at all in nude and SCID mice [17].

Results of this study indicated that both methods of pretreatment can improve the implantation rate of Ramos tumors in athymic BALB/c mice. Use of WBI-pretreatment was associated with tumor implantation rate up to 100%, rapid induction of tumor growth, and synchronous growth of the tumors. Pretreatment with cyclophosphamide yielded less favorable results, but is easy to carry out, with good tumor implantation rate, 80%, in this experiment.

Acknowledgments

We thank G. Grutters of the Central Animal Laboratory and W. Brouwer, physicist, of the Dept. of Radiotherapy for their support

References

1 Postema EJ, Boerman OC, Oyen WJG, Raemaekers JMM, Corstens FHM. Radioimmunotherapy of B-cell non-Hodgkin's lymphoma. *Eur J Nucl Med* 2001; 28: 1725-1735.

2. Ghetie MA, Gordon BE, Podar EM, Vitetta ES. Effect of sublethal irradiation of SCID mice on growth of B-cell lymphoma xenografts and on efficacy of chemotherapy and/or immunotoxin therapy. *Lab Anim Sci* 1996; 46: 305-309.

3. Ghetie MA, Podar EM, Gordon BE, Pantazis P, Uhr JW, Vitetta ES. Combination immunotoxin treatment and chemotherapy in SCID mice with advanced, disseminated Daudi lymphoma. *Int J Cancer* 1996; 68: 93-96.

4. Liu C, Lambert JM, Teicher BA, Blattler WA, O'Connor R. Cure of multidrug-resistant human B-cell lymphoma xenografts by combinations of anti-B4-blocked ricin and chemotherapeutic drugs. *Blood* 1996; 87: 3892-3898.

5. van Horssen PJ, Preijers FW, van Oosterhout YV, de Witte T. Highly potent CD22-recombinant ricin A results in complete cure of disseminated malignant B-cell xenografts in SCID mice but fails to cure solid xenografts in nude mice. *Int J Cancer* 1996; 68: 378-383.

6. Vuist WM, Buitenen F, de Rie MA, Hekman A, Rumke P, Melief CJ. Potentiation by interleukin 2 of Burkitt's lymphoma therapy with anti-pan B (anti-CD19) monoclonal antibodies in a mouse xenotransplantation model. *Cancer Res* 1989; 49: 3783-3788.

7. Leonard JE, Johnson DE, Felsen RB, Tanney LE, Royston I, Dillman RO. Establishment of a human B-cell tumor in athymic mice. *Cancer Res* 1987; 47: 2899-2902.

8. Sharkey RM, Behr TM, Mattes MJ, Stein R, Griffiths GL, Shih LB, Hansen HJ, Blumenthal RD, Dunn RM, Juweid ME, Goldenberg DM. Advantage of residualizing radiolabels for an internalizing antibody against the B-cell lymphoma antigen, CD22. *Cancer Immunol Immunother* 1997; 44: 179-188.

9. Mattes MJ, Shih LB, Govindan SV, Sharkey RM, Ong GL, Xuan H, Goldenberg DM. The advantage of residualizing radiolabels for targeting B-cell lymphomas with a radiolabeled anti-CD22 monoclonal antibody. *Int J Cancer* 1997; 71: 429-435.

10. Illidge TM, Cragg MS, McBride HM, French RR, Glennie MJ. The importance of antibody-specificity in determining successful radioimmunotherapy of B-cell lymphoma. *Blood* 1999; 94: 233-243.

11. Illidge T, Honeychurch J, Howatt W, Ross F, Wilkins B, Cragg M. A new in vivo and in vitro B cell lymphoma model, π-BCL_1. *Cancer Biother Radiopharm* 2000; 15: 571-580.

12. DeNardo GL, DeNardo SJ, Wessels BW, Kukis DL, Miyao N, Yuan A. ^{131}I-Lym-1 in mice implanted with human Burkitt's lymphoma (Raji) tumors: loss of tumor specificity due to radiolysis. *Cancer Biother Radiopharm* 2000; 15: 547-560.

13. Silobrcic V, Zietman AL, Ramsay JR, Suit HD, Sedlacek RS. Residual immunity of athymic NCr/Sed nude mice and the xenotransplantation of human tumors. *Int J Cancer* 1990; 45: 325-333.

14. Nauta MM, Boven E, Schluper HM, Erkelens CA, Pinedo HM. Enhanced transplantability of human ovarian cancer lines in cyclophosphamide-pretreated nude mice. *Br J Cancer* 1986; 54: 331-335.

15. Cavacini LA, Giles-Komar J, Kennel M, Quinn A. Effect of immunosuppressive therapy on cytolytic activity of immunodeficient mice: implications for xenogeneic transplantation. *Cell Immunol* 1992; 144: 296-310.

16. Tomayko MM, Reynolds CP. Determination of subcutaneous tumor size in athymic (nude) mice. *Cancer Chemother Pharmacol* 1989; 24: 148-154.

17. Kapp U, Wolf J, von Kalle C, Tawadros S, Rottgen A, Engert A, Fonatsch C, Stein H, Diehl V. Preliminary report: growth of Hodgkin's lymphoma derived cells in immune compromised mice. *Ann Oncol* 1992; 3 Suppl 4: 21-23.

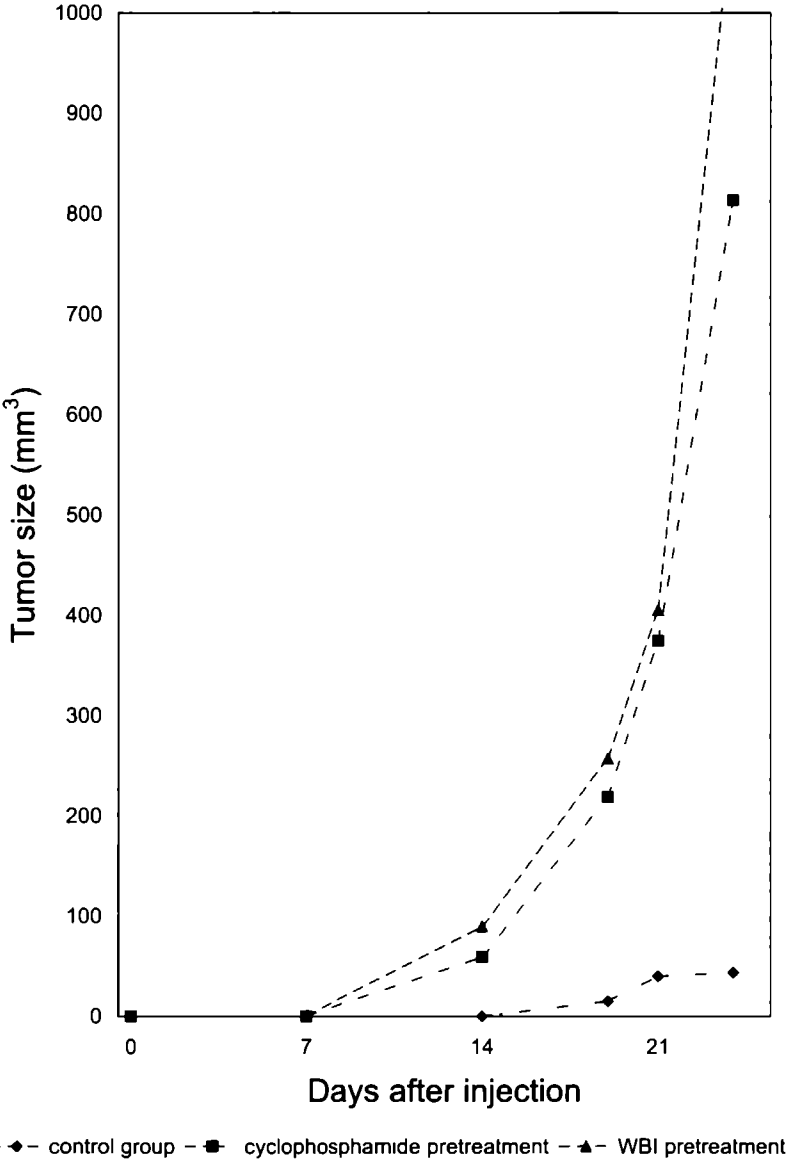

Figure 2 1 Mean tumor sizes in the three groups of mice

Chapter 3

Biodistribution of ^{131}I-, ^{186}Re-, ^{177}Lu-, and ^{88}Y-labeled hLL2 (epratuzumab) in nude mice with CD22-positive lymphoma

Ernst J. Postema
Cathelijne Frielink
Wim J.G. Oyen
John M.M. Raemaekers
David M. Goldenberg
Frans H.M. Corstens
Otto C. Boerman

Cancer Biotherapy & Radiopharmaceuticals 2003; 18: 525–533

Abstract

Radioimmunotherapy (RIT) is a new and effective treatment modality in patients with non-Hodgkin's lymphoma. The monoclonal antibody (mAb) hLL2 (epratuzumab), a humanized mAb directed against the CD22 antigen, and which internalizes, can be labeled with various radionuclides. The biodistribution of hLL2 labeled with ^{131}I, ^{186}Re, ^{177}Lu, and ^{88}Y was studied in nude mice with subcutaneous human lymphoma xenografts in order to determine the most suitable of these four radionuclides for RIT with hLL2.

Methods: Human Ramos lymphoma xenografts were transplanted in cyclophosphamide-pretreated athymic BALB/c mice. Four groups of mice were injected intravenously with ^{131}I-, ^{186}Re-, ^{88}Y-, or ^{177}Lu-labeled hLL2, respectively. To determine the non-specific tumor uptake, two groups of mice received ^{88}Y-labeled or ^{131}I-labeled control antibody, cG250. The biodistribution of the radiolabel was determined 1, 3, and 7 days postinjection (p.i.).

Results: Radiolabeled hLL2 had a higher tumor uptake than the non-specific mAb at all time-points, irrespective of the radiolabel used. Tumor accretion of ^{88}Y- and ^{177}Lu-hLL2 was higher than tumor uptake of ^{131}I- and ^{186}Re-hLL2. Activity in the bone, represented by the femur without bone marrow, was higher for ^{177}Lu- and ^{88}Y-hLL2 than for ^{131}I- and ^{186}Re-hLL2 on day 7 p.i.

Conclusion: The use of the residualizing radiolabels ^{88}Y and ^{177}Lu in combination with a mAb directed against an internalizing antigen resulted in higher uptake and better retention of the radiolabel in the tumor.

Introduction

Radioimmunotherapy is an effective treatment modality for patients with non-Hodgkin's lymphoma (NHL) Various monoclonal antibodies (mAbs) and radionuclides are being used for this purpose [1,2]. At present, only the murine ^{90}Y-labeled ibritumomab is approved for commercialization by the United States Food and Drug Administration [3]. Another radiolabeled murine antibody, ^{131}I-tositumomab, is currently being studied in phase III clinical trials [4]. Both mAbs are of murine origin and both are directed against CD20 In contrast, hLL2 (epratuzumab) is a humanized mAb targeting CD22 CD22 is a B-cell restricted marker, expressed on the B-cell surface during differentiation from the pre-B-cell stage [5]. Expression is lost during terminal differentiation to the plasma cell stage [5]. CD22 is rapidly internalized after binding the mAb LL2 [6]. Flow cytometric analysis of various Burkitt's lymphoma cell lines incubated with LL2 revealed

that 70% of Daudi cells, 42% of Raji cells, and 28% of Ramos cells were labeled with LL2 [7].

Currently, hLL2 is being investigated in clinical studies, labeled with ^{90}Y [8] and ^{186}Re [2,9] Previous studies, both in mice and humans, suggested a more favorable uptake in the tumor of ^{90}Y-labeled hLL2, represented by the γ-emitter ^{111}In labeled to hLL2, than of radioiodinated hLL2 [10,11]. At present, two other radionuclides, ^{186}Re and ^{177}Lu, could be of interest for RIT. ^{177}Lu is a radiometal with similar chemical properties as ^{90}Y . In contrast to ^{90}Y, it emits γ-radiation that could be used for imaging and dosimetric analysis. ^{186}Re is a group-VII element, like ^{99m}Tc, with ideal γ-emissions of 137 keV in 10% of disintegrations. The role of these radionuclides in combination with this internalizing mAb has not yet been determined *in vivo*. In the present study, the biodistribution of hLL2 labeled with four radionuclides, ^{131}I, ^{186}Re, ^{88}Y (as a representative of the pure β-emitter ^{90}Y), and ^{177}Lu, was compared in a nude mice model with human lymphoma xenografts.

Materials and methods

Cells

For the grafting of lymphoma xenografts, Ramos cells (CRL-1596, American Type Culture Collection, Manassas, VA) were cultured in RPMI 1640 medium supplemented with 10% fetal bovine serum, 100 U/ml of penicillin, 100 μg/ml streptomycin, and 100 m*M* L-glutamine. Cell cultures were kept in log phase and maintained in a humidified 5% CO_2 atmosphere at 37 °C. On the day of tumor cell inoculation, cell suspensions were centrifuged in 50-ml tubes at 1000 *g* for 5 minutes, resuspended in RPMI 1640 medium (10^8 cells/ml), and injected within 1 hour.

Animals and husbandry

Female, locally-bred BALB/c nude inbred strain mice were used. The mice were serologically screened for known rodent viruses according to recommendations of the Federation of European Laboratory Animal Science Associations (FELASA) and found to be negative for these viruses. The mice were housed behind strict barriers to maintain a specific pathogen-free status. At the start of the experiments, the mice were 6–8 weeks old. The mice were housed in wire- and filter-topped Macrolon type II cages (375 cm^2, Techniplast, Utrecht, The Netherlands), five mice per cage, with

autoclaved sawdust bedding (Woodyclean 3/4, BMI, Helmond, The Netherlands). Food pellets (Ssniff R/M-H, 10 mm, Ssniff Spezialdiaten GmbH, Soest, Germany) and acidified tap water (HCl, pH 2.5–3) were provided *ad libitum*. The animal room had a controlled photoperiod (07:00–19:00 hours light, 19:00–07:00 hours no light), temperature (21 °C), relative humidity (approximately 55%), and ventilation (15 air changes/hour). Animals were treated and used according to the ethical requirements of Dutch legislation. This investigation was approved by the internal review board for the use of laboratory animals.

Tumor grafts

Lymphoma xenografts were grafted as previously described [12]. The mice were injected with 0.1 mg/g cyclophosphamide (Endoxan-Asta, Dagra Pharma B.V., Diemen, The Netherlands) intraperitoneally. Twenty-four hours after pretreatment, 5×10^7 Ramos tumor cells in 0.2 ml were injected subcutaneously in the right flank of the mice. As soon as tumors were measurable, 2–3 weeks after implantation, mice were considered to be eligible for injection with radiolabeled hLL2 for the biodistribution study.

Antibodies, radionuclides, and labeling procedures

hLL2 (epratuzumab, vials of 52 mg/10 ml) was obtained from Immunomedics, Inc. (Morris Plains, NJ), and stored at 4–8 °C. The chimeric mAb, cG250, an antibody directed against carbonic anhydrase isoform IX, which is not expressed on lymphoma cells, was used as a negative control. It was stored, treated and labeled similarly to hLL2.

The radionuclide ^{131}I was obtained from MDS Nordion S.A. (Fleurus, Belgium), ^{186}Re from Mallinckrodt Medical BV (Petten, The Netherlands), ^{88}Y from Los Alamos National Laboratory (Los Alamos, NM), and ^{177}Lu from the University of Missouri Research Reactor (Columbia, MO). The physical properties of these radionuclides are listed in Table 3.1. Labeling of hLL2 with ^{131}I was performed using the iodogen method [13]. For labeling of ^{88}Y and ^{177}Lu, isothiocyanatobenzyl-diethylenetriaminepentaacetic acid (ITC-DTPA) was used as a chelator [14]. Mercaptoacetyltriglycine (MAG3) was used as a chelator for the labeling of the mAbs with ^{186}Re [15].

After labeling, the radiolabeled mAbs were separated from unbound radioactivity by PD10 column gel filtration. Radiochemical purity of all preparations exceeded 95%, as determined by ITLC on silicagel strips using 0.15 *M* citrate buffer, pH 5.0, as the mobile phase. The specific activity of each radiolabeled antibody preparation is listed in Table 3.2. Unlabeled

	Half-life	γ Energy (abundance)	Mean β energy
^{131}I	8.0 days	364 keV (81%)	192 keV
^{186}Re	3.8 days	137 keV (10%)	362 keV
^{88}Y	107 days	1,836 keV (99%)	—
^{90}Y	2.7 days	—	935 keV
^{177}Lu	6.7 days	208 keV	149 keV

Table 3.1: Physical properties of the radionuclides

	n	Radionuclide	mAb	Activity per animal	Antibody preparation specific activity
Group 1	29	^{131}I	hLL2	10 μCi (0.37 MBq)	2.9 μCi/mg
Group 2	26	^{186}Re	hLL2	50 μCi (1.85 MBq)	2.8 μCi/mg
Group 3	27	^{177}Lu	hLL2	50 μCi (1.85 MBq)	5.1 μCi/mg
Group 4	12	^{88}Y	hLL2	1 μCi (37 kBq)	0.1 μCi/mg
Group 5	21	^{131}I	cG250	10 μCi (0.37 MBq)	4.1 μCi/mg
Group 6	10	^{88}Y	cG250	1 μCi (37 kBq)	0.2 μCi/mg

Table 3.2: Groups of mice with lymphoma

hLL2 was added to the radiolabeled antibody preparations until a total protein dose of hLL2 of 50 μg per animal was attained.

Biodistribution and tumor dosimetry

All mice were injected intravenously with 50 μg radiolabeled hLL2 per animal via the tail vein on day 0. Six groups of at least 10 mice each were treated according to the radiolabel that was used (Table 3.2).

The animals in each group were sacrificed on day 1, 3, or 7 postinjection (p.i.), respectively, by CO_2 suffocation. Directly after death, blood was obtained by cardiac puncture. Tumor, thigh muscle, lung, liver, spleen, kidney, duodenum, and femur, without bone marrow, were dissected. The femur was flushed with 10 ml saline four times to remove the bone marrow. Periosteum was removed, and the femur dried for at least 1 hour. After weighing, the tissue samples and the calibration standards were counted in a well-type gamma counter (1480 Wizard 3'', Wallac, Turku, Finland). The amount of radioactivity in the samples was expressed as percentage of the injected dose per gram sample weight (% ID/g).

The absorbed tumor doses per administered unit of activity were esti-

mated using the biodistribution data [16]. The trapezoidal method was used, given the mean uptake in the tumor at the three different time-points, assuming that the activity at the time of injection was zero, and postulating that only physical decay was responsible for decline of activity in the tumor after 7 days p.i. [16]. After multiplication by the S values for each isotope, assuming uniformly distributed activity in small unit-density spheres, the absorbed tumor dose resulted, expressed as Gy/MBq.

Statistical analysis

For comparison of the four radiolabels, one-way analysis of variance (ANOVA) was performed, using Bonferroni post-test correction. For comparison of ^{131}I-hLL2 with ^{131}I-cG250, and ^{88}Y-hLL2 with ^{88}Y-cG250, respectively, unpaired *t*-test with Welch correction was used. Differences were considered statistically significant if $P < 0.05$.

Results

The human lymphoma xenograft was transplanted in a total of 125 mice. At the time of dissection the mean tumor weight was 0.49 g. The biodistribution of the radiolabeled antibody preparations on 1, 3, and 7 days p.i. is summarized in Table 3.3.

	Day 1 p.i. (% ID/g±SD)	Day 3 p.i. (% ID/g±SD)	Day 7 p.i. (% ID/g±SD)
Blood			
^{131}I-hLL2	13.32±1.64	9.73±3.45	5.25±1.96
^{186}Re-hLL2	16.26±1.40[a]	11.19±1.70	7.09±1.79
^{177}Lu-hLL2	15.29±2.97	11.52±1.72	8.74±1.47[a]
^{88}Y-hLL2	13.83±1.29	11.84±2.07	5.68±2.33
^{131}I-cG250	17.35±2.39[b]	13.64±1.54[b]	9.25±1.85[b]
^{88}Y-cG250	16.92±1.65[c]	15.11±0.88[c]	11.51±0.61[c]
Muscle			
^{131}I-hLL2	1.45±0.25	1.00±0.23	0.52±0.23
^{186}Re-hLL2	1.43±0.34	1.09±0.20	0.67±0.16
^{177}Lu-hLL2	1.26±0.26	1.00±0.18	0.90±0.19[a]
^{88}Y-hLL2	1.32±0.22	1.07±0.20	0.78±0.46
^{131}I-cG250	1.15±0.18[b]	0.88±0.08	0.67±0.12
^{88}Y-cG250	1.52±0.18	1.33±0.23	1.14±0.10
Tumor			
^{131}I-hLL2	4.75±1.03	4.40±0.99	2.27±1.08
^{186}Re-hLL2	4.52±1.16	6.05±1.57	3.92±1.40
^{177}Lu-hLL2	8.17±1.23[a]	12.01±3.69[a]	12.03±2.71[a]
^{88}Y-hLL2	6.64±1.61[a]	14.14±3.19[a]	8.34±3.18[a]
^{131}I-cG250	2.82±0.92[b]	2.05±0.10[b]	1.59±0.21
^{88}Y-cG250	3.35±0.45[c]	3.32±0.31[c]	2.84±0.14[c]
Lung			
^{131}I-hLL2	8.49±1.49	6.14±2.16	3.34±1.37
^{186}Re-hLL2	10.04±1.82	7.45±1.20	4.95±1.82
^{177}Lu-hLL2	8.79±1.56	7.67±0.96	6.67±1.13[a]
^{88}Y-hLL2	7.59±0.91	7.42±1.22	4.27±1.37
^{131}I-cG250	9.74±1.23	7.88±0.86[b]	4.91±0.76[b]
^{88}Y-cG250	8.52±0.62	8.80±0.91	6.99±0.95[c]
Spleen			
^{131}I-hLL2	3.55±0.78	2.60±0.93	1.38±0.65
^{186}Re-hLL2	4.91±0.63[a]	3.51±0.58	2.06±0.54
^{177}Lu-hLL2	5.39±1.59[a]	6.16±1.14[a]	7.81±1.44[a]
^{88}Y-hLL2	3.84±0.46	4.26±0.48[a]	3.98±1.06[a]
^{131}I-cG250	2.99±0.70	2.02±0.33	1.50±0.37
^{88}Y-cG250	4.53±0.39	4.51±0.41	6.34±0.62[c]
Kidney			
^{131}I-hLL2	4.27±0.51	2.99±0.88	1.61±0.56
^{186}Re-hLL2	5.04±0.61	3.54±0.47	2.21±0.61

	Day 1 p.i. (% ID/g±SD)	Day 3 p.i. (% ID/g±SD)	Day 7 p.i. (% ID/g±SD)
^{177}Lu-hLL2	5.71±0.94[a]	5.00±0.56[a]	4.09±0.53[a]
^{88}Y-hLL2	4.68±0.42	4.01±0.43	2.54±0.52
^{131}I-cG250	4.72±0.55	3.62±0.35	2.54±0.49[b]
^{88}Y-cG250	5.28±0.65	4.99±0.28[c]	4.35±0.48[c]
Liver			
^{131}I-hLL2	3.83±0.72	2.60±0.77	1.45±0.55
^{186}Re-hLL2	5.54±1.12[a]	3.65±0.50	1.94±0.46
^{177}Lu-hLL2	5.26±1.55	5.17±1.50[a]	4.23±0.78[a]
^{88}Y-hLL2	4.58±1.19	5.50±1.75[a]	5.96±2.09[a]
^{131}I-cG250	3.68±0.59	2.97±0.29	1.93±0.42
^{88}Y-cG250	6.64±0.47[c]	6.02±0.61	5.11±0.33
Duodenum			
^{131}I-hLL2	3.28±0.66	2.76±0.93	1.14±0.43
^{186}Re-hLL2	4.47±1.25[a]	3.05±0.59	1.80±0.61
^{177}Lu-hLL2	3.91±0.91	3.36±0.70	2.82±0.57[a]
^{88}Y-hLL2	2.81±0.28	2.80±0.98	1.62±0.60
^{131}I-cG250	3.52±0.53	2.89±0.56	2.01±0.46[b]
^{88}Y-cG250	3.37±0.50	2.72±0.35	2.70±0.74
Femur			
^{131}I-hLL2	0.50±0.11	0.39±0.20	0.22±0.10
^{186}Re-hLL2	0.80±0.25	0.50±0.15	0.24±0.14
^{177}Lu-hLL2	0.66±0.23	1.07±0.29[a]	1.43±0.26[a]
^{88}Y-hLL2	0.60±0.42	0.65±0.16	1.55±0.53[a]
^{131}I-cG250	0.60±0.17	0.58±0.15[b]	0.35±0.14
^{88}Y-cG250	0.77±0.21	0.73±0.08	1.20±0.48

[a]Uptake of hLL2 with this radiolabel significantly higher when compared with hLL2 with other radiolabel(s) at this time-point ($P < 0.05$)
[b]Uptake of ^{131}I-cG250 significantly different when compared to ^{131}I-hLL2 ($P < 0.05$)
[c]Uptake of ^{88}Y-cG250 significantly different when compared to ^{88}Y-hLL2 ($P < 0.05$)

Table 3.3: Biodistribution of radiolabeled antibodies in a human lymphoma model

The control antibodies ^{131}I- and ^{88}Y-cG250 had longer circulation times than ^{131}I- and ^{88}Y-hLL2, probably due to the fact that chimeric antibodies

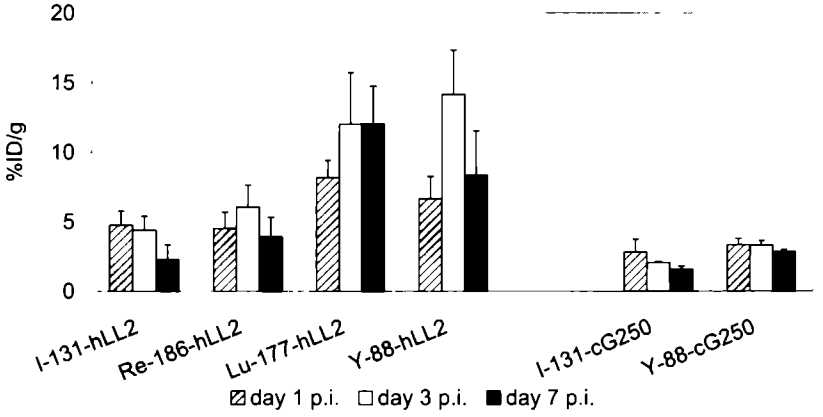

Figure 3.1: Uptake in lymphoma xenografts.

were used as control antibodies. There was no significant difference in amount of circulating radiolabeled hLL2 on the three time-points when comparing the four different radiolabels. Tumor uptake of ^{177}Lu- and ^{88}Y-hLL2 was significantly higher when compared with tumor accretion of ^{131}I- and ^{186}Re-hLL2 on days 1, 3, and 7 p.i. ^{131}I- and ^{88}Y-hLL2 tumor uptake was significantly higher when compared with ^{131}I- and ^{88}Y-cG250, respectively, at all time-points, as shown in Figure 3.1. Using the tumor uptake data and the mean tumor weight of 0.49 g, the aborbed tumor doses per administered unit of activity were estimated: 0.8 Gy/MBq for ^{131}I-hLL2, 1.0 Gy/MBq for ^{186}Re-hLL2, 2.1 Gy/MBq for ^{177}Lu-hLL2, and 3.2 Gy/MBq for ^{90}Y-hLL2.

The uptake in the liver and the spleen of ^{177}Lu and ^{88}Y was significantly higher when compared to the uptake of ^{186}Re and ^{131}I, both for radiolabeled hLL2 and for radiolabeled cG250. Uptake of ^{177}Lu in the kidney was significantly higher when compared with the other three radiolabels.

Since unbound ^{88}Y and ^{177}Lu tend to be incorporated in mineral bone, the activity in the bone was determined, as shown in Figure 3.2. The data show significantly higher accumulation in the bone of ^{88}Y and ^{177}Lu than of ^{131}I and ^{186}Re ($P < 0.05$ on day 7 p.i.).

Discussion

In the present study we have determined the biodistribution of the humanized anti-CD22 antibody LL2 labeled with different radionuclides in

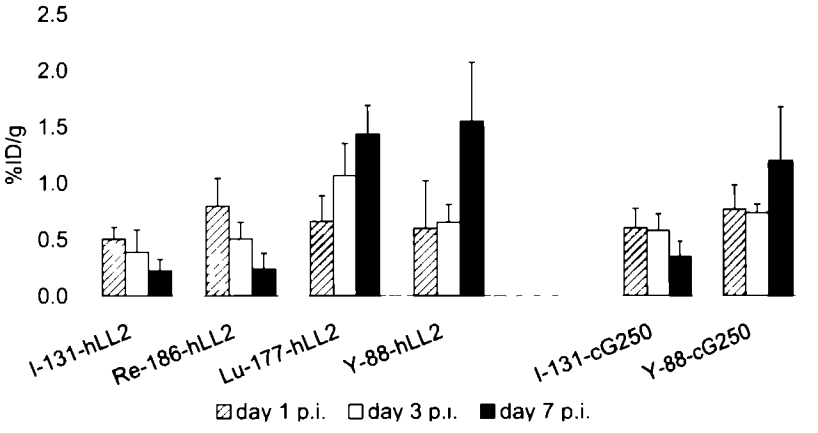

Figure 3.2: Uptake in femur.

nude mice with human lymphoma xenografts. The data show that uptake in the tumor varies from 2–14% ID/g, depending on the radionuclide and the time after injection. If the animals would have been treated at MTD, these uptake values would have led to an absorbed tumor dose of approximately 15 to 60 Gy. The fact that tumor uptake is not high may partly be due to the cell line used. As stated earlier, about 28% of Ramos cells are reactive with hLL2 [7]. However, with this cell line a workable animal model for these studies was obtained, as described earlier [12]. This study also indicated that tumor uptake of yttrium- and lutetium-labeled hLL2 is higher when compared to ^{131}I- and ^{186}Re-labeled hLL2. In a previous study, tumor uptake of the radioiodinated hLL2 did not exceed that of the non-specific control antibody in a mouse lymphoma model [17], but the present study shows a significant difference in tumor uptake of radioiodinated hLL2 over radioiodinated cG250. *In vivo*, ^{131}I-labeled hLL2 is rapidly catabolized within the lysosomes after internalization by the tumor cell. The radiolabel catabolites are rapidly released from the lysosomes and the cell [6,18]. To improve retention of the radioiodine in the cell, a residualizing iodine radiolabel, dilactilol-iodo-tyramine, was developed, leading to higher retention of ^{131}I in tumors in nude mice [18].

Other studies suggested to use radiometals, like ^{111}In, ^{90}Y, ^{177}Lu, or ^{67}Cu for radioimmunodetection and radioimmunotherapy, since these have a higher intracellular retention following internalization than iodine [10,11,17,19–21]. Not only absorbed doses in tumors appeared to be higher when using ^{90}Y-hLL2 instead of ^{131}I-hLL2, tumor-to-marrow, tumor-

to-lung and tumor-to-kidney ratios also increased in a clinical study [11]. Some studies suggest the use of ^{177}Lu instead of ^{90}Y [16,22]. ^{177}Lu has as an advantage over ^{90}Y in that it emits γ-radiation, which is useful for dosimetry and/or imaging. Since only 11% of disintegrations of ^{177}Lu are accompanied by medium-energy γ-rays, treatment could also be given on an outpatient basis in most countries. The present results show comparable uptake of ^{177}Lu and ^{90}Y in both tumor and other organs. Therefore, ^{177}Lu could be an interesting alternative for ^{90}Y. De Jong *et al.* recently suggested that the optimal tumor diameter for RIT with ^{90}Y-labeled peptides is 34 mm [22]. For RIT of smaller tumors, ^{90}Y is less suitable. At present, RIT is mostly studied in patients with recurrent or refractory lymphoma. ^{90}Y is a good choice, given the tumor size in this patient population. However, in patients with minimal residual disease receiving consolidation therapy, ^{177}Lu could be a better choice than ^{90}Y. In this experiment, uptake of ^{177}Lu in normal organs, such as spleen, liver, and kidneys, was highest compared with the other radionuclides, although this observation was not reported by others. This observation does not prove that absorbed doses in the organs mentioned will be higher, but attention should be paid to absorbed doses in normal organs in future RIT trials in patients. Looking at the favorable physical properties of ^{177}Lu, ^{67}Cu would be a suitable alternative radiometal that could be used for RIT of lymphoma. Studies in mice and patients with lymphoma showed that the use of ^{67}Cu-labeled anti-lymphoma mAb Lym-1 is more preferable than the use of ^{131}I-labeled Lym-1 [20,21]. Because of the high costs and sporadic production, ^{67}Cu was not included in our study, although a direct comparison of this radionuclide with ^{177}Lu and ^{90}Y would be very interesting.

Uptake in the bone of ^{177}Lu was as high as the bone accretion of ^{88}Y, suggesting that both radiometals are incorporated into the mineral bone to the same extent. This property could be disadvantageous for RIT. The bone marrow is the dose-limiting organ when giving non-myeloablative RIT. Incorporation of unbound radiometals in the bones could result in higher absorbed doses in the bone marrow, limiting the maximum activity dose of the radiolabeled antibody preparations that can be administered safely. A factor that might have influenced the uptake in the bone is the chelator used. The effect of the chelator was investigated by Govindan *et al.* in athymic mice with Ramos lymphoma xenografts; hLL2 was labeled with ^{88}Y using either benzyl-DTPA or 1,4,7,10-tetraazacyclododecane-N,N′,N″,N‴-tetraacetic acid (DOTA) [23]. Biodistributions of ^{88}Y-benzyl-DTPA-hLL2 and ^{88}Y-DOTA-hLL2 were comparable, except for the uptake in the bone, which was higher when benzyl-DTPA was used as a chelator [23]. This observation was even more pronounced in the recently published study,

comparing ^{88}Y-2-(4-isothiocyanatobenzyl)-6-methyl-DTPA-hLL2 with ^{88}Y-DOTA-hLL2 in the same animal model [24]. Up to 4-fold more yttrium was present in the bones after 7 and 10 days p.i. when using the former radiopharmaceutical, compared to the latter [24]. DeNardo *et al.* presented data concordant with these findings. Both ^{67}Cu and ^{90}Y did not show increased bone uptake when a macrocyclic chelator was used to label Lym-1, which was the case when DTPA was used as a chelator [19]. Therefore, the use of DOTA-hLL2 seems preferable in the clinical situation.

^{186}Re is not incorporated in mineral bone, and thus *in vivo* release of ^{186}Re does not cause enhanced radiation doses to the bone marrow. Although the physical characteristics of ^{186}Re seem to be ideal for RIT of lymphoma and despite the fact that unbound ^{186}Re is rapidly excreted mainly via urine, the uptake in tumors appears to be lower when compared to ^{90}Y- and ^{177}Lu-hLL2. This observation is in line with the results of Steffens *et al.* comparing ^{186}Re with ^{111}In and ^{125}I in combination with G250 in a renal cell carcinoma mouse model [25]. Shih *et al.* also concluded that upon internalization, ^{186}Re has relatively poor intracellular retention [26]. Although the clinical results with ^{186}Re-hLL2 are promising [9], it is suggested by the present study that ^{90}Y-hLL2 might be a better choice.

The clinical relevance of biodistribution studies and dosimetric analysis in animal models should not be overestimated. Although this study suggests that the combination of ^{90}Y or ^{177}Lu and hLL2 might be preferable, it remains to be demonstrated that clinical responses will be better when using these radionuclides, since there is no obvious difference in the therapeutic efficacy of ^{131}I-tositumomab as compared to ^{90}Y-ibritumomab, both targeting the same CD20 antigen. Response rates ranging from 60 to 80% have been obtained in comparable patient populations with both preparations [4, 27]. Other factors, such as (i) the way the radiolabeled antibody is handled *in vivo*, (ii) the chelator that is used, and (iii) the extent of myelotoxicity in a group of patients who have received prior myelosuppressive chemotherapy, are probably as important in determining the antitumor efficacy of radiolabeled antibody preparations.

In conclusion, although ^{186}Re has advantages over the radiometals ^{177}Lu and ^{90}Y when labeled to hLL2, the latter two display the most favorable tumor uptake. Like other studies, this investigation confirms that the biodistribution and tumor uptake of ^{131}I-hLL2 are the least suitable for this purpose.

Acknowledgments

This study was conducted with support of The Netherlands Organization for Health Research and Development (ZonMw), project # 920-03-073.

References

1. Postema EJ, Boerman OC, Oyen WJG, Raemaekers JMM, Corstens FHM. Radioimmunotherapy of B-cell non-Hodgkin's lymphoma. *Eur J Nucl Med* 2001; 28: 1725-1735.

2. Goldenberg DM. The role of radiolabeled antibodies in the treatment of non-Hodgkin's lymphoma: the coming of age of radioimmunotherapy. *Crit Rev Oncol Hematol* 2001; 39: 195-201.

3. Wagner HN, Jr, Wiseman GA, Marcus CS, Nabi HA, Nagle CE, Fink-Bennett DM, Lamonica DM, Conti PS. Administration guidelines for radioimmunotherapy of non-Hodgkin's lymphoma with ^{90}Y-labeled anti-CD20 monoclonal antibody. *J Nucl Med* 2002; 43: 267-272.

4. Leonard JP, Frenette G, Dillman RO, Gregory SA. Interim safety and efficacy results of Bexxar™ in a large multicenter expanded access study. *Blood* 2001; 98: 133a.

5. van Horssen PJ. General introduction: CD22-immunotoxins in treatment of B-cell leukaemias and lymphomas. *CD22-recombinant ricin A immunotoxin activity against malignant B-cells.* Katholieke Universiteit Nijmegen, Nijmegen 1999: 9-24.

6. Shih LB, Lu HHZ, Xuan H, Goldenberg DM. Internalization and intracellular processing of an anti-B-cell lymphoma monoclonal antibody, LL2. *Int J Cancer* 1994; 56: 538-545.

7. Pawlak-Byczkowska EJ, Hansen HJ, Dion AS, Goldenberg DM. Two new monoclonal antibodies, EPB-1 and EPB-2, reactive with human lymphoma. *Cancer Res* 1989; 49: 4568-4577.

8. Lindén O, Tennvall J, Cavallin-Ståhl E, Lindner KJ, Darte L, Ohlsson T, Hindorf C, Wingårdh K, Strand SE. A phase I/II trial with ^{90}Y hLL2 in recurrent B-cell lymphomas. Preliminary results. *Cancer Biother Radiopharm* 2000; 15: 413.

9. Postema EJ, Mandigers CMPW, Oyen WJG, Raemaekers JMM, Goldenberg DM, van Dongen GAMS, Corstens FHM, Boerman OC. Final results of a phase I radioimmunotherapy trial using ^{186}Re-epratuzumab for the treatment of patients with non-Hodgkin's lymphoma. *Cancer Biother Radiopharm* 2002; 17: 491.

10. Sharkey RM, Behr TM, Mattes MJ, Stein R, Griffiths GL, Shih LB, Hansen HJ, Blumenthal RD , Dunn RM, Juweid ME, Goldenberg DM. Advantage of residualizing radiolabels for an internalizing antibody against the B-cell lymphoma antigen, CD22. *Cancer Immunol Immunother* 1997; 44: 179-188.

11. Juweid ME, Stadtmauer E, Hajjar G, Sharkey RM, Suleiman S, Luger S, Swayne LC, Alavi A, Goldenberg DM. Pharmacokinetics, dosimetry, and initial therapeutic results with ^{131}I- and ^{111}In-/^{90}Y-labeled humanized LL2 anti-CD22 monoclonal antibody in patients with relapsed, refractory non-Hodgkin's lymphoma. *Clin Cancer Res* 1999; 5: 3292s-3303s.

12. Manders JMB, Postema EJ, Corstens FHM, Boerman OC. Enhancing tumor implantation and growth rate of Ramos B-cell lymphoma in nude mice. *Comp Med* 2002; 52: 36-38.

13. Fraker PJ, Speck JC, Jr. Protein and cell membrane iodinations with a sparingly soluble chloroamide, 1,3,4,6-tetrachloro-3a,6a-diphrenylglycoluril. *Biochem Biophys Res Commun* 1978; 80: 849-857.

14. Esteban JM, Schlom J, Gansow OA, Atcher RW, Brechbiel MW, Simpson DE, Colcher D. New method for the chelation of indium-111 to monoclonal antibodies: biodistribution and imaging of athymic mice bearing human colon carcinoma xenografts. *J Nucl Med* 1987; 28: 861-870.

15. Visser GWM, Gerretsen M, Herscheid JDM, Snow GB, van Dongen GAMS. Labeling of monoclonal antibodies with rhenium-186 using the MAG3 chelate for radioimmunotherapy of cancer: a technical protocol. *J Nucl Med* 1993; 34: 1953-1963.

16. Stein R, Govindan SV, Chen S, Reed L, Richel H, Griffiths GL, Hansen HJ, Goldenberg DM. Radioimmunotherapy of a human lung cancer xenograft with monoclonal antibody RS7: evaluation of ^{177}Lu and comparison of its efficacy with that of ^{90}Y and residualizing ^{131}I. *J Nucl Med* 2001; 42: 967-974.

17. Mattes MJ, Shih LB, Govindan SV, Sharkey RM, Ong GL, Xuan H, Goldenberg DM. The advantage of residualizing radiolabels for targeting B-cell lymphomas with a radiolabeled anti-CD22 monoclonal antibody. *Int J Cancer* 1997; 71: 429-435.

18. Stein R, Goldenberg DM, Thorpe SR, Basu A, Mattes MJ. Effects of radiolabeling monoclonal antibodies with a residualizing iodine radiolabel on the accretion of radioisotope in tumors. *Cancer Res* 1995; 55: 3132-3139.

19. DeNardo GL, DeNardo SJ, Meares CF, Kukis D, Diril H, McCall MJ, Adams GP, Mausner LF, Moody DC, Deshpande SV. Pharmacokinetics of copper-67 conjugated Lym-1, a potential therapeutic radioimmunoconjugate, in mice and in patients with lymphoma. *Antibody ImmunoConj Radiopharm* 1991; 4: 777-785.

20. DeNardo GL, Kukis DL, Shen S, DeNardo DA, Meares CF, DeNardo SJ. ^{67}Cu- *versus* ^{131}I-labeled Lym-1 antibody: comparative pharmacokinetics and dosimetry in patients with non-Hodgkin's lymphoma. *Clin Cancer Res* 1999; 5: 533-541.

21. DeNardo GL, DeNardo SJ, O'Donnell RT, Kroger LA, Kukis DL, Meares CF, Goldstein DS, Shen S. Are radiometal-labeled antibodies better than iodine-131-labeled antibodies: comparative pharmacokinetics and dosimetry of copper-67-, iodine-131-, and yttrium-90-labeled Lym-1 antibody in patients with non- Hodgkin's lymphoma. *Clin Lymphoma* 2000; 1: 118-126.

22. de Jong M, Breeman WAP, Bernard BF, Bakker WH, Visser TJ, Kooij PPM, van Gameren A, Krenning EP. Tumor response after [^{90}Y-DOTA^{0},Tyr^{3}]octreotide radionuclide therapy in a transplantable rat tumor model is dependent on tumor size. *J Nucl Med* 2001; 42: 1841-1846.

23. Govindan SV, Shih LB, Goldenberg DM, Sharkey RM, Karacay H, Donnelly JE, Losman MJ, Hansen HJ, Griffiths GL. ^{90}Yttrium-labeled complementarity-determining-region-grafted monoclonal antibodies for radioimmunotherapy: radiolabeling and animal biodistribution studies. *Bioconjug Chem* 1998; 9: 773-782.

24. Griffiths GL, Govindan SV, Sharkey RM, Fisher DR, Goldenberg DM. ^{90}Y-DOTA-hLL2: an agent for radioimmunotherapy of non-Hodgkin's lymphoma. *J Nucl Med* 2003; 44: 77-84.

25. Steffens MG, Kranenborg MHGC , Boerman OC, Zegwaart-Hagemeier NEM, Debruyne FMJ, Corstens FHM, Oosterwijk E. Tumor retention of ^{186}Re-MAG3, ^{111}In-DTPA and ^{125}I labeled monoclonal antibody G250 in nude mice with renal cell carcinoma xenografts. *Cancer Biother Radiopharm* 1998; 13: 133-139.

26. Shih LB, Thorpe SR, Griffiths GL, Diril H, Ong GL, Hansen HJ, Goldenberg DM, Mattes MJ. The processing and fate of antibodies and their radiolabels bound to the surface of tumor cells in vitro: a comparison of nine radiolabels. *J Nucl Med* 1994; 35: 899- 908.

27. Witzig TE. Radioimmunotherapy for patients with relapsed B-cell non-Hodgkin lymphoma. *Cancer Chemother Pharmacol* 2001; 48 Suppl 1: S91-S95.

Chapter 4

Final results of a phase I radioimmunotherapy trial using ^{186}Re-epratuzumab for the treatment of patients with non-Hodgkin's lymphoma

Ernst J. Postema
John M.M. Raemaekers
Wim J.G. Oyen
Otto C. Boerman
Caroline M.P.W. Mandigers
David M. Goldenberg
Guus A.M.S. van Dongen
Frans H.M. Corstens

Clinical Cancer Research 2003; 9: 3995s-4002s

Abstract

Purpose: Radioimmunotherapy (RIT) is an effective, new treatment modality for non-Hodgkin's lymphoma (NHL). The aim of this study was to determine the maximum tolerated dose and a first impression of the therapeutic potential of ^{186}Re-epratuzumab in patients with NHL.

Experimental Design: Patients with relapsed or refractory CD22-positive NHL of diverse histopathology and prior treatments received ^{99m}Tc-labeled epratuzumab (anti-CD22 IgG1), followed by RIT with ^{186}Re-epratuzumab 1 week later. Dose escalation of RIT was started at 0.5 GBq/m^2. Three patients were entered per dose level. If no dose-limiting toxicity occurred, the dose was increased by 0.5 GBq/m^2; otherwise three additional patients were included on that dose level.

Results: A total of 18 patients received a diagnostic dose of ^{99m}Tc-epratuzumab. Fifteen patients were actually treated with ^{186}Re-epratuzumab at four different dose levels, 0.5, 1.0, 1.5, and 2.0 GBq/m^2. During or after infusion of ^{186}Re-epratuzumab, no adverse reactions were seen. In all patients, a transient decrease of leukocyte and platelet levels was observed 1 month after treatment. At the 1.5-GBq/m^2 dose level, one grade 4 hematological toxicity was observed. At the highest dose level of 2 GBq/m^2, no grade 4 hematological toxicity was seen, but WBC and platelet counts of two of the three patients did not recover completely. One patient had a complete remission lasting 4 months. Four patients had a partial response, lasting 3, 3, 6, and 14 months, respectively. Four patients had stable disease for 3, 3, 7, and 9 months, respectively.

Conclusions: ^{186}Re-epratuzumab at a dose of 2.0 GBq/m^2 is well tolerated without major toxicity. A single dose of ^{186}Re-epratuzumab led to objective responses in 5 of 15 treated patients.

Introduction

In the last decade, radioimmunotherapy (RIT) has become a rather successful treatment modality for patients with refractory or relapsed non-Hodgkin's lymphoma (NHL) [1,2]. Several phase I/II studies with ^{131}I- or ^{90}Y-labeled monoclonal antibodies (mAbs) have shown promising therapeutic results. One radiolabeled antibody, ^{90}Y-labeled ibritumomab, has been approved recently for commercialization by the United States Food and Drug Administration after a successful randomized phase III trial [3–5]. In this study, radiolabeled antibody treatment was shown to be significantly more effective than treatment with unlabeled antibodies alone [5]. The two currently most widely studied and used mAbs are the murine

anti-CD20 antibodies, ibritumomab and tositumomab. Although study results confirm the enormous potential of these new drugs against NHL, they both have the disadvantage of being murine antibodies. The use of murine mAbs could induce the formation of human anti-mouse antibodies (HAMAs), eventually preventing repeated treatment with this radiopharmaceutical Therefore, the use of chimeric or, preferably, humanized antibodies is desirable.

Another important issue in RIT is the choice of the radionuclide to be used. Both ^{90}Y and ^{131}I are widely used in RIT. ^{131}I could be disadvantageous, however, because it emits high-energy, high-abundance γ-rays, requiring hospitalization of treated patients for radiation safety reasons. It also emits low-energy β-radiation with a limited penetration range in tissue, which could also be disadvantageous when treating patients with bulky disease ^{90}Y emits high-energy β-radiation but lacks γ-emissions, prohibiting scintigraphic evaluation after treatment. Rhenium-186 (^{186}Re) has ideal physical characteristics for RIT. It has medium-energy β-emissions and low-abundance γ-photons with ideal energy (137 keV) for scintigraphic imaging.

In this study, the humanized anti-CD22 mAb epratuzumab was used, which is also being investigated as an unlabeled mAb as well as a mAb labeled with the radionuclides ^{131}I and ^{90}Y. The aim of the study was to determine the safety and the maximum tolerated dose (MTD) of RIT using epratuzumab labeled with ^{186}Re.

Materials and methods

Patient population

This dose-escalation study was performed in patients with B-cell NHL who had relapsed after or did not respond to at least one line of treatment and who were not eligible for potentially curative high-dose chemotherapy followed by stem cell support. All patients had histologically proven, CD22-positive NHL. Patients had to have a life expectancy of at least 2 months and had to be at least 18 years of age. Patients had to have a WHO performance status of 0, 1, or 2 No other antitumor therapy should be given within at least 3 weeks before study entry. WBC count had to be at least 2.5×10^9/l, and platelet count had to be at least 75×10^9/l Patients were excluded in case of life-threatening infection, allergic diathesis with current complaints, organ failure, pregnancy, known seropositivity for HIV, > 25% bone marrow involvement by lymphoma as determined by bone marrow histology and histochemistry, concomitant treatment with other

investigational drugs, or spread of the malignancy to the central nervous system. The study was approved by the institutional review board of the University Medical Center Nijmegen. Written informed consent was obtained from all patients.

Antibody

Epratuzumab (hLL2) is a humanized monoclonal IgG1 antibody directed against CD22 on B cells [6]. CD22 is expressed in the cytoplasm of early pre-B and progenitor cells and appears on the surface of mature B cells. The CD22 antigen is broadly expressed on both normal and malignant B cells, with a distribution comparable to that of CD20, although antigen density may be more variable [7]. Unlabeled epratuzumab is used in clinical trials in chemotherapy-refractory NHL patients [8] and in combination with rituximab [9]. Initial data of the phase I/II dose-escalation study show that the lowest dose level at which objective responses were seen was the dose level with four weekly infusions of 240 mg/m^2 epratuzumab [8]. Epratuzumab was kindly provided by Immunomedics, Inc. (Morris Plains, NJ) as a sterile pyrogen-free solution.

Labeling

Epratuzumab was labeled with ^{99m}Tc using mercaptoacetyltriglycine (MAG3) as a chelator according to the method described by Visser *et al.* [10]. A preparation with a specific activity of 100 MBq/mg was prepared. Patients received 750 MBq of ^{99m}Tc-MAG3-epratuzumab. The protein dose of the preparation was adjusted to 0.5 mg/kg body weight with unlabeled epratuzumab.

^{186}Re-epratuzumab was prepared according to the same method [10]. Again, the protein dose of the preparation was adjusted to 0.5 mg/kg body weight by adding unlabeled epratuzumab to the radiolabeled preparation.

Protocol

Pretherapy evaluation consisted of history, physical examination, blood sampling for hematological and biochemical analysis, bone marrow histology and cytology, and computed tomography of the chest and abdomen. After inclusion, a diagnostic dose of 750 MBq of ^{99m}Tc-epratuzumab was administered i.v. over 45 min. One week after this diagnostic procedure, the patient was hospitalized overnight for RIT with ^{186}Re-epratuzumab. The infusion time of ^{186}Re-labeled epratuzumab was also 45 min. The

starting dose level was 0.5 GBq/m^2 body surface area. If no dose-limiting toxicity occurred (*i.e.*, no grade 3 or 4 non-hematological toxicity and no grade 4 hematological toxicity according to the National Cancer Institute Common Toxicity Criteria 2.0) in consecutive patients, the dose level was escalated by 0.5 GBq/m^2. Three patients were included at each dose level. If dose-limiting toxicity was observed in one patient at a specific dose level, three additional patients were treated at that same dose level. In case of dose-limiting toxicity in two or more patients at a particular dose level, the dose level below that level would be considered the MTD. Patients were monitored weekly for adverse reactions and toxicity. Patients were evaluated for responses 4–6 weeks after RIT, using physical examination, biochemical analysis, computed tomography scanning, and bone marrow examination, as far as involved at the start. In case of stable disease (SD) or responses, this procedure was repeated every 3 months thereafter.

Pharmacokinetics

Blood samples for pharmacokinetics were taken 10 min, 30 min, and 1, 2, 3, 4, and 24 h after injection of the diagnostic dose of ^{99m}Tc-epratuzumab. After RIT, blood samples were taken at the same time points and additionally after 2, 5, 7, and 14 days. mAb blood clearance rates were determined by counting the samples in a shielded well-type counter. The plasma clearance of ^{99m}Tc-epratuzumab was fit to a monoexponential function, and the blood clearance of ^{186}Re-epratuzumab was fit to a biexponential function. On the basis of these curves, $T_{1/2}$ (the time point when 50% of the activity was cleared from the circulation), $T_{1/2,\alpha}$ (representing the distribution phase), and $T_{1/2,\beta}$ (representing the elimination phase) were calculated.

HAHA analysis

Serum samples for human anti-human antibody (HAHA) analysis were obtained before the infusion with ^{99m}Tc-epratuzumab, before the infusion with ^{186}Re-epratuzumab, and 7, 14, 28, and 56 days after treatment. An ELISA performed by Immunomedics, Inc. was used to assess human anti-hLL2 antibodies. Results were reported as a number (in ng/ml) or as undetected (< 1 ng/ml). Levels above 50 ng/ml are considered to be elevated (results from Immunomedics, Inc.).

Scintigraphy

One hour and 1 day after injection of the diagnostic dose, a whole body scan was made with a double-head gamma camera (Siemens Multispect 2; Siemens Medical Solutions USA, Inc., Hoffmann Estates, IL) equipped with low-energy, high-resolution collimators. Scintigraphy after RIT was performed 1 h, 1 day, 2 days, and 5 days postinjection at a speed of 5 cm/min.

Dosimetry

Scans made after RIT were used for dosimetric analysis. Regions of interest (ROIs) were drawn around the whole body, heart, right lung, liver, spleen, left kidney, and testes. Background regions were drawn adjacent to these ROIs. Using the counts in the ROIs, corrected for background, residence times in the organs as listed above were estimated. These residence times were entered in MIRDOSE3, version 3.1 (Oak Ridge Associated Universities, Oak Ridge, TN) to calculate absorbed doses. For males, the adult phantom was used; for females, the adult female phantom was used. The absorbed dose in the bone marrow was calculated using the blood-derived method as described by Shen *et al.* [11].

Results

Patient characteristics

Eighteen patients (12 men and 6 women) were included, 15 of whom were actually treated. The mean age was 57 years (range, 41–75 years). Patient characteristics are listed in Table 4.1. The number of courses of chemotherapy and/or external beam radiation before inclusion in our study ranged from 1–7, with a median number of 4. Of these patients, three had had high-dose chemotherapy followed by autologous peripheral stem cell transplantation. Three patients were not treated with ^{186}Re-epratuzumab because of unfavorable biodistribution (n = 2), as described in "Scintigraphy" and because of an acute allergic reaction to the first, diagnostic infusion (n = 1), as described in "Toxicity" section. Patients were treated at four different dose levels, 0.5 GBq/m^2 (n = 3), 1.0 GBq/m^2 (n = 3), 1.5 GBq/m^2 (n = 6), and 2.0 GBq/m^2 (n = 3).

Toxicity

During or directly after infusion of the diagnostic dose of 750 MBq of ^{99m}Tc-epratuzumab, fever and chills were observed in 9 of 18 patients

within 1 h after infusion. This reaction was self-limiting and required no specific medical intervention. Chills lasted 30–45 min, whereas the fever lasted several hours. One patient experienced an acute allergic reaction with airway obstruction within half an hour after infusion, for which administration of clemastine and prednisolone and inhalation of albuterol and ipratropium were required. One patient had slight dyspnea during infusion, which diminished after stopping the infusion. After restart of the infusion at half speed, the dyspnea did not recur. Two patients had a vasovagal episode after infusion. Finally, one patient had herpetiform lesions on the left lower arm 1 week after the diagnostic infusion. During infusion of the therapeutic dose of ^{186}Re-epratuzumab, no clinical adverse reactions were seen in any of the patients. Within 1 h after infusion, fever was observed in only two patients. In all patients, platelet and leukocyte levels decreased 4–6 weeks after the therapeutic injection. The nadirs are listed in Table 4.1.

Patient		Age	Known with NHL for	No. of		Dose level	Nadir platelets	Nadir WBC		Duration
No.	Sex	(yrs)	(yrs)	pretreatments	Histology	(MBq/m^2)	($\times 10^9$/liter)	($\times 10^9$/liter)	Response[a]	(days)
1	M	51	1.7	3	Mantle cell lymphoma	500	81	2.2	SD	272
2	F	59	6.5	7	Follicle center cell lymphoma	500	98	1.0	PD	
3	F	57	10	4	Follicle center cell lymphoma	500	190[b]	4.7[b]	PD	
4	M	66	5.5	4	Diffuse large B-cell lymphoma	1000	57	2.2	CR	132
5	F	67	10	5	Small lymphocytic lymphoma	1000	87	3.5	SD	210
6	M	50	6	4	Follicle center cell lymphoma	1000	76	1.9	PR	84
7	M	41	2.3	3	Diffuse large B-cell lymphoma	1500	32	0.5	PD	
8	M	57	8	4	Small lymphocytic lymphoma	0	NA	NA	NA	
9	M	55	2.7	1	Mantle cell lymphoma	1500	16	3.1	PR	95
10	M	69	3.0	4	Marginal zone B-cell lymphoma	1500	21	8.4	SD	85
11	M	43	5.0	4	Follicle center cell lymphoma	1500	64	5.7	SD	90
12	F	61	7	5[c]	Follicle center cell lymphoma	1500	107	2.6	PD	
13	M	75	1.1	2	Mantle cell lymphoma	1500	162[b]	2.7	PD	
14	M	49	1.9	5[c]	Diffuse large B-cell lymphoma	2000	33	2.7	PD	
15	F	41	4.0	4[c]	Follicle center cell lymphoma	2000	25	2.2	PR	198
16	M	68	2.5	1	Mantle cell lymphoma	0	NA	NA	NA	
17	F	45	3.8	6	Marginal zone lymphoma	0	NA	NA	NA	
18	M	72	0.5	1	Diffuse large B-cell lymphoma	2000	102	3.5	PR	425

[a] PD, progressive disease; CR, complete response; NA, not applicable.

[b] No real nadir was observed: blood counts increased following therapy.

[c] One of the pretreatments consisted of autologous peripheral stem cell transplantation.

Table 4.1: Patient characteristics and therapeutic effects

Figures 4.1 and 4.2 depict the platelet and WBC count, respectively, over time. In only one patient was a grade 4 hematological toxicity observed (WBC of 0.5×10^9/l) 6 weeks postinfusion of 1.5 GBq/m^2. In patient 2 (0.5 GBq/m^2 dose level), an isolated WBC count drop was observed as early as 2 weeks after therapy and was probably caused by a viral infection. Other toxicity consisted of a facial zoster reactivation (n = 1), oral candidiasis (n = 1), and loss of taste (n = 1).

Pharmacokinetics

Elimination from the circulation of both ^{99m}Tc- and ^{186}Re-labeled epratuzumab varied widely between patients. Table 4.2 shows $T_{1/2}$, $T_{1/2,\alpha}$, and $T_{1/2,\beta}$ in all patients. The $T_{1/2,\beta}$ varied from 30.3 to 176.1 h, indicating that the antibody is circulating for a long time, as expected when using a humanized mAb. The percentage of the injected dose that was excreted via the urine is also listed in Table 4.2. Up to 45.9% of injected dose could be detected in the urine, indicating that after catabolization of the mAb, ^{186}Re-MAG3 is cleared renally.

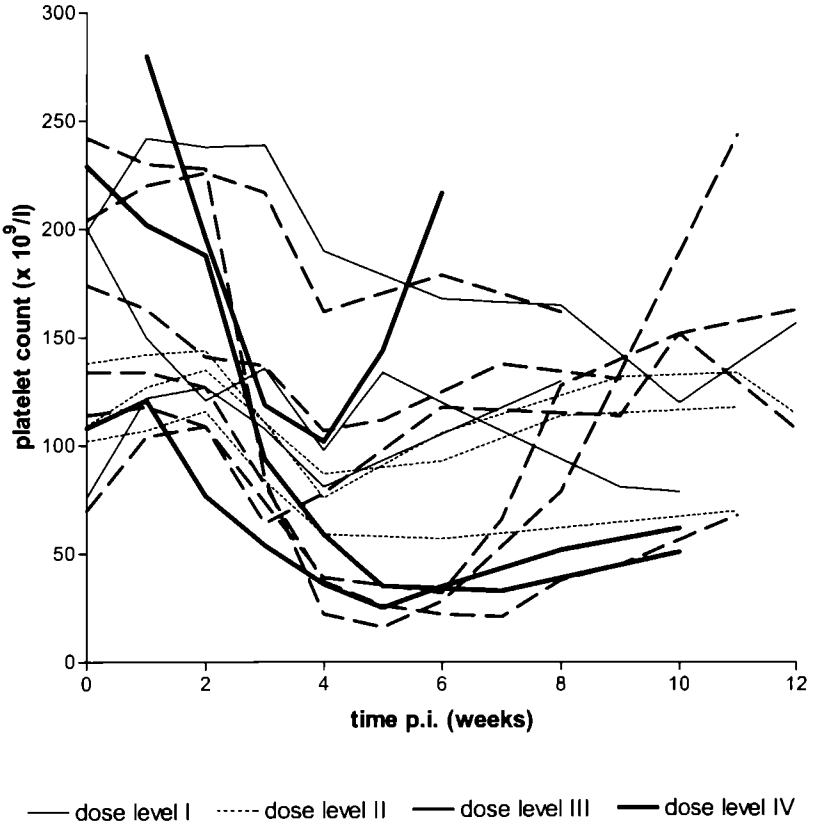

Figure 4.1: Platelet counts after RIT.

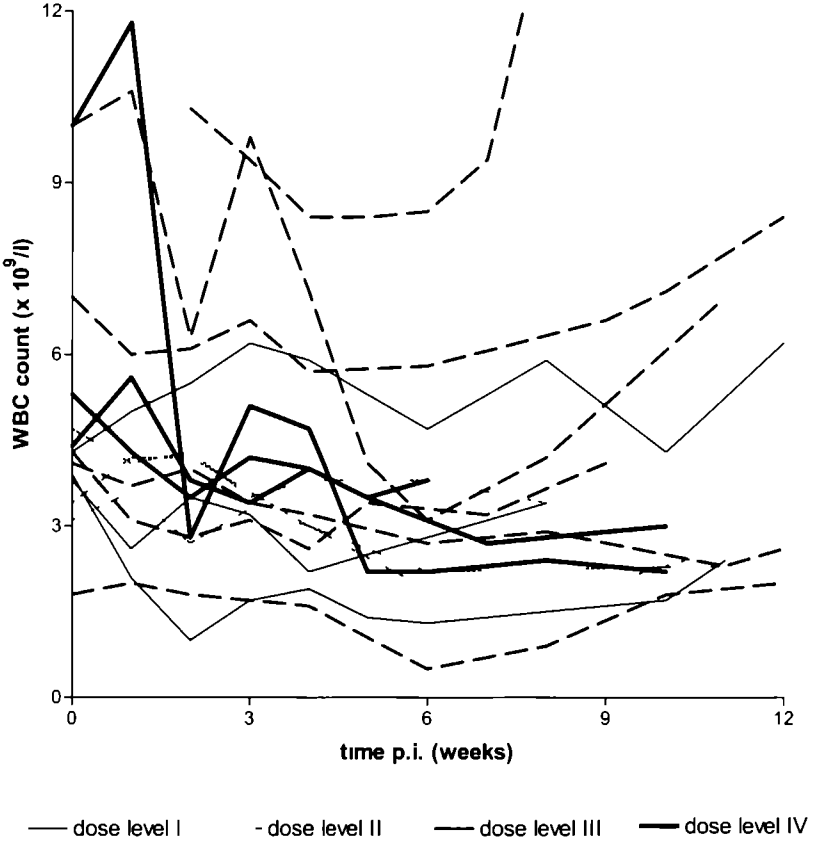

Figure 4 2 WBC counts after RIT

Patient no.	$T_{1/2}$ (in h) of ^{99m}Tc-epratuzumab	$T_{1/2,\alpha}$ (in h) of ^{186}Re-epratuzumab	$T_{1/2,\beta}$ (in h) of ^{186}Re-epratuzumab	% ID[a] in urine
1	20.68	0.69	30.34	45.9
2	28.44	3.42	31.03	27.9
3	ND	1.86	41.02	30.1
4	33.98	6.03	137.52	16.8
5	42.26	5.88	51.73	15.1
6	44.75	2.55	65.93	16.7
7	No pharmacokinetic data available			
8	10.28	NA	NA	NA
9	18.11	4.49	42.52	ND
10	30.16	1.38	63.61	21.1
11	15.61	No pharmacokinetic data available		
12	33.99	9.43	103.64	11.0
13	27.94	5.22	43.80	26.0
14	35.20	2.76	176.13	ND
15	No pharmacokinetic data available			
16	61.89	NA	NA	NA
17	30.00	NA	NA	NA
18	24.74	8.22	81.00	23.1

[a] % ID, percentage of injected dose; NA, not applicable; ND, not done

Table 4.2: Pharmacokinetic data of ^{99m}Tc- and ^{186}Re-labeled epratuzumab

HAHAs

A total of 90 samples of 18 patients were analyzed quantitatively for HAHAs. In seven patients, HAHA levels could be detected, ranging from 0.5 to 50 ng/ml. Six of these seven patients with detectable HAHAs had detectable HAHA levels before RIT. No positive HAHA results were obtained. Special attention was paid to serum samples of the patient experiencing an adverse reaction shortly after infusion of ^{99m}Tc-epratuzumab. Neither HAHA nor HAMA levels could be detected in serum samples obtained before infusion; 1, 3, and 4 h after infusion; and 1 and 9 days after infusion. There was no relation between the presence of low levels of HAHAs before treatment and the occurrence of chills and fever after the infusion of radiolabeled epratuzumab.

Scintigraphy

On scintigrams made 1 h and 1 day after injection of ^{99m}Tc-epratuzumab, mainly activity in the blood pool was observed. In some patients, lymphoma targeting was observed, as illustrated in Figure 4.3. Two patients appeared to have major bone marrow uptake after the diagnostic injection, as shown in Figure 4.4. Both patients were known to have bone marrow involvement (but < 25% involvement). Both patients were excluded from further RIT because treatment with ^{186}Re-epratuzumab could have resulted in serious and potentially irreversible myelotoxicity.

During the first days after RIT, visualization of lymphoma improved. Figure 4.5 shows scintigrams of a patient who had lymphoma localization in the inguinal regions.

Dosimetry

Doses absorbed in normal organs are listed in Table 4.3. The organ with the highest absorbed dose is the spleen because the spleen is a lymphoid organ housing CD22-positive cells and involved in NHL. All absorbed doses were far below critical values. Therefore, RIT with ^{186}Re-labeled epratuzumab is thought to be safe. Tumor dosimetry is not available yet. The dosimetric analysis will be discussed in more detail in Chapter 5.

Therapeutic effects

A summary of the therapeutic effects is listed in Table 4.1. One patient responded completely; for 4 months no lymphoma could be demonstrated. Four patients showed a partial response (PR) lasting 14, 6, 3, and 3 months,

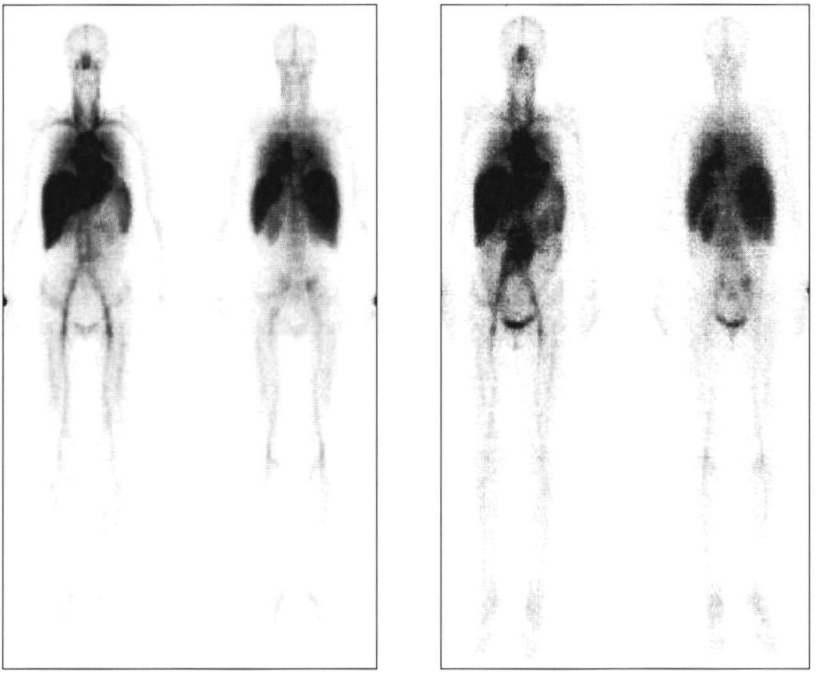

1 hour p.i. 1 day p.i.

Figure 4.3: Scintigraphy after infusion of ^{99m}Tc-epratuzumab, showing a normal biodistribution and targeting of an abdominal lymphoma.

respectively. Four patients had SD for 9, 7, 3, and 3 months, respectively, after RIT. Six patients progressed after RIT.

Discussion

The present study shows that RIT with ^{186}Re-labeled epratuzumab is safe, despite the fact that most patients were heavily pretreated before RIT. As expected, a transient decrease in blood counts was dose-limiting. Although grade 4 hematological toxicity was observed in only one patient treated at the third dose level of 1.5 GBq/m^2, the slow recovery of platelet counts in two of the three patients at the highest dose level suggests that further dose escalation was clinically unacceptable and would probably result in prolonged low blood cell counts, increasing the risk of side effects.

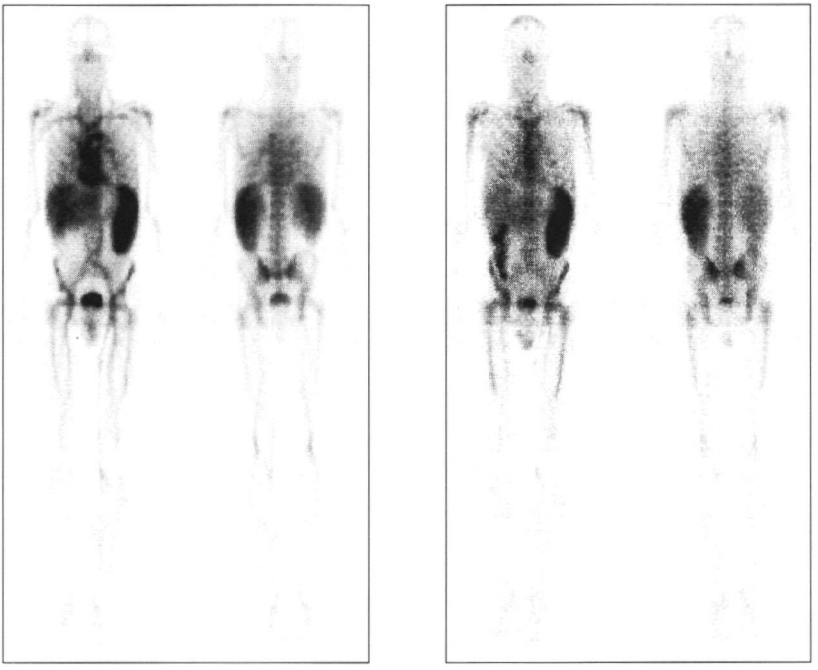

Figure 4.4: Scintigraphy after infusion of ^{99m}Tc-epratuzumab, showing unfavorable biodistribution with targeting of bone marrow and an enlarged spleen.

Platelet counts of one of the two patients recovered slowly, returning to normal within 5 months. The time to full recovery of the platelet counts of the other patient is unknown because he was treated in another hospital 12 weeks after RIT with other myelotoxic therapy. The Common Toxicity Criteria used to define toxicity did not classify prolonged cytopenia as a separate entity, although this aspect should be taken into consideration. Strictly speaking, no grade 4 toxicity was observed in the group treated at the dose level of 2.0 GBq/m^2. Therefore, a dose of 2.0 GBq/m^2 is considered to be the MTD.

The use of ^{186}Re has several advantages. First of all, being a group-VII element, ^{99m}Tc and ^{186}Re have similar chemical properties. ^{99m}Tc-labeled mAbs can therefore be used for an imaging procedure before RIT, representing ^{186}Re-labeled mAbs. The need for a diagnostic procedure was demonstrated in this study: two patients were considered to have < 25%

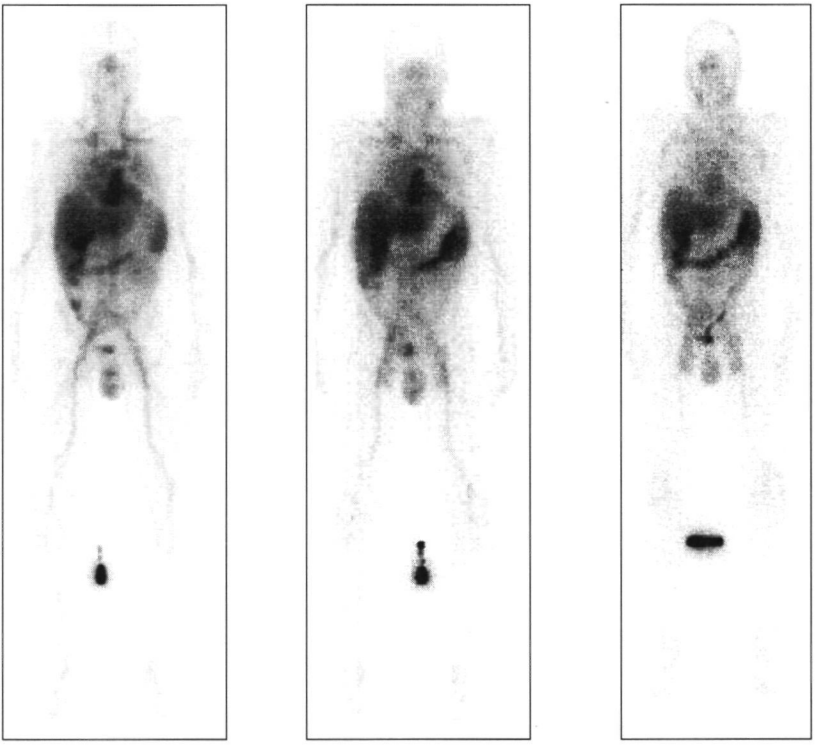

Figure 4.5: Scintigraphy after infusion of ^{186}Re-epratuzumab, showing targeting of inguinal lymphoma.

bone marrow involvement based on classical histological examination, but scintigraphy showed that uptake in the bone marrow was so extensive that RIT was contraindicated in these patients. Although taking bone marrow samples at more than one site can be advised to prevent sampling errors, a diagnostic procedure before RIT should be advocated.

A second advantage of the use of ^{186}Re is the fact that it emits low-energy, low-abundance γ-radiation. The γ-emissions are ideal for imaging, making it unnecessary to label mAbs with a second radiolabel to perform dosimetry. The quality of the images is high, comparable with the quality of images made using ^{99m}Tc. Because only 10% of disintegrations are accompanied by γ-emissions, the exposure rate after treatment is low, at

Organ	Mean absorbed doses ± standard deviation (mGy/MBq)	
	Males	Females
Red marrow	0.45 ± 0.15	0.51 ± 0.10
Lungs	0.69 ± 0.28	0.86 ± 0.19
Heart	0.64 ± 0.24	0.68 ± 0.24
Kidneys	1.29 ± 0.36	1.36 ± 0.09
Liver	0.75 ± 0.17	1.13 ± 0.31
Spleen	1.89 ± 0.93	2.33 ± 0.40

Table 4.3 Pharmacokinetic data of ^{99m}Tc and ^{186}Re-labeled epratuzumab

least lower than 5 μSv·m^2/h. In most countries, it is therefore possible to treat patients on an outpatient basis. Initial dosimetric analysis, as mentioned earlier, reveals that absorbed doses in normal organs are far below critical values. Further dosimetric analysis of the data of this study is currently in progress.

A disadvantage of the use of ^{186}Re-labeled mAbs is the laborious labeling procedure, especially when compared with the labeling of mAbs with radiometals such as ^{90}Y, ^{111}In, and ^{177}Lu . Another labeling procedure, using antibody sulfhydryl groups as effective carriers of reduced rhenium, as described by Griffiths *et al.* [12], is less laborious, but the low specific activity of this radioimmunoconjugate requires large amounts of antibodies. Moreover, the method requires extensive reduction of disulfide bridges in the antibody molecule, leading to a loss of immunoreactivity. This labeling procedure is not thought useful for preparing doses needed for RIT [12].

Another disadvantage may be the lower retention of the radiolabel ^{186}Re in the tumor when compared with ^{90}Y . Radiolabeled epratuzumab is rapidly internalized upon binding to a CD22-expressing target cell. Using radiometals such as ^{90}Y would result in retention of the radiolabel [13] Preclinical data suggest that although ^{186}Re is retained better than ^{131}I in a mouse lymphoma model, tumor uptake of ^{90}Y-labeled is significantly higher [14]. After processing of the radiolabeled mAb, ^{186}Re-MAG3 is excreted from the target cell and excreted renally, as shown in Table 4.2.

The ultimate goal of this study was to define a MTD for further analysis in a phase II study. In such a study, patients would receive repeated RIT cycles For this approach, a non-immunogenic mAb is required, such as the humanized epratuzumab. The formation of HAMAs is observed in a minority of heavily pretreated patients with NHL treated with murine anti-

CD20 mAbs [2,15]. Nevertheless, HAMA formation can be observed in over 60% of patients when treating patients more upfront with murine mAbs [16], prohibiting further treatment. When using epratuzumab, HAMA formation is not to be expected. The presence of HAHAs was determined before and after RIT with ^{186}Re-epratuzumab, showing that in six of seven patients HAHAs were already present before RIT. The levels were low, with a maximum of 50 ng/ml, in concordance with earlier observations [17], and below the threshold value for HAHA elevation in the test used. Other studies also reported that HAHA induction was hardly ever observed in patients who received epratuzumab [18,19]. Therefore, it should be feasible to repeatedly treat patients using radiolabeled epratuzumab.

In conclusion, RIT with ^{186}Re-epratuzumab is feasible and safe, with an MTD of 2.0 GBq/m^2. Even in this phase I study of refractive/relapsed patients who were heavily pretreated, objective responses were observed. A phase II study treating patients with repeated doses of radiolabeled epratuzumab is planned. Additional studies should reveal whether this approach leads to improved overall response rates, duration of responses, and survival of patients with NHL.

Acknowledgments

We thank Emile B. Koenders for assistance in administering the radiolabeled preparations and preparation of the calibration standards and pharmacokinetics samples. We also thank the referring physicians, Drs. Sinnige, Schuitemaker, Wittebol, De Vries, and Pruijt, for their close cooperation with our center in the treatment and follow-up of patients.

This study was conducted with the support of The Netherlands Organization for Health Research and Development (ZonMw), project # 920-03-073.

References

1. Postema EJ, Boerman OC, Oyen WJG, Raemaekers JMM, Corstens FHM. Radioimmunotherapy of B-cell non-Hodgkin's lymphoma. *Eur J Nucl Med* 2001; 28: 1725-1735.

2. Goldenberg DM. The role of radiolabeled antibodies in the treatment of non-Hodgkin's lymphoma: the coming of age of radioimmunotherapy. *Crit Rev Oncol Hematol* 2001; 39: 195-201.

3. Wagner HN, Jr, Wiseman GA, Marcus CS, Nabi HA, Nagle CE, Fink-Bennett DM, Lamonica DM, Conti PS. Administration guidelines for radioimmunotherapy of non-Hodgkin's lymphoma with ^{90}Y-labeled anti-CD20 monoclonal antibody. *J Nucl Med* 2002; 43: 267-272.

4. Wiseman GA, White CA, Sparks RB, Erwin WD, Podoloff DA, Lamonica D, Bartlett NL, Parker JA, Dunn WL, Spies SM, Belanger R, Witzig TE, Leigh BR. Biodistribution and dosimetry results from a phase III prospectively randomized controlled trial of Zevalin radioimmunotherapy for low-grade, follicular, or transformed B-cell non-Hodgkin's lymphoma. *Crit Rev Oncol Hematol* 2001; 39: 181-194.

5. Witzig TE, Gordon LI, Cabanillas F, Czuczman MS, Emmanouilides C, Joyce R, Bartlett NL, Wiseman GA, Grillo-López AJ, Multani P, White CA. Randomized controlled trial of yttrium-90-labeled ibritumomab tiuxetan radioimmunotherapy *versus* rituximab immunotherapy for patients with relapsed or refractory low-grade, follicular, or transformed B-cell non-Hodgkin's lymphoma. *J Clin Oncol* 2002; 20: 2453-2463.

6. Leung SO, Goldenberg DM, Dion AS, Pellegrini MC, Shevitz J, Shih LB, Hansen HJ. Construction and characterization of a humanized, internalizing, B-cell (CD22)-specific, leukemia/lymphoma antibody, LL2. *Mol Immunol* 1995; 32: 1413-1427.

7. Press OW, Leonard JP, Coiffier B, Levy R, Timmerman J. Immunotherapy of non-Hodgkin's lymphomas. *Hematology (Am Soc Hematol Educ Program)* 2001; 221-240.

8. Leonard JP, Coleman M, Schuster MW, Chadburn A, Ely S, Yagan N, Sharkey RM, Hansen HJ, Goldenberg DM. Epratuzumab, a new anti-CD22, humanized, monoclonal antibody for the therapy of non-Hodgkin's lymphoma (NHL): phase I/II trial results. *Blood* 1999; 94: 92a-93a.

9. Leonard JP, Coleman M, Matthews JC, Fiore JM, Dosik A, Shore T, Kapushoc H, Macri M, Wegener WA, Cesano A, Goldenberg DM. Epratuzumab (anti-CD22) and rituximab (anti-CD20) combination immunotherapy for non-Hodgkin's lymphoma: preliminary response data. *Proc Am Soc Clin Oncol* 2002; 21: 266a.

10. Visser GWM, Gerretsen M, Herscheid JDM, Snow GB, van Dongen GAMS. Labeling of monoclonal antibodies with rhenium-186 using

the MAG3 chelate for radioimmunotherapy of cancer: a technical protocol. *J Nucl Med* 1993; 34: 1953-1963.

11. Shen S, DeNardo GL, Sgouros G, O'Donnell RT, DeNardo SJ. Practical determination of patient-specific marrow dose using radioactivity concentration in blood and body. *J Nucl Med* 1999; 40: 2102-2106.

12. Griffiths GL, Goldenberg DM, Diril H, Hansen HJ. Technetium-99m, rhenium-186, and rhenium-188 direct-labeled antibodies. *Cancer* 1994; 73: 761-768.

13. Sharkey RM, Behr TM, Mattes MJ, Stein R, Griffiths GL, Shih LB, Hansen HJ, Blumenthal RD , Dunn RM, Juweid ME, Goldenberg DM. Advantage of residualizing radiolabels for an internalizing antibody against the B-cell lymphoma antigen, CD22. *Cancer Immunol Immunother* 1997; 44: 179-188.

14. Postema EJ, Frielink C, Oyen WJG, Raemaekers JMM, Goldenberg DM, Corstens FHM, Boerman OC. Biodistribution of ^{131}I-, ^{186}Re-, ^{177}Lu-, and ^{88}Y-labeled hLL2 (epratuzumab) in nude mice with CD22-positive lymphoma. *Cancer Biother Radiopharm* 2003; 18: 525-533.

15. Witzig TE. Radioimmunotherapy for patients with relapsed B-cell non-Hodgkin lymphoma. *Cancer Chemother Pharmacol* 2001; 48 Suppl 1: S91-S95.

16. Kaminski MS, Estes J, Tuck M, Mann J, Fisher S, Kison P, Regan D, Stagg R, Kroll SM, Magnuson DE, Wahl RL. Iodine I 131 tositumomab therapy for previously untreated follicular lymphoma. *Proc Am Soc Clin Oncol* 2000; 19: abstract 11.

17. Juweid ME, Stadtmauer E, Hajjar G, Sharkey RM, Suleiman S, Luger S, Swayne LC, Alavi A, Goldenberg DM. Pharmacokinetics, dosimetry, and initial therapeutic results with ^{131}I- and ^{111}In-/^{90}Y-labeled humanized LL2 anti-CD22 monoclonal antibody in patients with relapsed, refractory non-Hodgkin's lymphoma. *Clin Cancer Res* 1999; 5: 3292s-3303s.

18. Behr TM, Wormann B, Gramatzki M, Riggert J, Gratz S, Béhé M, Griesinger F, Sharkey RM, Kolb H-J, Hiddemann W, Goldenberg DM, Becker W. Low- *versus* high-dose radioimmunotherapy with humanized anti-CD22 or chimeric anti-CD20 antibodies in a broad spectrum of B cell-associated malignancies. *Clin Cancer Res* 1999; 5: 3304s-3314s.

19. Lindén O, Cavallin-Ståhl E, Strand SE, Hindorf C, Tennvall J, Stenberg L, Ohlsson T, Darte L. 90-Yttrium-epratuzumab in patients with B-cell lymphoma failing chemotherapy, using a dose fractionated schedule. *Cancer Biother Radiopharm* 2002; 17: 490.

Chapter 5

Dosimetric analysis of radioimmunotherapy with ^{186}Re-epratuzumab

Ernst J. Postema
Wilhelmina C.A.M. Buijs
Michel de Groot
John M.M. Raemaekers
Otto C. Boerman
David M. Goldenberg
Frans H.M. Corstens
Wim J.G. Oyen

Presented at the *50th Annual Meeting of the Society of Nuclear Medicine*, June 21-25, 2003, New Orleans, LA
Journal of Nuclear Medicine 2003; 44: 32P-33P

Abstract

Objective: Radioimmunotherapy (RIT) is an effective treatment modality for non-Hodgkin's lymphoma (NHL). In our center, ^{186}Re-epratuzumab has been used for this purpose in a phase I dose-escalation study. The primary aim of this study was to assess the maximum tolerated dose (MTD) and safety of ^{186}Re-epratuzumab in patients with NHL. This article describes the dosimetric analysis of RIT using ^{186}Re-labeled epratuzumab in a phase I study in patients with refractory or relapsed NHL, in relation to safety and toxicity of this treatment modality.

Methods: Patients with relapsed or refractory CD22-positive NHL received ^{99m}Tc-labeled epratuzumab (anti-CD22 IgG; Immunomedics, Inc., Morris Plains, NJ), followed by RIT with ^{186}Re-epratuzumab 1 week later. A total of 15 patients were treated with i.v. doses of 0.5, 1 0, 1.5, or 2.0 GBq/m^2. Whole body scintigraphy was acquired directly after, and at 1, 2, and 5 days following RIT. Regions of interest were drawn around normal organs to estimate residence times.

Results: During or after infusion of ^{186}Re-epratuzumab, no adverse reactions were seen. Dose limiting toxicity consisted of transient leuko- and thrombocytopenia. MTD was established at 2.0 GBq/m^2. One patient had a complete remission lasting 4 months, and 4 patients had a partial response, lasting 3, 3, 6, and 14 months, respectively. Thirteen (9 males, 4 females) of 15 patient studies could be used for dosimetric analysis. The absorbed dose in the spleen, an organ often involved in NHL, was highest, with a mean of 1.89 ± 0.93 mGy/MBq for males and 2.33 ± 0.40 mGy/MBq for females All absorbed doses were within safe ranges. No correlation could be found between toxicity observed and the absorbed doses.

Conclusion: RIT with ^{186}Re-epratuzumab seems to be safe, and even at lower activity dosages, therapeutic responses were observed. Dosimetric analysis did not reveal high absorbed doses to normal organs.

Introduction

Radioimmunotherapy (RIT) of non-Hodgkin's lymphoma (NHL) is a successful new treatment option [1,2]. Toxicity due to this therapeutic approach consists mainly of transient hematological toxicity when low dosages of radioactivity are used, whereas cardiopulmonary toxicity is dose-limiting in myeloablative RIT [3]. Dosimetry is the tool used to estimate absorbed doses to normal organs, in order to explain or to predict toxicity. In some cases, when using ^{131}I-labeled monoclonal antibodies (mAbs), dosimetry is even used to determine the amounts of activity to be

administered [4]. Other studies, describing the use of ^{90}Y-labeled mAbs, showed that dosimetry neither correlated with the toxicity observed, nor is needed to safely dose and administer radioactive mAbs [5,6].

In the present study, ^{186}Re-labeled mAbs were used to treat patients with NHL. ^{186}Re decays by both β- and γ-emission. The mean energy of both β-emissions is 362 keV (71% of disintegrations) and 309 keV (22%), respectively. The low-energy (137 keV), low-abundance (10%) γ-radiation is ideal for scintigraphy to be used for dosimetric analysis It also permits treatment on an outpatient basis, even at high doses, according to Dutch regulations.

This paper describes the dosimetric analysis of RIT using ^{186}Re-labeled epratuzumab in a phase I study in patients with refractory or relapsed NHL, in relation to safety and toxicity of this treatment modality.

Materials and methods

Patient eligibility

This dose-escalation study was conducted in patients with B-cell NHL who had relapsed after or did not respond to at least one line of treatment and who were not eligible for potentially curative high-dose chemotherapy followed by stem cell support. All patients had histologically-proven, CD22-positive, NHL. Patients had to have a life expectancy of at least 2 months and had to be at least 18 years of age. Patients had to have a WHO performance status of 0, 1, or 2. No other antitumor therapy was given within at least three weeks prior to study entry. White blood cell (WBC) count had to be at least 2.5×10^9/l and platelet count at least 75×10^9/l. Patients were excluded in case of life-threatening infection, allergic diathesis with current complaints, organ failure, pregnancy, known seropositivity for human immunodeficiency virus (HIV), over 25% bone marrow involvement by lymphoma determined by bone marrow histology and histochemistry, concomitant treatment with other investigational drugs, or spread of the malignancy to the central nervous system. The study was approved by the institutional review board of the UMC Nijmegen. Written informed consent was obtained from all patients.

Epratuzumab

Epratuzumab (hLL2) is a humanized monoclonal IgG1 antibody directed against CD22 on B cells [7]. Unlabeled epratuzumab is used in clinical trials in chemotherapy-refractory NHL patients [8], and in combination with

rituximab [9]. Initial data of the phase I/II dose escalation study show that the lowest dose level at which objective responses were seen was the dose level with four weekly infusions of 360 mg/m^2 of epratuzumab [8]. Epratuzumab was kindly provided by Immunomedics, Inc., Morris Plains, NJ, as a sterile pyrogen-free solution. Epratuzumab was labeled with ^{186}Re using *S*-benzoyl-mercaptoacetyltriglycine (MAG3) as a chelator by the method as described by Visser *et al.* at the Radionuclide Center of the VU University Medical Center, Amsterdam, The Netherlands [10].

Study design

The present clinical trial was an uncontrolled dose-escalation study. After inclusion, a diagnostic dose of 750 MBq ^{99m}Tc-epratuzumab was administered intravenously. One week after this diagnostic procedure the patient was hospitalized overnight for RIT with ^{186}Re-epratuzumab. Patients were treated at four different dose levels, 0.5, 1.0, 1.5, and 2.0 GBq ^{186}Re per m^2 body surface area (BSA). Three patients were included at each dose level, except for the dose level of 1.5 GBq/m^2, at which 6 patients were treated. Patients were monitored weekly for adverse reactions and toxicity. Patients were evaluated for responses 4–6 weeks after RIT, using physical examination, biochemical analysis, CT scanning, and bone marrow examination, if involved at the start. In case of stable disease or responses, this procedure was repeated every 3 months.

Scintigraphy

Whole body scintigrams for visual assessment of biodistribution and for dosimetric analysis were acquired within one hour after injection, and 1, 2, and 5 days p.i. In an Adams' phantom, a known aliquot of the injected dose (gamma camera standard) was scanned at the same time for reference purposes. Images were acquired using a Siemens double-head gamma camera. The images were processed at ICON workstations using a locally developed dosimetry tool. This tool allows copying and transferring regions of interest (ROIs) between various whole body studies. ROIs were drawn around the gamma camera standard, the whole body, the heart and its background, the right lung and its background, the liver, the spleen and its background, the left kidney and its background, the skull, and the testes, if applicable, and their background. All images were reviewed by one physician.

Dosimetry

Background correction

The activity in the body and the activity in the standard were determined as the geometric mean of the counts in the anterior image and the counts in the posterior image, without background correction. The activity in the heart was determined as the geometric mean of the counts in the anterior and in the posterior ROI minus background. The background in the anterior image was calculated by multiplying the counts per pixel in the ROI for the background of the heart by the number of pixels in the ROI of the heart. Similarly, the background in the posterior image was calculated. The partial background subtraction was used: only a fraction of the counts in the background ROIs was subtracted [11]. This fraction (F) was calculated by dividing abdomen thickness minus organ thickness by the abdomen thickness. For the heart, F equals 0.5 [11].

The activity in the lungs, spleen, and kidneys were determined as the geometric mean of the counts in the anterior and in the posterior ROI, minus F = 0.66 times the background in the anterior and the posterior image, respectively [12]. The background for each organ was calculated similarly as the background of the heart (see above). The activity in the lungs was assumed to be two times the amount of activity in the right lung. The activity in the kidneys was assumed to be two times the amount of activity in the left kidney. The activity in the liver was determined as the geometric mean of the counts in the anterior and in the posterior ROI. No background correction was made, since the liver occupies almost the entire thickness of the patient's abdomen [11]. The bone marrow in the skull is thought to represent 8.4% of the total bone marrow mass in the body. Therefore, counts in the skull were divided by 0.084 to obtain the total activity in the bone marrow. The activity in the testes was determined using the anterior image only.

Attenuation correction

The attenuation of the activity in the whole body and the abdominal organs was considered to be caused by 11.25 cm of tissue between the center of the patient and the skin. The attenuation of activity in the intrathoracic organs is less, because the lungs contain air, leading to less attenuation. Therefore the residence times of these organs are multiplied by 0.85 to correct for the differences in attenuation in the abdomen and thorax.

The residence times of the activity in the testes were multiplied by 0.25. The attenuation of the testes by an overlying layer of 1.5 cm soft

tissue can be defined using equation 5.1, in which μ equals 0.144 cm^{-1} for 137 keV photons in tissue, and x = 1.5 cm of tissue. The attenuation of the abdomen can be defined using the same equation and x = 11.25 cm. By dividing $A_{11\,25}$ by $A_{1\,5}$, a correction factor of 0.25 is obtained.

$$A_x = A_0 \cdot e^{-\mu x}. \tag{5.1}$$

Similarly, the activity in the skull was corrected, assuming a mean path of x = 9 cm, leading to a correction factor of 0.72.

Residence times

Background and attenuation correction were applied as described above to each imaging time-point to yield time–activity curves for each organ. The activity in the whole body at each time-point was decay-corrected. Time–activity curves for the whole body were obtained by assuming no biological clearance of injected activity at the first imaging time-point. The decay-corrected counts were fit to a single component exponential clearance expression, yielding the biological half-life. Assuming that 100% of the injected dose was present at the first imaging time-point, the percentage of the injected dose for each following scan was calculated by dividing counts of each following scan by the counts of the first scan These data were fit in a single component exponential clearance expression, yielding the residence time value of the whole body. Residence times in all organs were calculated using the trapezoidal method. First, a linear extrapolation between the assumed uptake fraction of 0 at time of injection and the measured fractional uptake at the time of the first image was made, not corrected for physical decay. From each time-point to each next time-point a line was drawn between the fractions of uptake. The sum of the areas under all these lines was calculated. The remaining area under the curve from the end of data collection until infinity was determined by considering only physical decay of the radionuclide.

Absorbed doses

The absorbed dose to the organs was calculated using the MIRD schema. Tumor, heart (contents), lungs, liver, spleen, kidneys, red marrow, testes, urinary bladder, and the rest of the body (remainder) were considered as source organs. For the bladder, the dynamic bladder model was used. A voiding interval of 4 h was assumed. Using the counts for the whole body, the biological half-life was determined, as described previously. Biological half-life and voiding interval were entered into the dynamic bladder

model, yielding the residence time in the urinary bladder. The calculated residence times, as described in the previous section, were entered into the MIRDOSE3 computer program, version 3.1 (Oak Ridge Associated Universities, Oak Ridge, TN) [13], to compute the absorbed doses, using the reference adult software phantom for the male patients. For the female patients, the adult female phantom was used.

Statistical analysis

Associations between myelotoxicity and doses were calculated with Microsoft® Excel 2002 software using Pearson correlation test

Results

Patient characteristics

Eighteen patients (12 men and 6 women) were included, of whom 15 were actually treated. The mean age was 57 years (range 41-75). Patient characteristics are listed in Table 4 1, and are described in more detail in Chapter 4 of this thesis. The number of courses of chemotherapy and/or external beam radiation prior to inclusion in our study ranged from 1-7, with a median number of 4

During or directly after infusion of the diagnostic dose of 750 MBq ^{99m}Tc-epratuzumab, fever and chills were observed in 9 out of 18 patients within 1 hour after infusion. This reaction was self-limiting and required no specific medical intervention. One patient experienced an acute allergic reaction with airway obstruction within half an hour after infusion. Other infusion-related side effects were mild and did not require medical intervention. During infusion of the therapeutic dose of ^{186}Re-epratuzumab, no clinical adverse reactions were seen in any of the patients. Within one hour after infusion, fever was observed in only two patients. In all patients, platelet and leukocyte levels decreased 4-6 weeks after the therapeutic injection A grade 4 hematological toxicity was observed (WBC of 0.5×10^9/l) 6 weeks post infusion of 1.5 GBq/m^2 in only one patient. In patient # 2 (0.5 GBq/m^2 dose level), an isolated WBC count drop was observed as early as two weeks after therapy, probably caused by a viral infection.

A summary of the therapeutic effects is listed in Table 4.1. One patient responded completely; for 4 months no lymphoma could be demonstrated. Four patients showed a partial response lasting 14, 6, 3, and 3 months, respectively. Four patients had stable disease for 9, 7, 3, and 3 months, respectively, after RIT. Six patients progressed following RIT.

Target organ	#1	#4	#6	#7	#8	#9	#10	#12	#15	mean±SD
Adrenals	0.149	0.243	0.147	0.197	0.154	0.148	0.122	0.165	0.150	0.164±0.036
Brain	0.144	0.237	0.141	0.190	0.149	0.142	0.118	0.160	0.143	0.158±0.035
Gallbladder wall	0.151	0.243	0.147	0.197	0.155	0.147	0.122	0.165	0.150	0.164±0.036
LLI wall	0.146	0.240	0.143	0.193	0.151	0.144	0.120	0.163	0.146	0.161±0.036
Small intestine	0.147	0.240	0.144	0.194	0.152	0.145	0.121	0.163	0.146	0.161±0.035
Stomach	0.147	0.240	0.144	0.195	0.152	0.145	0.121	0.163	0.147	0.162±0.035
ULI wall	0.147	0.240	0.144	0.194	0.152	0.145	0.120	0.163	0.146	0.161±0.035
Heart wall	0.364	0.814	0.686	0.780	0.459	0.977	0.293	0.520	0.767	0.629±0.230
Kidneys	1.300	2.000	1.270	0.999	1.370	1.330	0.909	0.850	1.620	1.294±0.361
Liver	0.939	0.636	0.793	0.966	0.793	0.650	0.437	0.662	0.892	0.752±0.171
Lungs	0.522	0.836	0.490	0.678	0.565	0.975	0.198	1.010	0.963	0.693±0.275
Muscle	0.145	0.238	0.142	0.191	0.150	0.143	0.119	0.161	0.145	0.159±0.035
Pancreas	0.150	0.243	0.147	0.198	0.154	0.147	0.123	0.165	0.150	0.164±0.036
Red marrow	0.475	0.854	0.583	0.784	0.516	0.760	0.213	0.631	0.586	0.600±0.193
Bone surfaces	0.347	0.614	0.411	0.552	0.374	0.516	0.180	0.448	0.414	0.428±0.127
Skin	0.143	0.235	0.140	0.189	0.148	0.141	0.118	0.159	0.143	0.157±0.035
Spleen	1.940	1.610	2.500	3.780	0.984	1.140	2.250	0.723	2.040	1.885±0.930
Testes	1.880	0.715	0.612	0.613	0.460	0.358	0.256	0.308	0.257	0.607±0.506
Thymus	0.146	0.240	0.144	0.193	0.151	0.146	0.120	0.163	0.147	0.161±0.035
Thyroid	0.145	0.238	0.142	0.191	0.150	0.143	0.119	0.161	0.144	0.159±0.035
Urinary bladder wall	0.623	0.261	0.500	0.408	0.583	0.485	0.723	0.485	0.481	0.505±0.131
Total body	0.193	0.290	0.192	0.253	0.193	0.199	0.142	0.207	0.204	0.208±0.042

LLI = lower large intestine; ULI = upper large intestine

Table 5.1: Absorbed doses (mGy/MBq) to normal organs in male patients

Absorbed doses

The absorbed doses for male and female patients are listed in Tables 5.1 and 5.2, respectively. The organ with the highest absorbed dose appeared to be the spleen, with a mean of 1.89 ± 0.93 mGy/MBq for males and 2.33 ± 0.40 mGy/MBq for females. Other organs absorbing doses exceeding 0.5 mGy/MBq were the kidneys, liver, lungs, heart, urinary bladder wall, and the testes. The mean absorbed doses to the red marrow were 0.60 ± 0.19 mGy/MBq and 0.61 ± 0.14 mGy/MBq for male and female patients, respectively.

Correlation between toxicity and absorbed doses

Since hematologic toxicity appeared to be dose-limiting, and since no other serious toxicity was observed, platelet and WBC nadir levels were compared with a) whole body absorbed dose, b) red marrow absorbed dose, c) total injected activity, d) injected dosage per m^2 BSA, e) injected dosage per kg body weight, and f) the number of prior chemotherapies. The results of this analysis are summarized in Table 5.3. Correlations between nadir of platelets and WBCs, and the 6 parameters mentioned above, could not be found.

Discussion

Dosimetric analysis of RIT using ^{186}Re-epratuzumab showed absorbed doses that are comparable to absorbed doses when using other ^{186}Re-labeled mAbs, like humanized bivatuzumab [14], chimeric cU36 [15], and intraperitoneally administered murine NR-LU-10 [16], although the kidney doses induced by the latter were remarkably lower. The lack of correlation between hematological toxicity and dosages was also described in other lymphoma RIT studies [5,17]. Nevertheless, some other RIT trials were able to determine factors associated with hematological toxicity [14,15,18]. The method to estimate the absorbed dose to the red marrow probably plays a major role. If there is no targeting of the bone marrow, a blood-derived method can be safely used [19]. Unfortunately, in lymphoma patients, the red marrow quite often contains lymphoma. Therefore, the red marrow is a potential target. A camera-derived method to estimate the absorbed marrow dose is preferable. If the marrow doses of the patients described in this study would have been calculated using a blood-derived method, as described in the previous chapter of this thesis, the mean marrow dose would have been underestimated: 0.45 mGy/MBq

Target organ	#2	#3	#5	#11	mean±SD
Adrenals	0.190	0.220	0.251	0.266	0.232±0.034
Brain	0.184	0.212	0.244	0.259	0.225±0.033
Breasts	0.184	0.212	0.243	0.259	0.225±0.033
Gallbladder wall	0.191	0.222	0.251	0.265	0.232±0.033
LLI wall	0.187	0.215	0.247	0.262	0.228±0.034
Small intestine	0.187	0.216	0.247	0.262	0.228±0.033
Stomach	0.188	0.217	0.248	0.263	0.229±0.033
ULI wall	0.187	0.216	0.248	0.263	0.229±0.034
Heart wall	0.528	0.490	0.674	1.010	0.676±0.237
Kidneys	1.410	1.400	1.410	1.230	1.363±0.088
Liver	0.936	1.570	1.100	0.907	1.128±0.307
Lungs	0.667	0.807	1.130	0.828	0.858±0.195
Muscle	0.185	0.214	0.245	0.260	0.226±0.033
Ovaries	0.187	0.216	0.247	0.262	0.228±0.033
Pancreas	0.191	0.221	0.251	0.266	0.232±0.033
Red marrow	0.441	0.570	0.700	0.746	0.614±0.137
Bone surfaces	0.326	0.408	0.492	0.524	0.438±0.089
Skin	0.183	0.211	0.242	0.257	0.223±0.033
Spleen	2.470	2.830	1.960	2.060	2.330±0.400
Thymus	0.186	0.215	0.247	0.262	0.228±0.034
Thyroid	0.184	0.213	0.244	0.259	0.225±0.033
Urinary bladder wall	0.794	0.618	0.537	0.571	0.630±0.114
Uterus	0.187	0.216	0.247	0.262	0.228±0.033
Total body	0.235	0.284	0.308	0.316	0.286±0.036

LLI = lower large intestine; ULI = upper large intestine

Table 5.2: Absorbed doses (mGy/MBq) to normal organs in female patients

instead of 0.60 mGy/MBq in male patients, and 0.51 mGy/MBq instead of 0.61 mGy/MBq in female patients.

In this study, only dosimetric analysis for safety assessment was performed, whereas no lymphoma dosimetry was done. Other studies showed a wide variety of tumor doses, ranging from 0.6–243 Gy in case of treatment with ^{90}Y-ibritumomab [20] and 0.4–18 Gy after treatment with ^{131}I-tositumomab [17]. Although mean and median tumor doses vary, in both cases there was no correlation found between these doses and response to treatment, although there seems to be a tendency that higher absorbed doses can be achieved in smaller tumors than in larger ones, though not statistically significant [17]. Lymphoma dosimetry in RIT has some limitations. Not all lymphomas were clearly visible on scintigraphy, although they responded to RIT. Secondly, even low absorbed lymphoma doses, as

	Platelet nadir	WBC nadir
Whole body dose (Gy)	−0.03	−0.14
Red marrow dose (Gy)	−0.14	−0.36
Dosage (GBq)	−0.31	0.04
Dose level (GBq/m^2)	−0.32	0.06
Dosage/kg (GBq/kg)	−0.30	−0.01
Prior chemotherapies	−0.04	−0.20

Table 5.3: Correlation coefficients r between doses and toxicity

low as 4 Gy, are associated with responses to treatment [21]. Absorbed doses alone do not account for responses, due to the intrinsic antitumor activity of the mAbs themselves [17,21]. Therefore, tumor dosimetry is of limited value in planning RIT of patients with non-Hodgkin's lymphoma.

Conclusions

RIT with ^{186}Re-epratuzumab seems to be safe, and therapeutic responses were observed even at lower dosages. Dosimetric analysis did not reveal high absorbed doses to normal organs. A correlation between dosimetric parameters and toxicity could not be found.

Acknowledgments

This study was conducted with support of The Netherlands Organization for Health Research and Development (ZonMw), project # 920-03-073.

References

1. Postema EJ, Boerman OC, Oyen WJG, Raemaekers JMM, Corstens FHM. Radioimmunotherapy of B-cell non-Hodgkin's lymphoma. *Eur J Nucl Med* 2001; 28: 1725-1735.

2. Wagner HN, Jr, Wiseman GA, Marcus CS, Nabi HA, Nagle CE, Fink-Bennett DM, Lamonica DM, Conti PS. Administration guidelines for radioimmunotherapy of non-Hodgkin's lymphoma with ^{90}Y-labeled anti-CD20 monoclonal antibody. *J Nucl Med* 2002; 43: 267-272.

3. Press OW, Eary JF, Appelbaum FR, Martin PJ, Badger CC, Nelp WB, Glenn SD, Butchko G, Fisher D, Porter B, Matthews DC, Fisher LD,

Bernstein ID. Radiolabeled-antibody therapy of B-cell lymphoma with autologous bone marrow support. *N Engl J Med* 1993; 329: 1219-1224.

4. Wahl RL, Kroll S, Zasadny KR. Patient-specific whole-body dosimetry: principles and a simplified method for clinical implementation. *J Nucl Med* 1998; 39: 14S-20S.

5. Wiseman GA, Kornmehl E, Leigh B, Erwin WD, Podoloff DA, Spies S, Sparks RB, Stabin MG, Witzig T, White CA. Radiation dosimetry results and safety correlations from ^{90}Y-ibritumomab tiuxetan radioimmunotherapy for relapsed or refractory non-Hodgkin's lymphoma: Combined data from 4 clinical trials. *J Nucl Med* 2003; 44: 465-474.

6. Sharkey RM, Brenner A, Burton J, Hajjar G, Toder SP, Alavi A, Matthies A, Tsai DE, Schuster SJ, Stadtmauer EA, Czuczman MS, Lamonica D, Kraeber-Bodere F, Mahe B, Chatal JF, Rogatko A, Mardirosian G, Goldenberg DM. Radioimmunotherapy of non-Hodgkin's lymphoma with ^{90}Y-DOTA humanized anti-CD22 IgG (^{90}Y-epratuzumab): Do tumor targeting and dosimetry predict therapeutic response? *J Nucl Med* 2003; 44: 2000-2018.

7. Leung SO, Goldenberg DM, Dion AS, Pellegrini MC, Shevitz J, Shih LB, Hansen HJ. Construction and characterization of a humanized, internalizing, B-cell (CD22)-specific, leukemia/lymphoma antibody, LL2. *Mol Immunol* 1995; 32: 1413-1427.

8. Leonard JP, Coleman M, Ketas JC, Chadburn A, Ely S, Furman RR, Wegener WA, Hansen HJ, Ziccardi H, Eschenberg M, Gayko U, Cesano A, Goldenberg DM. Phase I/II trial of epratuzumab (humanized anti-CD22 antibody) in indolent non-Hodgkin's lymphoma. *J Clin Oncol* 2003; 21: 3051-3059.

9. Leonard JP, Coleman M, Matthews JC, Fiore JM, Dosik A, Shore T, Kapushoc H, Macri M, Wegener WA, Cesano A, Goldenberg DM. Epratuzumab (anti-CD22) and rituximab (anti-CD20) combination immunotherapy for non-Hodgkin's lymphoma: preliminary response data. *Proc Am Soc Clin Oncol* 2002; 21: 266a.

10. Visser GWM, Gerretsen M, Herscheid JDM, Snow GB, van Dongen GAMS. Labeling of monoclonal antibodies with rhenium-186 using the MAG3 chelate for radioimmunotherapy of cancer: a technical protocol. *J Nucl Med* 1993; 34: 1953-1963.

11. Buijs WCAM, Oyen WJG, Dams ETM, Boerman OC, Siegel JA, Claessens RAMJ, van der Meer JWM, Corstens FHM. Dynamic distribution and dosimetric evaluation of human non-specific immunoglobulin G labelled with ^{111}In or ^{99m}Tc. *Nucl Med Commun* 1998; 19: 743-751.

12. Buijs WCAM, Siegel JA, Boerman OC, Corstens FHM. Absolute organ activity estimated by five different methods of background correction. *J Nucl Med* 1998; 39: 2167-2172.

13. Stabin MG. MIRDOSE: personal computer software for internal dose assessment in nuclear medicine. *J Nucl Med* 1996; 37: 538-546.

14. Postema EJ, Borjesson PKE, Buijs WCAM, Roos JC, Marres HAM, Boerman OC, de Bree R, Lang M, Munzert G, van Dongen GAMS, Oyen WJG. Dosimetric analysis of radioimmunotherapy with ^{186}Re-labeled bivatuzumab in patients with head and neck cancer *J Nucl Med* 2003; 44: 1690-1699.

15. Colnot DR, Quak JJ, Roos JC, van Lingen A, Wilhelm AJ, van Kamp GJ, Huijgens PC, Snow GB, van Dongen GAMS. Phase I therapy study of ^{186}Re-labeled chimeric monoclonal antibody U36 in patients with squamous cell carcinoma of the head and neck. *J Nucl Med* 2000; 41: 1999-2010.

16. Breitz HB, Durham JS, Fisher DR, Weiden PL, DeNardo GL, Goodgold HM, Nelp WB. Pharmacokinetics and normal organ dosimetry following intraperitoneal rhenium-186-labeled monoclonal antibody. *J Nucl Med* 1995; 36: 754-761.

17. Sgouros G, Squeri S, Ballangrud ÅM, Kolbert KS, Teitcher JB, Panageas KS, Finn RD, Divgi CR, Larson SM, Zelenetz AD. Patient-specific, 3-dimensional dosimetry in non-Hodgkin's lymphoma patients treated with ^{131}I-anti-B1 antibody: Assessment of tumor dose-response. *J Nucl Med* 2003; 44: 260-268.

18. Breitz HB, Fisher DR, Wessels BW. Marrow toxicity and radiation absorbed dose estimates from rhenium-186-labeled monoclonal antibody. *J Nucl Med* 1998; 39: 1746-1751.

19. Shen S, Meredith RF, Duan J, Brezovich I, Khazaeli MB, LoBuglio AF. Comparison of methods for predicting myelotoxicity for non-marrow targeting I-131-antibody therapy. *Cancer Biother Radiopharm* 2003; 18: 209-215.

20. Wiseman GA, White CA, Sparks RB, Erwin WD, Podoloff DA, Lamonica D, Bartlett NL, Parker JA, Dunn WL, Spies SM, Belanger R, Witzig TE, Leigh BR. Biodistribution and dosimetry results from a phase III prospectively randomized controlled trial of Zevalin radioimmunotherapy for low-grade, follicular, or transformed B-cell non-Hodgkin's lymphoma. *Crit Rev Oncol Hematol* 2001; 39: 181-194.

21. Hindorf C, Lindén O, Stenberg L, Tennvall J, Strand SE. Change in tumor-absorbed dose due to decrease in mass during fractionated radioimmunotherapy in lymphoma patients. *Clin Cancer Res* 2003; 9: 4003s-4006s.

Chapter 6

Radioimmunotherapy of head and neck cancer

Introduction

Head and neck cancer

Head and neck cancer refers to malignant tumors that arise in the mucosa of the upper aerodigestive tract including the oral cavity, pharynx, larynx, nasal cavity, and paranasal sinuses. Squamous cell carcinoma of the head and neck (HNSCC) account for 90% of these tumors. Malignant tumors arising in adjacent structures including the salivary glands, soft tissues, and bone develop relatively infrequently. Worldwide, the annual incidence is more than 500,000 cases of HNSCC, accounting for approximately 5% of all newly diagnosed malignant neoplasms in North Western Europe and the United States [1,2]. About one third of the patients present with early stage disease (stage I and II), whereas the remaining patients present with advanced disease (stage III and IV). Tumor spread from the primary site is dictated by the local anatomy, each site having its own pattern of dissemination. Lymphatic dissemination is an important mechanism in the spread of HNSCC. After penetration of the basement membrane of the epithelium, cancer cells enter the lymphatic system, pass through the lymphatic vessels, and settle in the subcapsular sinus of the first draining lymph node. A tumor-infiltrated lymph node can act as a source for further dissemination into the surrounding lymphatics or the blood stream, the latter resulting in distant metastases

Staging of the neck in head and neck cancer

The status of the lymph nodes is the single most important tumor-related prognostic factor of HNSCC [3]. For optimal treatment planning, it is essential to know the exact involvement of the nodes. If metastases in the neck are detected, the neck should be treated. In many institutions, diagnosis of the neck is still based on palpation. However, palpation is far from reliable for the detection of lymph node metastases Histopathological evaluations have demonstrated that both the false-positive rate of 20% and the false-negative rate of 20–30% are unsatisfactorily high [4]. Modern imaging techniques, such as computed tomography (CT), magnetic resonance imaging (MRI), ultrasound (US), and especially US-guided fine-needle aspiration cytology (FNAC), are more reliable than palpation, but also leave much room for improvement. Using the most optimal radiological criteria, the overall error of CT and MRI in the preoperative detection of lymph node metastases in neck sides is about 20% [5,6]. From the perspective of local tumor control, especially a neck without palpable lymph nodes (N0) remains a diagnostic dilemma as it still is at risk for harboring occult

metastases. For diagnosis of the N0 neck, US-guided fine-needle aspiration cytology (USgFNAC) has a higher sensitivity and specificity than CT and MRI. In experienced hands, the sensitivity for the N0 neck can reach 73% with a specificity of 100% [7]. Despite this, USgFNAC also has some unfavorable aspects: (i) it is an invasive method, (ii) it only gives diagnostic information of a selected part of the neck and not on the primary tumor or distant metastases, and (iii) its accuracy is strongly dependent on the skill of the ultrasonographer and the cytopathologist. With respect to the latter, selection of lymph nodes to be aspirated is not easy and is based on known patterns of lymphatic spread and on lymph node size and morphology as assessed with US. Inaccuracies of USgFNAC result from absence of enlarged nodes, aspiration of the wrong lymph node, failure of cytological analysis due to the presence of few tumor cells, or the presence of micrometastases in parts of the lymph nodes not aspirated (sampling error).

The presence or absence of lymph node and distant metastases has a major impact on the choice of treatment. There is still a great need for a sensitive, specific and minimally invasive method to detect occult (micro)metastases in the lymph nodes in the neck as well as at distant sites.

Treatment of head and neck cancer

Therapy usually consists of surgery, radiotherapy, or a combination of these modalities. Generally, patients with stage I and II disease, undergo either surgery or radiotherapy with curative intent. Cure will be achieved in 70–85% of these patients. For patients with local or regional advanced disease (stage III and IV), the prognosis is much worse. Frequently, a combination of surgery and radiotherapy is used. It is disappointing that the survival rates of patients with advanced stage head and neck cancer have not improved much over the last decades. Although many studies have observed a decrease of local and particularly of regional failures, because of the widespread use of combined surgery and radiotherapy, this is not reflected in a proportional increase of the five-year survival rates. As fewer patients die from uncontrolled disease in the head and neck, more are exposed to the risk of disseminated disease below the clavicles [8]. It is obvious that there is a great demand for a systemic treatment effective in destroying (micro)metastases at distant sites and minimal residual disease at the local and regional level. Initially, hope was high for chemotherapy to play this role, but unfortunately these expectations have not been materialized. Clearly, a more tumor-selective systemic therapy is needed.

Radioimmunotherapy of cancer

One of the novel approaches for selective treatment of cancer is the use of monoclonal antibodies (mAbs) conjugated with radionuclides. In the last decade, successes have been obtained with radioimmunotherapy (RIT) of non-Hodgkin's lymphoma, leading to FDA approval of the anti-CD20 mAbs yttrium-90 (^{90}Y)-ibritumomab (Zevalin) [9] and iodine-131 (^{131}I)-tositumomab (Bexxar). For solid tumors, however, such promising results have not yet been observed, although some studies have reported encouraging results with RIT for small metastatic lesions or as adjuvant treatment [10,11,12]. Several radioimmunoconjugates are currently evaluated in phase III clinical RIT trials [13]. While in the last two decades radiolabeled mAbs have been administered to thousands of patients with various types of tumors, the application of mAbs for detection and treatment of HNSCC has started relatively late One of the main reasons for the slow progress has been the lack of mAbs with a high specificity for HNSCC and a restricted reactivity with normal tissues. Only recently, the use of radiolabeled mAbs has been considered as a realistic alternative approach for detection and treatment of HNSCC. This paper deals with the factors influencing tumor treatment by RIT. The progress in RIT of head and neck cancer will be summarized and its feasibility will be discussed.

Target antigens

The hybridoma technology allowed the development of mAbs specifically directed against each particular cellular antigen. In general, mice are immunized with tumor cells or a purified tumor antigen. Spleen cells from the immunized mice are fused with myeloma cells, which can be propagated indefinitely and have the ability to produce mAbs. As such, the resulting hybridoma cells receive the genetic information for the production of specific mAbs from the splenic B lymphocytes and the growth potential and mAb-production and secretion machinery from the myeloma cells. After the cell fusion procedure, a hybridoma cell clone can be selected that produces a murine mAb with the desired antigen-specificity. In the last decade, new technology became available for the direct selection of human mAbs by using phage display libraries [14] or transgenic mice [15].

An ideal antigenic target for RIT is abundantly expressed by all tumors in the patient population, at the outer cell surface of all tumor cells, and not by normal tissues. Unfortunately, tumor-specific antigens have only been found in experimentally induced tumors and not in so-called spontaneous tumors. The majority of identified antigens in human tumors,

however, represent tumor-associated antigens, present on tumor tissue but also detectable on normal tissues. Expression of the target antigen in normal tissues can be acceptable for radioimmunoscintigraphy (RIS) when this normal tissue is poorly accessible for mAbs, or when it is localized at a site outside the anatomic region of interest. However, for RIT also the latter is unacceptable. Other factors influencing the suitability of antigens for tumor targeting, are internalization and shedding. If the antigen-antibody complex is internalized after binding of the radiolabeled mAb, optimal cellular retention of the targeted radionuclides is of importance for RIT, since the longer time the radionuclides stay in or near the targeted cell, the higher the radiation dose that will be delivered. Shedding of an antigen by the tumor into the blood stream is considered to be disadvantageous, since circulating antigen can trap the circulating radiolabeled mAb before the mAb reaches the tumor and thus makes tumor targeting less effective. Moreover, the formed complexes may accumulate in tissues with a highly developed reticuloendothelial system such as liver, spleen, bone marrow, and lung.

Monoclonal antibodies

Nowadays, mAbs can be produced in large quantities, at acceptable costs for marketing, and with a quality that fulfils the requirements of the FDA and the European Medicines Evaluation Agency. Most mAbs were originally of murine origin. Administration of a murine mAb usually results in the formation of human anti-mouse antibodies (HAMAs). To decrease immunogenicity, the mAb molecule can be restructured to human-mouse chimeric or even humanized versions, using recombinant DNA techniques [16]. Fully human mAbs can be produced via phage display libraries [14] or by transgenic mice that contain a human immunoglobulin gene repertoire [15]. High binding affinity of the mAb to the target structure is generally considered necessary, as it minimizes the risk of competing low affinity interactions in normal tissues or of interactions with circulating antigen. However, with respect to RIT application, it has been claimed that an intermediate affinity mAb will perform better than a mAb with extremely high affinity, since it distributes more extensively and more homogeneously throughout solid tumor masses [17]. So far, at least 30 mAbs directed against HNSCC have been described in literature. These mAbs can be divided in three main categories:

1. *mAbs reactive with squamous cell carcinoma and not with other tumor types:* A general shortcoming of this group of mAbs is their reactivity with normal squamous epithelia. When such mAbs are used

in RIS or RIT, uptake of radioactivity in the normal oral mucosa can occur. This can hamper tumor detection in the head and neck area when applied in RIS, while in RIT mucositis might occur.

2. *Pan-carcinoma mAbs:* These mAbs are not only directed against HNSCC, but also against other tumor types. A general shortcoming of these mAbs is there heterogenous reaction pattern with HNSCC, and their reactivity with several normal tissues.

3. *mAbs recognizing stromal and/or endothelial cells of the tumor:* Most recently a third group of mAbs has become available. These mAbs do not recognize antigens expressed on tumor cells themselves, but they recognize antigens on stromal and/or endothelial cells of the tumor. These mAbs may be especially attractive because stromal and endothelial markers are expressed by a diversity of tumor types, and are well accessible for mAbs [18-21]. Also for this category of mAbs, cross reactivity with normal tissues might form a limitation.

Many of the mAbs described in literature are poorly characterized with respect to their reactivity profile on normal and malignant tissues. It is difficult to speculate about their suitability for RIS and RIT. Only a few mAbs have been administered to HNSCC patients for RIS, and even less for RIT. So far, none of them is routinely used for several reasons. High costs for production of a batch of mAbs for clinical use restrict preliminary clinical evaluation for RIS. Despite promising preclinical results, there is the inherent risk that the mAb is not suitable for RIS or RIT already at an early stage of clinical studies. However, it is also possible that a mAb, though not selective enough for application in RIT, is well qualified for other therapeutic approaches with mAbs. The latter seems to be the case with mAbs directed against the Epidermal Growth Factor Receptor (EGFR) [22].

Radiolabeled monoclonal antibodies

The choice of the radionuclide to be coupled to the mAb depends on the antibody used, the properties of the antigen, and the purpose of the radiolabel: imaging, treatment, or treatment planning. In the latter application, RIS is performed as a scouting procedure prior to RIT, to enable the confirmation of tumor targeting and the estimation of radiation dose delivery to both tumors and normal tissues (*i.e.* dosimetry). For RIT, a therapeutic radionuclide is preferably a beta-emitter with a half-life of several days, as discussed in the previous chapters of this thesis.

The stability of the radioconjugate *in vivo* and the internalization of the antibody-antigen complex are also of main importance. The radioimmunoconjugate should be as stable as possible. Unbound radionuclides could result in uptake in normal organs, possibly leading to unwanted side-effects. For instance, unbound radiometals like ^{90}Y accumulate in mineral bone, and therefore cause an increase of the bone marrow dose. The effect of internalization of a mAb on RIT depends on the conjugated radionuclide. For example, degradation of ^{131}I-, ^{186}Re- and ^{188}Re-labeled mAbs will result in a rapid clearance of these radionuclides from the tumor. In contrast, upon internalization ^{177}Lu-, ^{67}Cu-, or ^{90}Y-labeled mAbs are processed, and the radionuclides will be trapped intracellularly in lysosomes [23]. Therefore, the phenomenon of internalization should be taken into account when choosing a radionuclide for RIT.

Radioimmunotherapy of head and neck cancer

Radiolabeled mAbs are exploited in order to irradiate tumors from the closest distance as possible, with low radiation burden to surrounding, healthy tissue. Therefore, β-emitting radionuclides have to be used, since the range of β-particles in tissue does not exceed several millimeters (10–100 cell diameters). Advantages of RIT over other mAb-based therapies are the previously mentioned cross-fire effect, the possibility to perform imaging and dosimetry, and the independence of phenomenons like mAb internalization, patient's immunocompetence, and multi-drug resistance Taking into account the availability of suitable mAbs and the fact that HNSCC is a radiosensitive tumor type, initiation of clinical RIT trials in patients with HNSCC was a logical next step.

Chimeric mAb U36 was selected for the first clinical RIT trial in HNSCC patients, as this mAb is broadly applicable for targeting squamous tumors as well as adenocarcinomas. Colnot *et al.* described the clinical use of the chimeric mAb U36, labeled with ^{186}Re, in patients with recurrent HNSCC, either locally or at distant sites [24]. Thirteen patients received 0.74 GBq ^{99m}Tc-labeled U36 (2 mg), followed 1 week later by a single dose of ^{186}Re-labeled U36 (12 or 52 mg) in radiation dose-escalating steps of 0.4, 1.0, and 1.5 GBq/m^2. The radiopharmaceutical was well-tolerated and excellent targeting of tumor lesions was seen in all patients. Dose-limiting myelotoxicity (thrombocytopenia being most prominent) was the only toxicity observed, and the maximum tolerated dose (MTD) was reached at 1.0 GBq/m^2. Pharmacokinetics varied between patients treated at the same dose level and were accurately predicted by the diagnostic procedure. In two patients with dose-limiting myelotoxicity, the tumor size was reduced

by RIT, while in one patient treated at MTD stable disease for six months was observed.

In RIT, myelotoxicity generally is dose-limiting. A nadir of platelets and granulocytes typically occurs at 4-6 weeks after RIT. In this trial, the absorbed dose for bone marrow at MTD ranged from 0.73 to 1.10 Gy. The MTD of 1.0 GBq/m^2 is lower than MTDs found in comparable trials using ^{186}Re-labeled mAbs. With the murine mAb NR-LU-10 and the chimeric mAb NR-LU-13, MTDs of 3.3 GBq/m^2 and 2.2 GBq/m^2 were found, respectively [25,26]. In a phase I study using the ^{186}Re-labeled anti-CD22 humanized mAb LL2, an MTD of 2.0 GBq/m^2 was established [27]. Three factors might have contributed to the low MTD: (i) a longer half-life of ^{186}Re-labeled chimeric mAb U36 in the blood, (ii) the definition of dose-limiting toxicity, defining grade 4 thrombocytopenia as platelet counts below 25×10^9/l instead of below 10×10^9/l, and (iii) the pretreatment of the patients, although the lymphoma patients in the previously mentioned RIT trial were more heavily pretreated.

A noteworthy observation of the ^{186}Re-U36 trial was the development of human anti-chimeric antibodies (HACAs) in 35% of the patients. Immunogenicity was also observed with a second anti-CD44v6 mAb, the high affinity murine mAb BIWA 1 [28]. To reduce immunogenicity, humanized versions of BIWA 1 were developed, as described by Verel *et al.* [29]. One of these mAbs called BIWA 4 (bivatuzumab), was selected for further clinical evaluation. BIWA 4 was labeled with ^{186}Re and studied in a dose-escalation study [30]. The results of this study are described in the next two chapters of this thesis.

Future approaches

The dose-limiting organ in non-myeloablative RIT is the red marrow. Therefore, ways are being explored to overcome this limitation. When treating non-Hodgkin's lymphoma patients, high, myeloablative doses of radiolabeled mAbs can be given in combination with stem cell transplantation [31,32]. An alternative way to increase hematologic tolerability is the harvest of stem cell-containing whole blood, without separation of the stem cells from the blood. This procedure, which can be performed in a routine clinical setting at relatively low cost, was introduced in a RIT trial in HNSCC by Colnot *et al.* [33]. The procedure and rationale in brief: before RIT, granolocyte colony-stimulating factor (G-CSF: 10 μg/kg/day) was administered s.c. on an outpatient basis during 5 days. This treatment resulted in a rise of CD34+ stem cells in the peripheral blood. On day 6, immediately prior to the administration of ^{186}Re-labeled U36, 1 liter of

whole blood was harvested and kept unprocessed at 4 °C until reinfusion 72 h later. At that time, only 25% of the total ^{186}Re-labeled U36 dose had remained in the blood. It was anticipated that the radiation level would be low enough to allow homing and proliferation of the CD34+ cells in the bone marrow before myelotoxicity would become manifest (4–6 weeks p.i.), thereby reducing the severity of myelotoxicity. Indeed, when applying this technique the MTD more than doubled. Although the bone marrow dose ranged from 2.1 to 2.8 Gy, more than two times higher than in the previous phase I trial with U36 [24], myelotoxicity exceeding grade 3 was not observed. Stable disease for 3–7 months was observed in five of nine patients, and in all patients treated at the highest dose level of 2.0 GBq/m^2

Another possibility to increase the administered activity dose is the reduction of the circulation time of radioactivity by introducing multi-step treatment schedules Paganelli *et al.* treated a HNSCC patient by infusing non-radioactive biotinylated anti-CEA mAbs, followed by administration of streptavidin 36 h later [34]. As the last step in this pre-targeting approach, 18 h after the streptavidin infusion, 2.6 GBq of the fast clearing ^{90}Y-DOTA-biotin was infused. This patient, having a T4N3M0 HNSCC of the right tonsil that relapsed after chemo-radiation therapy, responded with a complete remission to RIT. No hematologic toxicity was observed. Still, the dose absorbed by the tumor was less than 10 Gy [34] Therefore, the authors state that this treatment modality should preferably be used in combination with external beam radiation

Maraveyas *et al.* came to the same conclusion [35]. They studied the use of radioiodinated HMFG1 mAbs in patients undergoing surgery. With specimens obtained during surgery, absorbed tumor doses could be estimated. When giving ^{131}I-HMFG1 RIT, an absorbed tumor dose of approximately 3–4 Gy was achieved [35]. Since also other RIT studies suggest that tumor doses of at most 20 Gy can be achieved, it is realistic to expect future application of RIT of HNSCC in an adjuvant setting. Especially the treatment of minimal residual disease seems to be attractive as it was demonstrated that mAb uptake and dose delivery are approximately 4 times higher in small-volume tumors (1 cm^3) than in the large-volume tumors (50 cm^3) [36].

Also some novel approaches might be particular attractive for application in head and neck cancer. For example, it was shown that the anti-EGFR mAb 425 strongly enhanced the efficacy of RIT with ^{186}Re-labeled U36 in HNSCC-bearing nude mice [37]. Also other studies showed synergism when combining EGFR inhibitors with irradiation [38,39]. Taking into account the high expression of EGFR in most HNSCC and its absence on bone marrow cells, such approach holds promise for future clinical application

Conclusions

RIT of HNSCC has been applied in only a small number of patients. Myelotoxicity appeared to be dose-limiting. Nevertheless, data suggest that RIT could play a role as an adjuvant treatment of HNSCC.

Acknowledgments

This chapter was adapted from excerpts of the publication *Radioimmunodetection and radioimmunotherapy of head and neck cancer: A review* by Borjesson, Postema, De Bree, Leemans, Kairemo, and Van Dongen (*Oral Oncol* 2004).

References

1. Parkin DM, Bray F, Ferlay J, Pisani P. Estimating the world cancer burden: Globocan 2000. *Int J Cancer* 2001; 94: 153-156.

2. Vokes EE, Weichselbaum RR, Lippman SM, Hong WK. Head and neck cancer. *N Engl J Med* 1993; 328: 184-194.

3. Leemans CR, Tiwari R, Nauta JJP, van der Waal I, Snow GB. Regional lymph node involvement and its significance in the development of distant metastases in head and neck carcinoma. *Cancer* 1993; 71: 452-456.

4. Ali S, Tiwari RM, Snow GB. False-positive and false-negative neck nodes. *Head Neck Surg* 1985; 8: 78-82.

5. van den Brekel MWM, Stel HV, Castelijns JA, Nauta JJ, van der Waal I, Valk J, Meyer CJ, Snow GB. Cervical lymph node metastasis: assessment of radiologic criteria. *Radiology* 1990; 177: 379-384.

6. van den Brekel MWM, Castelijns JA, Croll GA, Stel HV, Valk J, van der Waal I, Golding RP, Meyer CJ, Snow GB. Magnetic resonance imaging vs palpation of cervical lymph node metastasis. *Arch Otolaryngol Head Neck Surg* 1991; 117: 663-673.

7. van den Brekel MWM, Castelijns JA, Stel HV, Luth WJ, Valk J, van der Waal I, Snow GB. Occult metastatic neck disease: detection with US and US-guided fine-needle aspiration cytology. *Radiology* 1991; 180: 457-461.

8. Taneja C, Allen H, Koness RJ, Radie-Keane K, Wanebo HJ. Changing patterns of failure of head and neck cancer. *Arch Otolaryngol Head Neck Surg* 2002; 128: 324-327.

9. Wagner HN, Jr, Wiseman GA, Marcus CS, Nabi HA, Nagle CE, Fink-Bennett DM, Lamonica DM, Conti PS. Administration guidelines for radioimmunotherapy of non-Hodgkin's lymphoma with ^{90}Y-labeled anti-CD20 monoclonal antibody. *J Nucl Med* 2002; 43: 267-272.

10. Hird V, Maraveyas A, Snook D, Dhokia B, Soutter WP, Meares C, Stewart JS, Mason P, Lambert HE, Epenetos AA. Adjuvant therapy of ovarian cancer with radioactive monoclonal antibody. *Br J Cancer* 1993; 68: 403-406.

11. Juweid ME, Sharkey RM, Behr T, Swayne LC, Dunn R, Siegel J, Goldenberg DM. Radioimmunotherapy of patients with small-volume tumors using iodine-131-labeled anti-CEA monoclonal antibody NP-4 F(ab')2. *J Nucl Med* 1996; 37: 1504-1510.

12. Behr TM, Sharkey RM, Juweid ME, Dunn RM, Vagg RC, Ying Z, Zhang CH, Swayne LC, Vardi Y, Siegel JA, Goldenberg DM. Phase I/II clinical radioimmunotherapy with an iodine-131-labeled anti-carcinoembryonic antigen murine monoclonal antibody IgG. *J Nucl Med* 1997; 38: 858-870.

13. Trikha M, Yan L, Nakada MT. Monoclonal antibodies as therapeutics in oncology. *Curr Opin Biotechnol* 2002; 13: 609-614.

14. Kretzschmar T, von Ruden T. Antibody discovery: phage display. *Curr Opin Biotechnol* 2002; 13: 598-602.

15. Kellermann SA, Green LL. Antibody discovery: the use of transgenic mice to generate human monoclonal antibodies for therapeutics. *Curr Opin Biotechnol* 2002; 13: 593-597.

16. Hazra DK, Britton KE, Lahiri VL, Gupta AK, Khanna P, Saran S. Immunotechnological trends in radioimmunotargeting: from 'magic bullet' to 'smart bomb'. *Nucl Med Commun* 1995; 16: 66-75.

17. Adams GP, Schier R, McCall AM, Simmons HH, Horak EM, Alpaugh RK, Marks JD, Weiner LM. High affinity restricts the localization and tumor penetration of single-chain fv antibody molecules. *Cancer Res* 2001; 61: 4750-4755.

18. Welt S, Divgi CR, Scott AM, Garin-Chesa P, Finn RD, Graham M, Carswell EA, Cohen A, Larson SM, Old LJ, Rettig WJ. Antibody targeting in metastatic colon cancer: a phase I study of monoclonal antibody F19 against a cell-surface protein of reactive tumor stromal fibroblasts. *J Clin Oncol* 1994; 12: 1193-1203.

19. Posey JA, Khazaeli MB, DelGrosso A, Saleh MN, Lin CY, Huse W, LoBuglio AF. A pilot trial of Vitaxin, a humanized anti-vitronectin receptor (anti alpha v beta 3) antibody in patients with metastatic cancer. *Cancer Biother Radiopharm* 2001; 16: 125-132.

20. Hicklin DJ, Witte L, Zhu Z, Liao F, Wu Y, Li Y, Bohlen P. Monoclonal antibody strategies to block angiogenesis. *Drug Discov Today* 2001; 6: 517-528.

21. Santimaria M, Moscatelli G, Viale GL, Giovannoni L, Neri G, Viti F, Leprini A, Borsi L, Castellani P, Zardi L, Neri D, Riva P. Immunoscintigraphic detection of the ED-B domain of fibronectin, a marker of angiogenesis, in patients with cancer. *Clin Cancer Res* 2003; 9: 571-579.

22. Mendelsohn J. Antibody-mediated EGF receptor blockade as an anticancer therapy: from the laboratory to the clinic. *Cancer Immunol Immunother* 2003; 52: 342-346.

23. Mattes MJ, Griffiths GL, Diril H, Goldenberg DM, Ong GL, Shih LB. Processing of antibody-radioisotope conjugates after binding to the surface of tumor cells. *Cancer* 1994; 73: 787-793.

24. Colnot DR, Quak JJ, Roos JC, van Lingen A, Wilhelm AJ, van Kamp GJ, Huijgens PC, Snow GB, van Dongen GAMS. Phase I therapy study of ^{186}Re-labeled chimeric monoclonal antibody U36 in patients with squamous cell carcinoma of the head and neck. *J Nucl Med* 2000; 41: 1999-2010.

25. Breitz HB, Weiden PL, Vanderheyden JL, Appelbaum JW, Bjorn MJ, Fer MF, Wolf SB, Ratliff BA, Seiler CA, Foisie DC. Clinical experience with rhenium-186-labeled monoclonal antibodies for radioimmunotherapy: results of phase I trials. *J Nucl Med* 1992; 33: 1099-1109.

26. Weiden PL, Breitz HB, Seiler CA, Bjorn MJ, Ratliff BA, Mallet R, Beaumier PL, Appelbaum JW, Fritzberg AR, Salk D. Rhenium-186-labeled chimeric antibody NR-LU-13: pharmacokinetics, biodistribution and immunogenicity relative to murine analog NR-LU-10. *J Nucl Med* 1993; 34: 2111-2119.

27. Postema EJ, Raemaekers JMM, Oyen WJG, Boerman OC, Mandigers CMPW, Goldenberg DM, van Dongen GAMS, Corstens FHM. Final results of a phase I radioimmunotherapy trial using ^{186}Re-epratuzumab for the treatment of patients with non-Hodgkin's lymphoma. *Clin Cancer Res* 2003; 9: 3995s-4002s.

28. Stroomer JWG, Roos JC, Sproll M, Quak JJ, Heider KH, Wilhelm BJ, Castelijns JA, Meyer R, Kwakkelstein MO, Snow GB, Adolf GR, van Dongen GAMS. Safety and biodistribution of ^{99m}Technetium-labeled anti-CD44v6 monoclonal antibody BIWA 1 in head and neck cancer patients. *Clin Cancer Res* 2000; 6: 3046-3055.

29. Verel I, Heider KH, Siegmund M, Ostermann E, Patzelt E, Sproll M, Snow GB, Adolf GR, van Dongen GAMS. Tumor targeting properties of monoclonal antibodies with different affinity for target antigen CD44V6 in nude mice bearing head-and-neck cancer xenografts. *Int J Cancer* 2002; 99: 396-402.

30. Börjesson PKE, Postema EJ, Roos JC, Colnot DR, Marres HAM, van Schie MH, Stehle G, de Bree R, Snow GB, Oyen WJG, van Dongen GAMS. Phase I therapy study with ^{186}Re-labeled humanized monoclonal antibody BIWA 4 (bivatuzumab) in patients with head and neck squamous cell carcinoma. *Clin Cancer Res* 2003; 9: 3961s-3972s.

31. Press OW, Eary JF, Appelbaum FR, Martin PJ, Nelp WB, Glenn S, Fisher DR, Porter B, Matthews DC, Gooley T. Phase II trial of ^{131}I-B1 (anti-CD20) antibody therapy with autologous stem cell transplantation for relapsed B cell lymphomas. *Lancet* 1995; 346: 336-340.

32. Behr TM, Griesinger F, Riggert J, Gratz S, Béhé M, Kaufmann CC, Wormann B, Brittinger G, Becker W. High-dose myeloablative radioimmunotherapy of mantle cell non-Hodgkin lymphoma with the iodine-131-labeled chimeric anti-CD20 antibody C2B8 and autologous stem cell support. Results of a pilot study. *Cancer* 2002; 94: 1363-1372.

33. Colnot DR, Ossenkoppele GJ, Roos JC, Quak JJ, de Bree R, Borjesson PK, Huijgens PC, Snow GB, van Dongen GA. Reinfusion of unprocessed, granulocyte colony-stimulating factor-stimulated whole blood allows dose escalation of ^{186}Re-labeled chimeric monoclonal antibody U36 radioimmunotherapy in a phase I dose escalation study. *Clin Cancer Res* 2002; 8: 3401-3406.

34. Paganelli G, Orecchia R, Jereczek-Fossa B, Grana C, Cremonesi M, de Braud F, Tradati N, Chinol M. Combined treatment of advanced

oropharyngeal cancer with external radiotherapy and three-step radioimmunotherapy. *Eur J Nucl Med* 1998; 25: 1336-1339.

35. Maraveyas A, Stafford N, Rowlinson-Busza G, Stewart JS, Epenetos AA. Pharmacokinetics, biodistribution, and dosimetry of specific and control radiolabeled monoclonal antibodies in patients with primary head and neck squamous cell carcinoma. *Cancer Res* 1995; 55: 1060-1069.

36. de Bree R, Roos JC, Plaizier MA, Quak JJ, van Kamp GJ, den Hollander W, Snow GB, van Dongen GAMS. Selection of monoclonal antibody E48 IgG or U36 IgG for adjuvant radioimmunotherapy in head and neck cancer patients. *Br J Cancer* 1997; 75: 1049-1060.

37. van Gog FB, Brakenhoff RH, Stigter-van Walsum M, Snow GB, van Dongen GAMS. Perspectives of combined radioimmunotherapy and anti-EGFR antibody therapy for the treatment of residual head and neck cancer. *Int J Cancer* 1998; 77: 13-18.

38. Milas L, Mason K, Hunter N, Petersen S, Yamakawa M, Ang K, Mendelsohn J, Fan Z. In vivo enhancement of tumor radioresponse by C225 antiepidermal growth factor receptor antibody. *Clin Cancer Res* 2000; 6: 701-708.

39. Bianco C, Tortora G, Bianco R, Caputo R, Veneziani BM, Caputo R, Damiano V, Troiani T, Fontanini G, Raben D, Pepe S, Bianco AR, Ciardiello F. Enhancement of antitumor activity of ionizing radiation by combined treatment with the selective epidermal growth factor receptor-tyrosine kinase inhibitor ZD1839 (Iressa). *Clin Cancer Res* 2002; 8: 3250-3258.

Chapter 7

Phase I therapy study with ^{186}Re-labeled humanized monoclonal antibody BIWA 4 (bivatuzumab) in patients with head and neck squamous cell carcinoma

Pontus K.E. Borjesson
Ernst J. Postema
Jan C. Roos
David R. Colnot
Henri A.M. Marres
Mathijs H. van Schie
Gerd Stehle
Remco de Bree
Gordon B. Snow
Wim J.G. Oyen
Guus A.M.S. van Dongen

Clinical Cancer Research 2003; 9: 3961s-3972s

Abstract

Purpose: In previous studies, we have shown the potential of radioimmunotherapy (RIT) with ^{186}Re-labeled chimeric monoclonal antibody (mAb) U36 for treatment of head and neck cancer. A limitation of this anti-CD44v6 mAb, however, appeared to be its immunogenicity, resulting in human anti-chimeric antibodies in 40% of the patients. Aiming for a less immunogenic anti-CD44v6 mAb, the humanized mAb BIWA 4 (bivatuzumab) was introduced. In the present phase I RIT study, we determined the safety, maximum tolerated dose (MTD), pharmacokinetics, immunogenicity, and therapeutic potential of ^{186}Re-labeled BIWA 4 in patients with squamous cell carcinoma of the head and neck.

Experimental Design: Twenty patients with inoperable recurrent and/or metastatic head and neck squamous cell carcinoma received a single dose of ^{186}Re-labeled BIWA 4 in radiation dose-escalation steps of 0.74, 1.11, 1.48, 1.85, and 2.22 GBq/m^2 (20, 30, 40, 50, and 60 mCi/m^2). Three patients received a second dose at least 3 months after the initial dose. After each administration, whole-body images as well as planar and tomographic images of the head and neck region were obtained, and the pharmacokinetics and the development of human anti-human antibody responses were determined. Radiation absorbed doses were calculated for whole body, red marrow, organs, and tumor.

Results: First and second administrations were all well tolerated, and targeting of tumor lesions proved to be excellent. The only significant manifestations of toxicity were dose-limiting myelotoxicity consisting of thrombo- and leukocytopenia and, to a lesser extent, oral mucositis (grade 2). Grade 4 myelotoxicity was seen in two patients treated with 2.22 GBq/m^2. The MTD was established at 1.85 GBq/m^2, at which level dose-limiting myelotoxicity was seen in one of six patients. Stable disease, varying between 6 and 21 weeks, was observed in three of six patients treated at the MTD level. The median tumor dose, recalculated to MTD level, was 12.4 Gy. The absorbed dose in red marrow was 0.49 ± 0.03 mGy/MBq for males and 0.64 ± 0.03 mGy/MBq for females. Two patients experienced a human anti-human antibody response. Pharmacokinetics showed consistency across patients and within the three patients receiving ^{186}Re-BIWA 4 on two occasions.

Conclusions: This study shows that ^{186}Re-labeled BIWA 4 can safely be administered, also in a repeated way. The MTD was established at 1.85 GBq/m^2. In comparison with the previously described anti-CD44v6 mAb U36, the humanized mAb BIWA 4 seems to be less immunogenic. The fact that antitumor effects were seen in incurable patients with bulky

disease justifies the evaluation of RIT with ^{186}Re-labeled BIWA 4 in an adjuvant setting.

Introduction

Squamous cell carcinoma, the predominant histological type among tumors of the head and neck, accounts for approximately 5% of all malignant tumors in Europe and the United States. In 2000, an estimated 551,100 new cases of squamous cell carcinoma of the head and neck (HNSCC) of the oral cavity, pharynx, or larynx were diagnosed worldwide [1]. Early stages (stage I/II) of HNSCC generally have a good prognosis after surgery or radiotherapy. Unfortunately, this does not hold true for advanced-stage disease (stage III/IV) as present in about two-thirds of all HNSCC patients. Despite improvements in locoregional treatment modalities, the rate of locoregional recurrence still is near 40%, whereas approximately 25% of these patients develop distant metastases. With respect to the latter, autopsy studies have shown incidences up to 57% [2–5]. In particular, patients with multiple lymph node metastases are at risk for the development of locoregional recurrences and distant metastases [6,7]. Considering these figures, it is plausible that many of the advanced-stage HNSCC patients harbor residual tumor cells after surgery and radiotherapy. The role of adjuvant chemotherapy for this group of patients has not proven to be beneficial, and therefore the development of an effective adjuvant systemic treatment is a major challenge.

Selective targeting of radionuclides to HNSCC by use of monoclonal antibodies (mAbs) as in radioimmunotherapy (RIT) might contribute to a more effective treatment of advanced-stage disease. Because HNSCC is relatively radiosensitive compared with other solid tumors, RIT can become a realistic option. To date, most successes in the field of RIT have been achieved in patients with hematological malignancies, such as non-Hodgkin's lymphomas, where high rates of partial and complete responses have been observed [8]. In the treatment of B-cell non-Hodgkin's lymphoma, most experience has been gained with iodine-131- and yttrium-90-labeled anti-CD20 mAbs such as tositumomab and ibritumomab, respectively [9–13].

These successes have motivated us to explore the additional value of RIT against HNSCC. In the selection of a suitable target antigen in HNSCC, CD44 splice variants containing the v6 domain appeared to be the most promising thus far. The CD44 protein family consists of isoforms, encoded by standard exons and up to nine alternatively spliced variant exons (v2–v10), which are expressed in a tissue-specific way and involved

in physiological functions such as signal transduction, growth factor binding, cell adhesion, and cell migration. Expression of v6-containing CD44 variants has been related to aggressive behavior of various tumor types and was shown to be particularly high and homogeneous on the outer cell surface of HNSCC [14,15].

In the past decade, the development of CD44v6-directed RIT in HNSCC has shown encouraging progress. For this purpose, two murine mAbs (mmAbs) became available, designated mmAb U36 and mmAb BIWA 1. Although BIWA 1 resembles U36, it binds to a different epitope with a 35-fold higher affinity [16]. According to the numbering of Kugelman *et al.* [17], the epitope recognized by BIWA 1 consists of amino acids 360–370, and the epitope recognized by mAb U36 consists of amino acids 365–376.

Biodistribution studies with radiolabeled mAbs U36 and BIWA 1 in HNSCC patients undergoing surgery showed promising biodistribution patterns with selective tumor targeting and high tumor uptake for both mAbs [18,19]. Unfortunately, administration of BIWA 1 resulted in human antimurine antibody (HAMA) responses in 11 of 12 patients [19], a problem also observed after injection of mmAb U36, although to a lesser extent [18].

Subsequent phase I RIT studies with chimeric (human/mouse) mAb U36 (cmAb U36) showed favorable targeting and (although not a primary objective) promising antitumor effects [20,21]. However, chimerization of mAb U36 had not resulted in a decrease of the immunogenicity because 5 of 12 patients showed development of human anti-chimeric antibodies (HACAs) [20]. Formation of HAMAs or HACAs should be eliminated to prevent allergic reactions and rapid clearance of the radioimmunoconjugate, especially when multiple administrations of the radioimmunoconjugate are anticipated. The engineering of humanized mAbs (hmAbs), being almost completely human apart from a small part of the antigen-binding sites, became the next approach to deal with this problem. In several studies, hmAbs showed excellent tumor targeting in combination with low or no immunogenicity [22,23].

To reduce immunogenicity, two humanized BIWA versions were developed, called BIWA 4 and BIWA 8. The intermediate-affinity mAb BIWA 4 was selected for further clinical evaluation rather than the high-affinity mAb BIWA 8 because of its superior tumor targeting in HNSCC-bearing nude mice [16].

In the present study, RIT with ^{186}Re-labeled hmAb BIWA 4 was evaluated in 20 head and neck cancer patients with regard to safety, maximum tolerated dose (MTD), pharmacokinetics, immunogenicity, and preliminary therapeutic potential. Three of these patients received a second

dose, which was the same or slightly different from the first dose.

Materials and methods

Patient eligibility

Patients with clinical evidence of recurrent locoregional and/or metastatic HNSCC, for whom no curative option was available, were candidates. A histologically confirmed HNSCC in the past was required for inclusion. Other eligibility criteria were an age between 18 and 80 years, a Karnofsky performance status above 60, and a life expectancy of at least 3 months. An interval of at least 4 weeks from the last chemotherapy or radiotherapy was required, as well as good recovery from prior treatment. Patients were excluded if their WBC count was less than 3.0×10^9/l, if their granulocyte count was less than 1.5×10^9/l, if their platelet count was less than 100×10^9/l, if the bilirubin level was greater than 30 μmol/l (upper limit of laboratory normals, 20 μmol/l), or if the serum creatinine concentration was greater than 150 μmol/l (upper limit of laboratory normals, 110 μmol/l). Other exclusion criteria were pregnancy, life-threatening infection, severe allergic condition, organ failure, hematological disorders, recent myocardial infarction on electrocardiogram or unstable angina pectoris, congestive heart failure, and bronchial asthma. Also, premenopausal women were excluded when not surgically sterile or not practicing acceptable means of birth control. The study was reviewed and approved by the institutional ethics committees of the VU University Medical Center (Amsterdam, The Netherlands) and UMC Nijmegen (Nijmegen, The Netherlands). All patients gave written informed consent after receiving a thorough explanation of the study.

hmAb BIWA 4 (bivatuzumab) and the v6 domain of CD44

mmAb BIWA 1 (Boehringer Ingelheim, Vienna, Austria), the parental mAb of BIWA 4, was generated by immunizing BALB/c mice with glutathione *S*-transferase fusion protein containing the human CD44 domains v3-v10 [14]. The epitope recognized by BIWA 1 has been mapped to the v6 domain of CD44. Homogenous expression of v6-containing CD44 isoforms has been observed in squamous cell carcinoma of the head and neck, lung, skin, esophagus, and cervix, whereas heterogeneous expression was found in adenocarcinomas of the breast, lung, colon, pancreas, and stomach. In normal tissues, expression has been found in epithelial tissues such as skin, breast, and prostate myoepithelium and bronchial epithelium [24].

Generation, production, and characterization of BIWA 4 have been described previously [16]. In short, mRNA was isolated from the BIWA 1 hybridoma cell line (Boehringer Ingelheim) using the QuickPrep mRNA Purification Kit (Pharmacia, Uppsala, Sweden). cDNA from heavy and light chain variable regions was generated by reverse transcription-PCR. Fragments were cloned into the TA cloning vector pCR II (Invitrogen, Groningen, The Netherlands) and sequenced. Two expression vectors derived from the plasmid pAD CMV1 [25] were constructed, carrying the constant regions of human γ-1 and of the human κ light chain, respectively. Subsequently humanized versions of the BIWA 1 heavy and light chain variable regions (generated by CDR grafting) were cloned in front of the immunoglobulin constant regions of the abovementioned expression vectors, resulting in the hmAb BIWA 4.

BIWA 4 was stably expressed in Chinese hamster ovary cells, whereas high producers were selected as described previously [16]. Cultivation was performed in proprietary serum-free medium TH-7 (Boehringer Ingelheim, Biberach an der Riss, Germany). Bulk substance from fermentation runs (titer after harvest, 90 mg/l) was purified according to a generic downstream process for mAbs consisting of ultra/diafiltration, affinity chromatography on protein A-Sepharose, microwave treatment at 80°C, nanofiltration, ultra/diafiltration, anion exchange chromatography on Q-Sepharose, and ultra/diafiltration. The bulk substance was formulated in PBS (pH 7.4) containing 0.02% Tween 20, filter sterilized, and dispensed aseptically into vials. Each vial contained 5 ml of BIWA 4 at a concentration of 5 mg/ml.

Radiolabeling and quality controls

For coupling of ^{186}Re to BIWA 4, the chelate *S*-benzoylmercaptoacetyltriglycine (MAG3) was used as described previously [26]. ^{186}Re and MAG3 were obtained from Mallinckrodt, Inc. (Petten, The Netherlands). The mean specific activity of ^{186}Re at the time of labeling was 11 ± 3 MBq/nmol (0.31 ± 0.07 mCi/nmol). After synthesis of ^{186}Re-MAG3, an esterification with tetrafluorophenol was performed. Subsequently, the ester was purified and conjugated to BIWA 4. Radiolabeled BIWA 4 was purified on a PD10 column (Pharmacia-Biotech, Woerden, The Netherlands) with 0.9% NaCl containing 5 mg/ml ascorbic acid (pH 5) as the eluent. Finally, the conjugates were filter sterilized. These procedures result in a sterile final product with endotoxin levels of < 5 endotoxin units per ml, as demonstrated in five preceding validation runs. The molar ratio of ^{186}Re-MAG3 to BIWA 4 was always < 4. The radiochemical purity of the conjugates as

assessed by high-performance liquid chromatography and thin-layer chromatography was always > 95% (mean, 98 ± 1.3%). After each preparation of ^{186}Re-BIWA 4, the immunoreactivity was determined by measuring binding to 0.1% paraformaldehyde-fixed cells of the HNSCC cell line UM-SCC-11B as described previously [16]. The immunoreactive fraction of the ^{186}Re-BIWA 4 preparations, as determined by a modified Lineweaver-Burk plot, ranged from 81% to 100% (mean, 90 ± 6.9%).

Prestudy screening and radiological assessment

The medical history and physical condition of all patients were examined, and routine laboratory analyses were performed, including complete blood cell counts, serum electrolytes, urine sediment, liver enzymes, and renal and thyroid functions. An electrocardiogram and a radiograph of the thorax were obtained. For all patients with locoregional tumor recurrence, a CT and/or magnetic resonance imaging (MRI) scan of the head and neck region was performed before treatment as has been described previously [18], and in cases with distant metastases, a CT scan of the region of interest was obtained. CT and/or MRI scans were also obtained at 6 weeks after administration for evaluation of RIT efficacy. To this end, perpendicular diameters of tumors were assessed by an experienced radiologist in both centers. In case of stable disease, follow-up assessments were, if possible, performed every 4 weeks.

For dosimetry, tumor volume was assessed by drawing regions of interest on consecutive CT or MRI slices with a VoxelQ system (Picker International, Highland Heights, OH), as described previously [20]. This system enables three-dimensional reconstruction and automated volume calculation.

Study design

RIT was performed with a starting activity dose of 0.74 GBq/m^2, followed by escalation with 0.37-MBq/m^2 increments of ^{186}Re-labeled BIWA 4. All patients received 50 mg of BIWA 4, a dose that was found to result in optimal tumor uptake and tumor : nontumor ratios in a preceding mAb dosefinding study in which doses of 25, 50, and 100 mg BIWA 4 were evaluated [27]. A complete pretreatment assessment was performed before the study, and blood samples were taken for pharmacokinetic analyses. Monitoring of vital functions (blood pressure, pulse rate, temperature, and breathing rate) was performed at the screening visit; before infusion; at 10, 60, 120, and 240 min after infusion; and 6 weeks after infusion. Patients

who developed an objective response or stable disease after the first dose of ^{186}Re-BIWA 4 were eligible for a second administration. They underwent the same visit schedule as for the first administration. As a safety precaution, all repeated administrations were conducted at least 3 months after the first administration, and the same inclusion/exclusion criteria were used as for the first dose.

Safety

After treatment, patients were admitted for approximately 21 h in a special treatment room at the Department of Nuclear Medicine, and thereafter they stayed an additional 3 days in a single room at the Department of Otolaryngology/ Head and Neck Surgery. Dose rates (in μSv/h) were measured 1 h after administration at a distance of 100 cm with a γ-radiation dose rate counter [at VU University Medical Center, Berthold LB 1230 (EG&G, Wildbad, Germany); at UMC Nijmegen, Automess 6150 AD 2 (Automess GmbH, Ladenburg, Germany)]. The patients were discharged 4 days after administration of ^{186}Re-BIWA 4, and the set of pretreatment laboratory analyses was repeated weekly for at least 6 weeks. The severity of toxicities was graded according to the National Cancer Institute Common Toxicity Criteria (CTC), version 2.0. The MTD was defined as the dose level at which grade 4 hematological or grade 3 non-hematological toxicity developed in not more than one of six patients.

Tumor response

Tumor response was assessed according to the WHO guidelines using physical examination or radiographic criteria. Stable disease was defined as a decrease of $< 50\%$ or an increase of $< 25\%$ of the sum of the perpendicular diameter products and no appearance of new lesions, which had to persist for at least 4 weeks. Progression was defined as a $\geq 25\%$ increase in the size of one or more lesions or the appearance of a new lesion.

Imaging studies

Simultaneously acquired planar anterior and posterior whole-body scans were obtained within 1 h after administration of the radioimmunoconjugate; 21, 48, 72, and 144 h after administration of the radioimmunoconjugate; and, if feasible, for up to 2 weeks after administration of the radioimmunoconjugate. For all scintigraphic studies, a large field-of-view gamma

camera [at VU University Medical Center, Dual Head Genesys Imaging System (ADAC Laboratories, Milpitas, CA); at UMC Nijmegen, Siemens Multispect 2 (Siemens, Erlangen, Germany)] equipped with low-energy high-resolution parallel-hole collimators and connected to a computer system [at VU University Medical Center, Pegasys (ADAC Laboratories); at UMC Nijmegen, ICON version 7.1 (Siemens)] was used. Camera quality control was performed at each imaging session. With the aliquot retained from the radioimmunoconjugate preparation for injection, a weighed dilution of the injected patient dose was prepared as standard, put in an Adams' phantom, and measured simultaneously during whole-body imaging. Lateral, anterior, and posterior planar images of the head and neck region were acquired at 21, 48, 72, and 144 h. Single photon emission computed tomography (SPECT) images were acquired at 72 h. Acquisition parameters for planar and SPECT images were as described previously [18], with a Hanning filter used for postfiltering (cutoff at 1 cycle/cm). In each of the study centers, all images were interpreted by one experienced examiner, who was unaware of the site of recurrence and/or the presence of distant metastases.

Dosimetry

Dosimetry to assess dose delivery to whole body, bone marrow, organs, and tumor was performed as described previously [20]. Patients 5 and 17 were excluded from dosimetric analysis due to insufficient data. In short, whole-body scintigraphy was used to draw regions around organs and sites of interest. Residence times in these organs and sites were calculated and entered in the MIRDOSE3 computer program, version 3.1 (Oak Ridge Associated Universities, Oak Ridge, TN). If CT/MRI scanning before treatment with ^{186}Re-BIWA 4 showed a measurable tumor lesion, and if this lesion was visible on scintigraphy after RIT, dosimetry of the tumor was performed. The red marrow dose was calculated using a blood-derived method as described previously [20,28].

Pharmacokinetics

Serial blood samples were taken from a peripheral vein of the arm opposite to the infusion site at the following time points: preinfusion; at the end of the infusion; and at 5 and 30 min and 1, 2, 4, 16, 21, 48, 72, and 144 h after administration of ^{186}Re-BIWA 4. Preliminary results obtained from the first four patients showed that blood sampling at additional time points in the second week after administration would improve the charac-

terization of the ^{186}Re-BIWA 4 pharmacokinetics. Therefore, for patients 5–20, blood samples were also taken at 240 and 336 h after administration. Plasma samples were prepared for determination of the concentration of immunoreactive BIWA 4 by validated ELISA methods, essentially as described previously [19]. In this sandwich-type ELISA, microtiter plates were absorptively coated with the fusion protein GST-CD44v6. In a first step, BIWA 4 in the plasma sample bound to the immobilized antigen CD44v6. After incubation, unbound BIWA 4 and plasma components were removed by washing. In a second step, rabbit anti-human IgG labeled with horseradish peroxidase (DAKO, Copenhagen, Denmark) was used for detection of bound BIWA 4, and tetramethyl-benzidine (Kirkegaard & Perry, Gaithersburg, MD) was used for detection of enzyme activity.

In addition, whole-blood and serum samples were prepared and counted in a gamma counter [at VU University Medical Center, 1470 Wizard (Wallac, Turku, Finland); at UMC Nijmegen, 1480 Wizard (Wallac)], and radioactivity levels were expressed as percentage of injected dose per kilogram (% ID/kg). Background activity and decay were corrected for, and the % ID/kg was determined by comparison with an aliquot retained from the conjugate preparation for injection.

Human anti-BIWA 4 response

Evaluation of the immunogenicity of the BIWA 4 radioimmunoconjugate was conducted by determination of human anti-hmAbs in serum samples taken before administration of ^{186}Re-BIWA 4 and 1 and 6 weeks after administration, using a validated bridging ELISA. In short, BIWA 4 antibodies labeled with the chelator MAG3 were immobilized onto microtiter plates. Antibodies to BIWA 4-MAG3 present in the serum sample bound simultaneously to the solid phase and to biotinylated BIWA 4-MAG3 that was added at the same time in a fixed amount. Streptavidin coupled to horseradish peroxidase (Boehringer Mannheim, Mannheim, Germany) was used for signal generation by the peroxidase/tetramethyl-benzidine system. Due to the lack of a positive human anti-BIWA 4 serum, which would be desirable as a standard, the validation of the present assay was done with a rabbit antiserum from an animal that was previously immunized with nonradioactive ^{185}Re-MAG3-BIWA 4. The assay only enabled the relative measurement of the human anti-human antibody (HAHA) titer in equivalents of the anti-BIWA 4 titer of the reference rabbit serum. For an easier handling of data, the dilution factors of the rabbit reference serum were converted into Boehringer Ingelheim titer units. The titer unit was defined as dilution of the rabbit reference serum (1:x) multiplied by 18,000.

Assay performance during the study was assessed by back-calculation of calibration standards, tabulation of the standard curve fit function parameters, measurement of quality control samples, and construction of a precision profile. Triplicate determinations in three randomly assigned wells of a microtiter plate were used for unknown samples, calibration standards, and quality controls. The lower and upper limits of determination of the assay were 0.180 and 60 Boehringer Ingelheim titer units (1:100,000 to 1:300 dilution of the rabbit reference serum). A serum sample was considered HAHA positive only if all of the following criteria were met: (a) the measured titer was above the lower limit of determination/quantification; (b) the titer in the postinjection sample was at least two times higher than that in the preinjection sample; (c) the sample could be serially diluted with a strong correlation between titer and dilution factor; (d) the titer could be blocked by addition of BIWA 4; and (e) the titer could not be blocked by a non-specific IgG mAb.

Results

Twenty patients (14 males and 6 females; age range, 42–73 years; mean age, 58 years) entered this study. Their characteristics are shown in Table 7.1. Thirteen patients had received surgical treatment of their disease at an earlier stage. All patients had been treated previously with radiotherapy, and some of them had also been treated with chemotherapy. Two patients were treated at the lowest dose level of 0.74 GBq/m^2, four patients were treated at 1.11 GBq/m^2 (one patient more than planned because of death of one of the patients during follow-up), three patients were treated at 1.48 GBq/m^2, six patients were treated at 1.85 GBq/m^2, and five patients were treated at 2.22 GBq/m^2. Three patients received a second administration of 1.85 GBq/m^2 ^{186}Re- BIWA 4 (Table 7.2).

Patient no.	Sex	Age (yrs)	Site of disease	Prior treatment besides radiotherapy
1	M	61	Oral cavity, and metastasis parotid gland, bilateral	Surgery + MTX[a] + Cis
2	F	53	Neck recurrence, right side	Surgery
3	M	61	Neck recurrence, left side	Surgery
4	M	55	Oral cavity, and neck recurrence, left side	Surgery + MTX
5	F	65	Hypopharynx, and metastases thoracic wall and lung	Doce + Cis + 5-FU
6	M	63	Parotic gland, and neck recurrence, left side	Cis + 5-FU
7	M	67	Neck recurrence, bilateral	Surgery
8	M	42	Neopharynx, and neck recurrence, right side	Surgery
9	F	50	Neck recurrence, right side, and metastasis left lung	Cis
10	M	58	Tonsillar cavity and base of tongue, right side	Cis + Vin + Bleo + MTX
11	M	62	Hypopharynx, neck recurrence left side, and lung metastasis	MTX
12	M	51	Neck recurrence, bilateral, and lung metastasis, bilateral	None
13	F	55	Floor of mouth, and lung metastasis	Surgery
14	M	55	Neck recurrence, right side	Surgery
15	M	73	Neck recurrence at tracheostoma	Surgery
16	F	66	Nasal vestibule and neck recurrence, right side	Surgery + Cis
17	M	53	Multiple s.c. metastases	Surgery
18	M	55	Recurrent disease mandibula, left side	Surgery + MTX[b]
19	M	49	Skin metastasis neck, left side, and lung metastasis, right side	Surgery + Doce + Cis + 5-FU
20	F	67	Oropharynx and sinus maxillaris, right side, and lung metastasis	Cyclo + Etopo + Doxorub

[a] MTX, methotrexate; Cis, cisplatin; Doce, docetaxel; 5-FU, fluorouracil; Vin, vincristin; Bleo, bleomycin, Cyclo, cyclophosphamide; Etopo, etoposide; Doxorub, doxorubicin

[b] MTX prescribed for rheumatoid arthritis.

Table 7.1 Patient and tumor characteristics

Patient no.	Dose ^{186}Re (GBq/m^2)	Total dose (GBq)	Platelet nadir	Toxicity grade	WBC nadir	Toxicity grade	Granulocyte nadir	Toxicity grade	Significant non-hematological toxicity[a]
1	0.74	1 27	199	0	10.1	0	9 55	0	None
2	0.74	1.18	321	0	7.5	0	6.45	0	Facial edema (1)
3	1.11	2.06	52	2	1.8	3	1 30	2	None
4	1 11	1.98	183	0	7.4	0	6 36	0	None
5	1.11	1.64	NA[b]	NA	NA	NA	NA	NA	Quincke's edema (3), Rash (3)
6	1.11	2.08	143	0	5.2	0	4 42	0	None
7	1.48	2.76	277	0	10.6	0	9 33	0	None
8	1.48	2.60	89	1	3.0	1	2 43	0	None
9	1.48	2.40	202	0	4.9	0	4 12	0	None
10	1.85	3 38	89	1	3.4	0	2 01	0	None
11a	1.85	3.12	122	0	4 5	0	2 34	0	Gout (2), Loss of taste (2)
11b[c]	1 85	3.17	209	0	6.4	0	4 75	0	Loss of taste (2)
12a	1.85	3.34	117	1	2 3	2	1 45	2	Oral mucositis (2)
12b[c]	1.85	3.35	43	3	1 7	3	0 99	3	Oral mucositis (2)
13	2.22	3.61	25	3	0 7	4	0 23	4	Fever (3), febrile neutropenia (3), oral mucositis (2), Candida stomatitis (2)
14a	2 22	3.83	78	1	2.7	2	1 70	1	Oral mucositis (2)
14b[c]	1.85	3.16	80	1	3 9	0	2 89	0	Oral mucositis (1)
15	2 22	4.00	47	3	2 0	2	0 96	3	None
16	2 22	3.31	18	3	1 2	3	0 70	3	Fever (3), febrile neutropenia (3), oral mucositis (2), Candida stomatitis (2), petechiae (1)
17	2 22	3.61	12	3	0 4	4	0 03	4	Fever (4), febrile neutropenia (4), increased anemia (4), fatigue (3)
18	1.85	3.22	8	4	0.9	4	1 52	1	Minor signs of petechiae (1)
19	1 85	3.67	94	1	2.3	2	1 52	1	None
20	1 85	2.57	65	2	2 9	2	2 00	0	None

[a] Possibly related to study drug

[b] NA, not applicable due to insufficient follow-up.

[c] Patient received ^{186}Re-BIWA 4 on two occasions.

Table 7 2 Administered dose and toxicity

Safety and non-hematological toxicity

Administration of ^{186}Re-BIWA 4 was tolerated well, and no side effects were observed directly after and during the first few days after treatment. No changes occurred in the physical parameters during the first few days after administration, and no changes in blood parameters indicated toxicity of organs such as the liver or kidneys. Non-hematological toxicity defined as drug-related CTC grade 3 or 4 occurred in four patients (Table 7.2). One patient (patient 5) treated at the 1.11-GBq/m^2 dose level was admitted to the hospital because of unexplained seizures 5 days after treatment. During hospitalization, Quincke's edema or angioedema caused respiratory distress 8 days after the start of RIT, which was treated with infusion of prednisolone and inhalation of bronchodilatators. After treatment for low serum sodium levels and treatment with antiepileptic drugs, the patient left the hospital again 11 days after the start of RIT. She was found dead at home 22 days after start of treatment. No signs indicating a relationship between antibody administration and death were noticed, but the possibility of a relationship could not be excluded. Permission for autopsy was not given by the relatives. Analysis of pre- and posttreatment serum samples showed absence of HAHA. Because this patient was not evaluable for hematological toxicity and antitumor response, an extra patient was treated at the 1.11-GBq/m^2 dose level.

Febrile neutropenia occurred in patients 13 and 16 (both CTC grade 3) and in patient 17 (CTC grade 4), all of whom were treated at the 2.22-GBq/m^2 dose level. All three patients received empirical antibiotic and antimycotic treatment until WBC counts had recovered and the patients were afebrile. CTC grade 3 fatigue occurred in patient 17 at approximately 4 weeks after administration of 2.22 GBq/m^2 ^{186}Re-BIWA 4. The fatigue was most likely related to the aggravation of the pre-existing anemia. Main non-hematological toxicity consisted of mild (maximum CTC grade 2) mucositis (Figure 7.1) in two of the six patients treated at the 1.85-GBq/m^2 dose level and in three of the five patients treated at the 2.22-GBq/m^2 dose level. This form of toxicity is most likely drug-related because the CD44v6 target antigen is known to be expressed in normal mucosa. The mucositis usually started 1–2 weeks after administration of the conjugate and disappeared 2 weeks after onset. Most other toxicity was not related to the conjugate, except for reversible loss of taste in one patient, observed after both injections of ^{186}Re-BIWA 4.

For patients treated at the MTD level, mean radiation dose rate measured 1 h after injection at a distance of 100 cm was 4.9 μSv/h. These dose rates would result in cumulative doses far less than the annual limit of 2 mSv, which, according to Dutch guidelines for radionuclide therapy, is

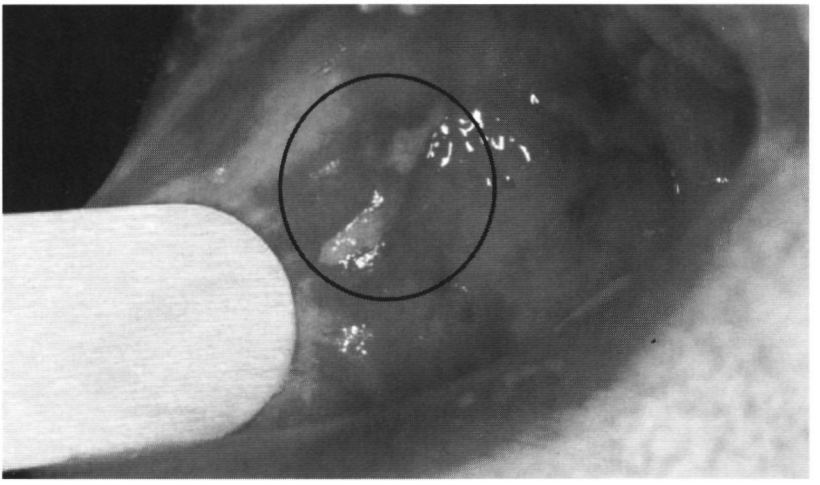

Figure 7.1: Example of oral mucositis (patient 12). Mucositis (encircled) occurred in this patient from day 11–32 after injection of 1.85 GBq/m^2 ^{186}Re- BIWA 4.

considered to be acceptable for medical personnel and family members.

Hematological toxicity

The bone marrow appeared to be the dose-limiting organ. A significant decrease of platelet and WBC counts was observed for patients treated at the highest dose levels, with a nadir of 4–5 weeks after injection of the conjugate (Figure 7.2). Hematological dose-limiting toxicity defined as drug-related CTC grade 4 was reported in three patients (Table 7.2). Reversible CTC grade 4 leukocytopenia and granulocytopenia were observed in two patients (patients 13 and 17) treated at 2.22 GBq/m^2, at 4 and 5 weeks after injection, respectively. In addition, the anemia present before entering the study worsened slowly in patient 17 and finally resulted in a CTC grade 4 anemia, which was treated with blood transfusions. Reversible CTC grade 4 thrombocytopenia and grade 4 leukocytopenia were observed in one patient (patient 18) treated at 1.85 GBq/m^2, who received concomitant treatment with methotrexate for rheumatoid arthritis. Clinical symptoms of thrombocytopenia in this patient consisted of mild petechiae. Patient received a total of two pooled donor units of platelets on day care basis. All three patients with grade 4 hematological toxicity received antibiotic and antimycotic treatment until WBC counts had recov-

ered and the patient was afebrile. MTD was established at 1.85 GBq/m^2. Nadirs of each individual patient are listed in Table 2. Drug-related thrombocytopenia and leukocytopenia occurred about 21 days after start of RIT, and the patients started recovering from these conditions before 6 weeks postinjection.

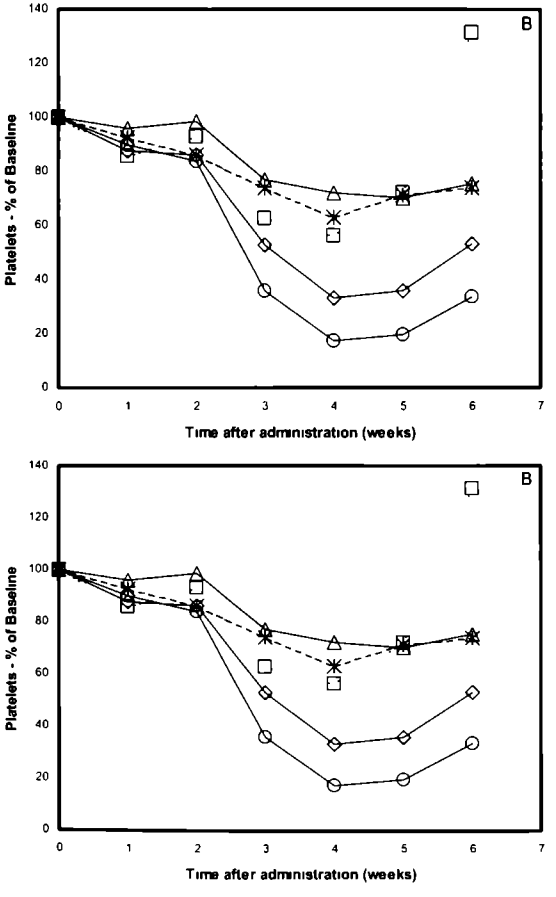

Figure 7.2· Relationship between myelotoxicity and administered ^{186}Re- BIWA 4 radioactivity dose Myelotoxicity, measured as mean percentage decrease from baseline for WBCs (A) and platelets (B) after administration of 0.74 (∗), 1.11 (□), 1.48 (△), 1 85 (◇), or 2.22 GBq/m^2(○).

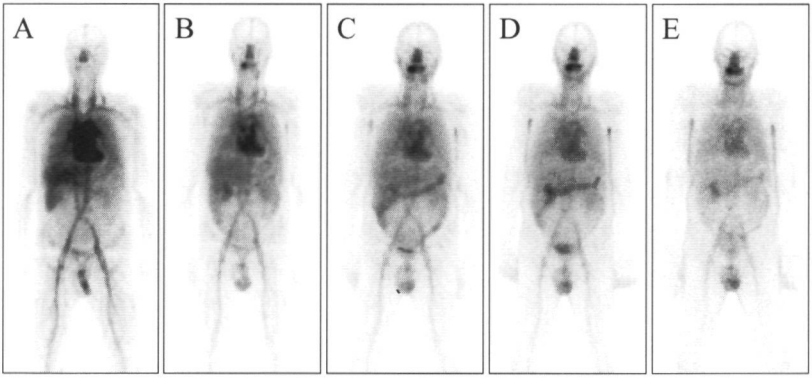

Figure 7.3: Whole-body scans of patient 10 acquired within 1 h (A) after administration of ^{186}Re-BIWA 4 and after 21 (B), 48 (C), 72 (D), and 144 h (E). Immediately after injection, activity is mainly present in blood pool. Relative uptake of the radioimmunoconjugate in the tumor in the right tonsillar cavity and base of tongue increases over time.

Imaging

Whole-body scans obtained directly after administration of ^{186}Re-BIWA 4 showed mainly blood-pool activity, which decreased over time. Representative whole-body scans are shown in Figure 7.3. At later intervals, a homogenous distribution was observed in the lungs, liver, spleen, and kidneys, whereas relative uptake at tumor sites gradually increased. In general, no selective accumulation at nontumor sites was visible except for uptake in squamous epithelia (oral mucosa, nasal mucosa, and skin), testes, feces, and urine (bladder). Planar and SPECT images obtained showed improved delineation of small tumors in the head and neck region (see Figure 7.4). However, visualization of distant metastases, concerning mainly lung metastases, was in most cases hampered by the presence of blood-pool activity and the small size of the lesions.

Pharmacokinetics

Concentrations of ^{186}Re-BIWA 4 were assessed by measuring immunoreactive BIWA 4 in plasma with an ELISA assay as well as by measuring radioactivity in serum. Because each patient received BIWA 4 as a 50-mg infusion, the immunoreactive BIWA 4 concentrations are presented as a group to demonstrate the consistency of data across patients (Fig-

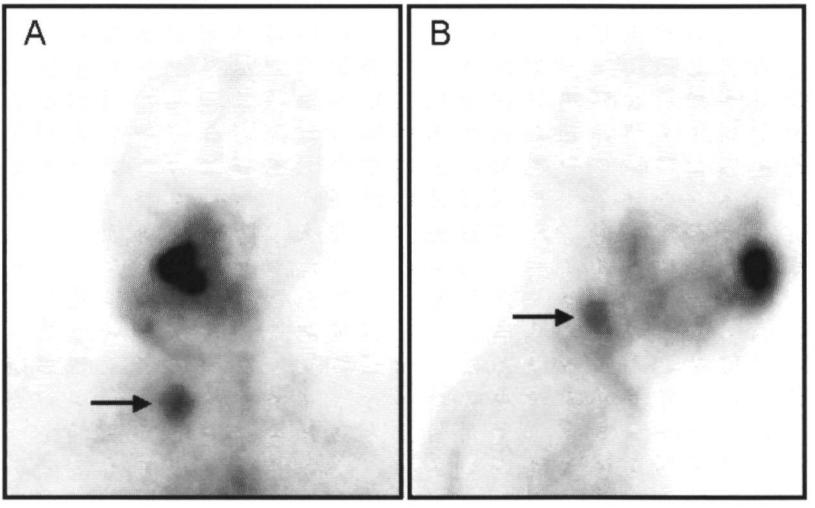

Figure 7.4: Frontal (A) and lateral (B) planar image of the head and neck region of patient 16, 72 h after administration of ^{186}Re-BIWA 4. Accumulation of radiolabeled hmAb BIWA 4 is visible in tumor recurrence in right nasal cavity, and at two cutaneous metastases in the neck (*arrows*).

ure 7.5A). In a similar way, the normalized (% ID/kg) radioactivity data are presented (Figure 7.5B). Overlaying the immunoreactivity and radioactivity data demonstrates that plasma BIWA 4 concentrations and radioactivity serum concentrations track each other well, indicating that the ^{186}Re-BIWA 4 conjugate remained stable after i.v. injection. This graphical consistency between plasma BIWA 4 concentrations and serum radioactivity concentrations was observed for each patient and within the three patients receiving ^{186}Re-BIWA 4 twice (Figure 7.6). However, modeling of the data revealed that the geometric mean serum half-life for the radioactive portion of ^{186}Re-BIWA 4 was significantly longer than the plasma half-life of BIWA 4 portion: 126.5 ± 36.3 *versus* 95.1 ± 15.9 h ($P < 0.001$). Differences noted in the modeling occurred at late time points, when most of the radioactivity was already eliminated or physically decayed. These data might indicate that a small proportion of injected radiolabeled BIWA 4 loses binding capacity at late time points after injection, by which detection in ELISA becomes impossible.

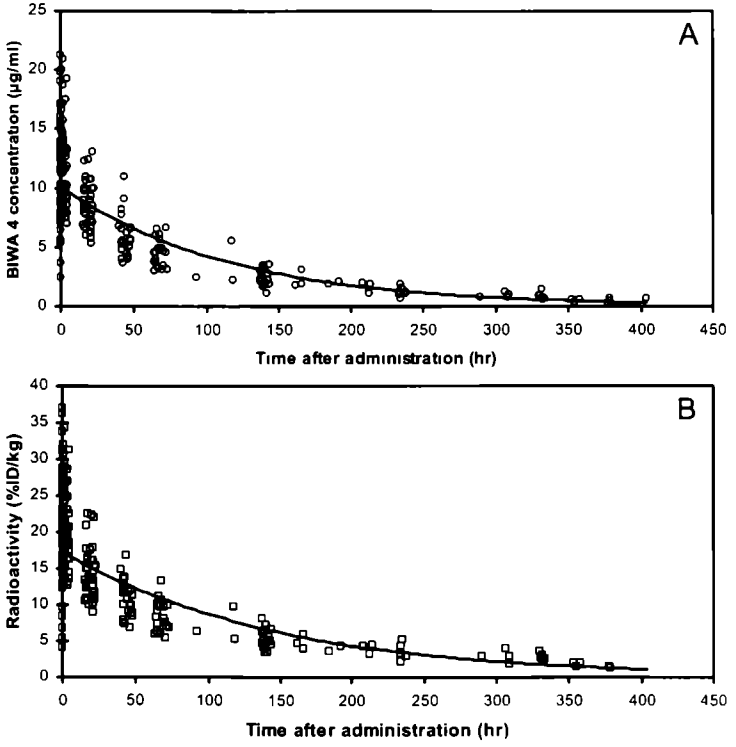

Figure 7.5: Average blood clearance curves of ^{186}Re-BIWA 4 as assessed by ELISA for measuring immunoreactive BIWA 4 in plasma (A) or by ^{186}Re radioactivity measurement in serum (B). Individual data points are depicted after administration of 50 mg of BIWA 4 labeled with 1.18–4.00 GBq of ^{186}Re to 20 HNSCC patients.

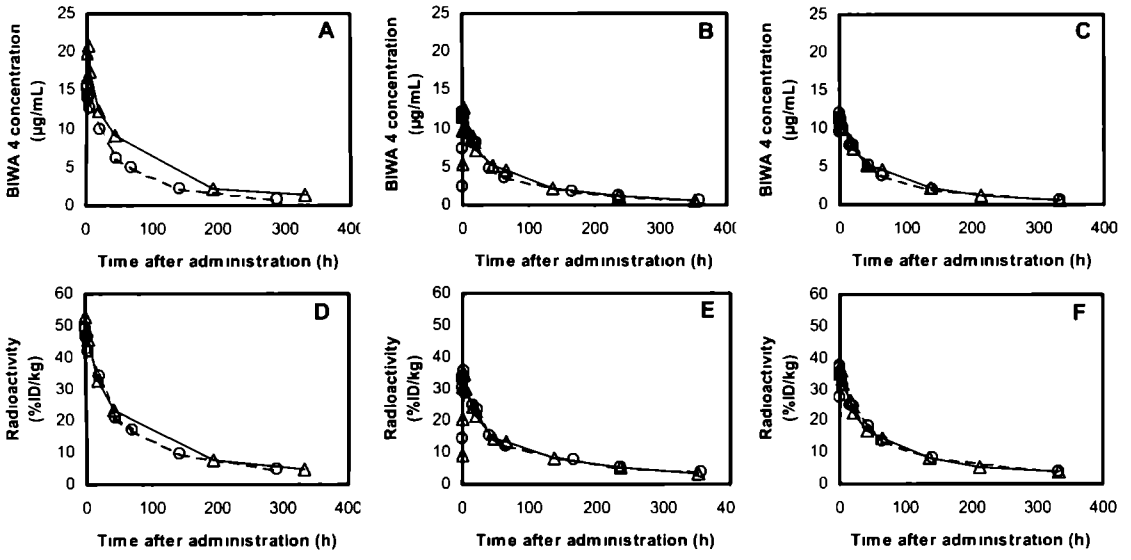

Figure 7 6: Blood clearance curves of ^{186}Re-BIWA 4 for patients who received the conjugate twice. Blood clearance was assessed by ELISA for measuring immunoreactive BIWA 4 in plasma (A-C) or by ^{186}Re activity measurement in serum (D-F), after the first (△) and second (○) administration of ^{186}Re-BIWA 4 to patients 11 (A and D), 12 (B and E), and 14 (C and F).

Dosimetry

Twenty-one patient studies [5 female, 13 male (of which 3 patients received two administrations)] could be used for dosimetry. The mean whole-body absorbed self-dose was 0.28 ± 0.02 mGy/MBq for males and 0.37 ± 0.03 mGy/MBq for females. The mean red marrow dose was 0.49 ± 0.03 mGy/MBq for males and 0.64 ± 0.03 mGy/MBq for females. The normal organ with the highest absorbed dose appeared to be the kidneys (mean dose in males, 1.61 ± 0.75 mGy/MBq; mean dose in females, 2.15 ± 0.95 mGy/MBq, which is not expected to lead to renal toxicity). The doses delivered to the tumors (n = 15), recalculated to the MTD level of 1.85 GBq/m^2, ranged from 3.8 to 76.4 Gy for tumors ranging in size from 285.9 to 5.1 cm^3. The median absorbed dose was 12.4 Gy. The largest tumor (285.9 cm^3) showed the lowest absorbed dose (3.8 Gy), whereas the two tumor localizations with the highest absorbed dose (65.1 and 76.4 Gy) appeared to be small lesions (11.5 and 5.1 cm^3, respectively). However, no clear correlation was found between tumor absorbed dose and tumor size.

Human anti-BIWA 4 response

HAHA analyses were evaluable for all patients. Two of the 20 patients (patients 10 and 17) showed a HAHA response (Table 7.3). For both patients, the titer of the week 6 sample was elevated and regarded as HAHA positive.

Tumor response

All patients treated with doses of up to 1.48 GBq/m^2 ^{186}Re-BIWA 4 showed progressive disease upon RIT. One patient (patient 5) was not evaluable for tumor size measurements, due to intercurrent death (see "Safety and non-hematological toxicity").

Three of the six patients (patients 10, 11, and 12) treated with 1.85 GBq/m^2 ^{186}Re-BIWA 4 developed stable disease after the first administration (Table 7.4). As a result, patients 11 and 12 received a second administration, and progressive disease was observed after a total of 18 weeks (patient 11) and 21 weeks (patient 12) after first administration of the trial drug.

One patient (patient 14) treated with 2.22 GBq/m^2 ^{186}Re-BIWA 4 experienced stable disease after the first treatment. Progressive disease was observed after a second treatment with 1.85 GBq/m^2 ^{186}Re-BIWA 4, approximately 24 weeks after the first administration of the trial drug.

Patient no.	BIWA 4 dose (mg)	HAHA titer Before RIT	1 week after RIT	6 weeks After RIT
1	50	< 0.180	< 0.180	< 0.180
2	50	< 0.180	< 0.180	< 0.180
3	50	< 0.180	0.570	0.784
4	50	< 0.180	< 0.180	< 0.180
5	50	< 0.180	< 0.180	< 0.180[a]
6	50	< 0.180	< 0.180	< 0.180
7	50	< 0.180	< 0.180	< 0.180
8	50	0.532	0.425	0.404
9	50	0.584	0.977	0.952
10	50	< 0.180	< 0.180	1.01[b]
11a	50	< 0.180	< 0.180	< 0.180
11b	50	< 0.180	< 0.180	< 0.180
12a	50	< 0.180	< 0.180	< 0.180
12b	50	< 0.180	< 0.180	< 0.180
13	50	< 0.180	< 0.180	< 0.180
14a	50	< 0.180	< 0.180	< 0.180
14b	50	< 0.180	< 0.180	< 0.180
15	50	< 0.180	< 0.180	< 0.180
16	50	< 0.180	< 0.180	< 0.180
17	50	< 0.180	< 0.180	25.2[b]
18	50	< 0.180	< 0.180	< 0.180
19	50	< 0.180	< 0.180	< 0.180
20	50	< 0.180	< 0.180	< 0.180

[a] Week-6 sample taken 2 weeks after RIT.
[b] Positive responses.

Table 7.3: Human anti-hmAb BIWA 4 antibody response

The overall time to progression for patients who did not respond to therapy ranged from 0 to 55 days, with a mean of about 5-6 weeks, irrespective of the treatment group. The survival time of the patients who did not obtain stable disease upon ^{186}Re-BIWA 4 treatment ranged from 21 to 219 days. For the four patients with stable disease, the survival time ranged from 217 to 403 days.

Patient no.	Dose ^{186}Re (GBq/m^2)	Pretreatment tumor measurements (mm^2)	Type of investigation	Response to therapy	Duration of response (weeks)
1	0.74	10,304/800/225	MRI	Progression	NA[a]
2	0.74	760	CT	Progression	NA
3	1.11	1,120	CT	Progression	NA
4	1.11	750	CT	Progression	NA
5	1.11	1,600/2,700/324	CT	Not evaluable	NA
6	1 11	600	CT	Progression	NA
7	1.48	396/1,428	MRI	Progression	NA
8	1.48	432	CT	Progression	NA
9	1.48	608/173/127	CT	Progression	NA
10	1.85	450	CT	Stable disease	6
11a	1.85	126/2,025	CT	Stable disease	18[b]
11b	1.85	126/2,025	CT		
12a	1.85	81/100/100/25/16	CT	Stable disease	21[b]
12b	1.85	81/81/100/25/16	CT		
13	2.22	1,900	CT	Progression	NA
14a	2.22	1,378	CT	Stable disease	24[b]
14b	1.85	1,440	CT		
15	2.22	2,250	Clinical	Progression	NA
16	2.22	2,100/225	CT	Progression	NA
17	2.22	216/196/289/350/196/100/196/150/16/80	Clinical	Progression	NA
18	1.85	396	CT	Progression	NA
19	1.85	750/144	CT	Progression	NA
20	1.85	180/14/165	MRI	Progression	NA

[a] NA, not applicable

[b] Patient received a second dose of ^{186}Re-BIWA 4, 3 months after the first administration

Table 7 4: Tumor response

Discussion

RIT with ^{186}Re-BIWA 4 seems to be safe, and no severe side effects were observed in this phase I study besides dose-limiting myelosuppression at a ^{186}Re dose level of 2.22 GBq/m^2 Furthermore, mild mucositis was observed at the highest ^{186}Re dose levels of 1.85 and 2.22 GBq/m^2. Mucositis is most probably caused by binding of ^{186}Re-BIWA 4 to the CD44v6 target antigen as present in oral mucosa. The MTD of ^{186}Re-BIWA 4 was established at 1.85 GBq/m^2, which seems to be higher than the 1.0 GBq/m^2 found in a previous phase I trial with the other anti-CD44v6 conjugate ^{186}Re-cmAb U36 [20] In the trial with ^{186}Re-cmAb U36, no mucositis became apparent. Because BIWA 4 and cmAb U36 have a comparable biological half-life in blood, differences in MTD cannot be explained by differences in pharmacokinetics. We believe that the large increments of the radiation dose-escalation steps used in the ^{186}Re-cmAb U36 phase I trial can partly explain the difference in MTD and that the use of smaller dose-escalation steps would most likely have resulted in a higher MTD for ^{186}Re-cmAb U36. Also, the heterogeneity of the HNSCC patient population might have contributed to this difference.

Of great importance is the low immunogenicity of this humanized mAb directed against the CD44v6 antigen. Ten percent of the patients treated in the present study developed HAHAs. In the meantime, 28 more patients have been treated with 25-100 mg of radiolabeled BIWA 4 in three parallel radioimmunoscintigraphy/biodistribution studies with HNSCC, non-small cell lung cancer, and breast cancer patients. HAHA responses were observed in none of these patients, resulting in an overall HAHA response rate of 4% for all four studies. This is considerably lower than the 40% HACAs as found with the cmAb U36 [20] and the 90% HAMAs as found with the parental mmAb BIWA 1 [19] None of the three patients who received a second administration developed HAHAs, which illustrates the possibility for repeated treatment with BIWA 4

Humanization of other mAbs has been performed with variable success. For instance, hmAb M195 elicited no immune response in a study group of 14 patients [23], compared with 37% HAMAs found with mmAb M195 [29] Furthermore, hmAb BrE-3 showed 14% HAHAs [22], compared with mmAb BrE-3, which showed immunogenicity in 46 7% [30] and 83% [31], respectively On the other hand, hmAb A33 elicited HAHAs in 26 of 41 patients [32] Although significantly lower as compared with its parental mmAb A33, for which HAMAs were found in all treated patients [33], this example illustrates that humanization does not always solve the problem of immunogenicity

A secondary objective in this phase I study was to determine the therapeutic effects of RIT with ^{186}Re-BIWA 4. Stabilization of tumor growth was observed in three of six patients treated at the MTD level, with durations ranging from 6 to 21 weeks. This is consistent with efficacy results obtained in previous phase I RIT trials with ^{186}Re-cmAb U36. In a first phase I trial with ^{186}Re-cmAb U36, stable disease was observed in one of six patients treated at MTD. In a second phase I trial with ^{186}Re-cmAb U36, reinfusion of granulocyte colony-stimulating factor-stimulated unprocessed whole blood was used to reduce myelotoxicity and to increase the MTD [21]. In this procedure, granulocyte colony-stimulating factor is administered s.c. at home during 5 days before the start of RIT. On day 0, just before administration of ^{186}Re-labeled mAb, 1 liter of whole blood is harvested and kept unprocessed at 4 °C until reinfusion after 72 h. Indeed, by using this facile procedure, the administered dose could be increased from 1.0 to 2.0 GBq/m^2, without exceeding grade 3 myelotoxicity and grade 2 mucositis. In this particular study, stable disease was observed in five of nine patients, for a period ranging from 3 to 7 months. All three patients treated at the highest dose level showed stable disease. Whether such a procedure for further dose escalation is also applicable for ^{186}Re-BIWA 4 remains to be established. It might well be that a second dose-limiting toxicity, most probably mucositis, will become manifest. Furthermore, it has to be considered that all HNSCC patients included in the phase I RIT trials described above had a history of external beam irradiation, which had caused severe mucositis in some of the patients.

The observation of antitumor effects in patients with bulky disease offers opportunities for further development of RIT with single or multiple doses of ^{186}Re-labeled BIWA 4 in an adjuvant setting. The tumor absorbed doses, recalculated to MTD level, ranged from 3.8 to 76.4 Gy, whereas the median absorbed dose was 12.4 Gy. The tumor with the highest absorbed dose of 76.4 Gy appeared to be a small lesion of 5.1 cm^3, which remained stable in size upon RIT (patient 10). It is unlikely that antitumor effects are caused by immune modulating effects because BIWA 4 lacks antibody-dependent cell-mediated cytotoxicity or complement-dependent cytotoxicity-mediating activity *in vitro*. Recently, we reported on the relationship between HNSCC size and mAb accumulation [34]. Data for this report were obtained from several radioimmunoscintigraphy and biodistribution studies with the anti-HNSCC mAbs E48 and U36 in HNSCC patients. mAb uptake in small-volume tumors (1 cm^3) was approximately 4 times higher than uptake in tumors with a large volume (> 50 cm^3). Therefore, in our view, these data justify evaluation of RIT with ^{186}Re-BIWA 4 as a systemic adjuvant treatment.

In conclusion, this study shows that RIT with ^{186}Re-BIWA 4 is safe. By using BIWA 4, a humanized anti-CD44v6 mAb, the rate of HAHA responses was reduced to a minimum, and repeated administrations appeared possible. The MTD was established at 1.85 GBq/m^2, at which dose level stabilization of disease was observed in three of six inoperable HNSCC patients with bulky disease. The application of RIT with ^{186}Re-BIWA 4 therefore holds promise, especially in an adjuvant setting.

Acknowledgments

We thank F.G. van Schaijk, M. Siegmund, and M.J.W.D. Vosjan for radiolabeling support and pharmacokinetic determinations; Dr. U. Kunz for pharmacokinetic and HAHA analyses; Prof. J.A. Castelijns and Dr. F. Joosten for CT and MRI examinations; M. van der Vlies for supervision on radiation safety issues; and Drs. E.F.I. Comans, R. Pijpers, P.G.H.M. Raymakers, M.A.W. Merkx, C.M.L. van Herpen, and Prof. P.C. Huijgens for clinical support.

References

1. Parkin DM, Bray F, Ferlay J, Pisani P. Estimating the world cancer burden: Globocan 2000. *Int J Cancer* 2001; 94: 153-156.

2. Vokes EE, Weichselbaum RR, Lippman SM, Hong WK. Head and neck cancer. *N Engl J Med* 1993; 328: 184-194.

3. Dennington ML, Carter DR, Meyers AD. Distant metastases in head and neck epidermoid carcinoma. *Laryngoscope* 1980; 90: 196-201.

4. Zbaren P, Lehmann W. Frequency and sites of distant metastases in head and neck squamous cell carcinoma. An analysis of 101 cases at autopsy. *Arch Otolaryngol Head Neck Surg* 1987; 113: 762-764.

5. Nishijima W, Takooda S, Tokita N, Takayama S, Sakura M. Analyses of distant metastases in squamous cell carcinoma of the head and neck and lesions above the clavicle at autopsy. *Arch Otolaryngol Head Neck Surg* 1993; 119: 65-68.

6. Leemans CR, Tiwari R, Nauta JJP, van der Waal I, Snow GB. Recurrence at the primary site in head and neck cancer and the significance of neck lymph node metastases as a prognostic factor. *Cancer* 1994; 73: 187-190.

7. Leemans CR, Tiwari R, Nauta JJP, van der Waal I, Snow GB. Regional lymph node involvement and its significance in the development of distant metastases in head and neck carcinoma. *Cancer* 1993; 71: 452-456.

8. Postema EJ, Boerman OC, Oyen WJG, Raemaekers JMM, Corstens FHM. Radioimmunotherapy of B-cell non-Hodgkin's lymphoma. *Eur J Nucl Med* 2001; 28: 1725-1735.

9. Witzig TE, White CA, Wiseman GA, Gordon LI, Emmanouilides C, Raubitschek A, Janakiraman N, Gutheil J, Schilder RJ, Spies S, Silverman DHS, Parker E, Grillo-Lpez AJ. Phase I/II trial of IDEC-Y2B8 radioimmunotherapy for treatment of relapsed or refractory CD20+ B-cell non-Hodgkin's lymphoma. *J Clin Oncol* 1999; 17: 3793-3803.

10. Witzig TE, Gordon LI, Cabanillas F, Czuczman MS, Emmanouilides C, Joyce R, Bartlett NL, Wiseman GA, Grillo-Lpez AJ, Multani P, White CA. Randomized controlled trial of yttrium-90-labeled ibritumomab tiuxetan radioimmunotherapy versus rituximab immunotherapy for patients with relapsed or refractory low-grade, follicular, or transformed B-cell non-Hodgkin's lymphoma. *J Clin Oncol* 2002; 20: 2453-2463.

11. Kaminski MS, Estes J, Zasadny KR, Francis IR, Ross CW, Tuck M, Regan D, Fisher S, Gutierrez J, Kroll SM, Stagg RJ, Tidmarsh GF, Wahl RL. Radioimmunotherapy with iodine ^{131}I tositumomab for relapsed or refractory B-cell non-Hodgkin lymphoma: updated results and long-term follow-up of the University of Michigan experience. *Blood* 2000; 96: 1259-1266.

12. Press OW, Eary JF, Appelbaum FR, Martin PJ, Nelp WB, Glenn S, Fisher DR, Porter B, Matthews DC, Gooley T. Phase II trial of ^{131}I-B1 (anti-CD20) antibody therapy with autologous stem cell transplantation for relapsed B cell lymphomas. *Lancet* 1995; 346: 336-340.

13. Press OW, Eary JF, Gooley T, Gopal AK, Liu S, Rajendran JG, Maloney DG, Petersdorf S, Bush SA, Durack LD, Martin PJ, Fisher DR, Wood B, Borrow JW, Porter B, Smith JP, Matthews DC, Appelbaum FR, Bernstein ID. A phase I/II trial of iodine-131-tositumomab (anti-CD20), etoposide, cyclophosphamide, and autologous stem cell transplantation for relapsed B-cell lymphomas. *Blood* 2000; 96: 2934-2942.

14. Heider KH, Sproll M, Susani S, Patzelt E, Beaumier P, Ostermann E, Ahorn H, Adolf GR. Characterization of a high-affinity monoclonal

antibody specific for CD44v6 as candidate for immunotherapy of squamous cell carcinomas. *Cancer Immunol Immunother* 1996; 43: 245-253.

15. Schrijvers AHGJ, Quak JJ, Uyterlinde AM, van Walsum M, Meijer CJLM, Snow GB, van Dongen GAMS. Mab U36, a novel monoclonal-antibody successful in immunotargeting of squamous-cell carcinoma of the head and neck. *Cancer Res* 1993; 53: 4383-4390.

16. Verel I, Heider KH, Siegmund M, Ostermann E, Patzelt E, Sproll M, Snow GB, Adolf GR, van Dongen GAMS. Tumor targeting properties of monoclonal antibodies with different affinity for target antigen CD44V6 in nude mice bearing head-and-neck cancer xenografts. *Int J Cancer* 2002; 99: 396-402.

17. Kugelman LC, Ganguly S, Haggerty JG, Weissman SM, Milstone LM. The core protein of epican, a heparan sulfate proteoglycan on keratinocytes, is an alternative form of CD44. *J Invest Dermatol* 1992; 99: 886-891.

18. de Bree R, Roos JC, Quak JJ, den Hollander W, Snow GB, van Dongen GAMS. Radioimmunoscintigraphy and biodistribution of technetium-99m-labeled monoclonal antibody U36 in patients with head and neck cancer. *Clin Cancer Res* 1995; 1: 591-598.

19. Stroomer JWG, Roos JC, Sproll M, Quak JJ, Heider KH, Wilhelm BJ, Castelijns JA, Meyer R, Kwakkelstein MO, Snow GB, Adolf GR, van Dongen GAMS. Safety and biodistribution of 99mTechnetium-labeled anti-CD44v6 monoclonal antibody BIWA 1 in head and neck cancer patients. *Clin Cancer Res* 2000; 6: 3046-3055.

20. Colnot DR, Quak JJ, Roos JC, van Lingen A, Wilhelm AJ, van Kamp GJ, Huijgens PC, Snow GB, van Dongen GAMS. Phase I therapy study of ^{186}Re-labeled chimeric monoclonal antibody U36 in patients with squamous cell carcinoma of the head and neck. *J Nucl Med* 2000; 41: 1999-2010.

21. Colnot DR, Ossenkoppele GJ, Roos JC, Quak JJ, de Bree R, Borjesson PK, Huijgens PC, Snow GB, van Dongen GA. Reinfusion of unprocessed, granulocyte colony-stimulating factor-stimulated whole blood allows dose escalation of ^{186}Relabeled chimeric monoclonal antibody U36 radioimmunotherapy in a phase I dose escalation study. *Clin Cancer Res* 2002; 8: 3401-3406.

22. Kramer EL, Liebes L, Wasserheit C, Noz ME, Blank EW, Zabalegui A, Melamed J, Furmanski P, Peterson JA, Ceriani RL. Initial clinical evaluation of radiolabeled MX-DTPA humanized BrE-3 antibody in patients with advanced breast cancer. *Clin Cancer Res* 1998; 4: 1679-1688.

23. Caron PC, Jurcic JG, Scott AM, Finn RD, Divgi CR, Graham MC, Jureidini IM, Sgouros G, Tyson D, Old LJ, Larson SM, Scheinberg DA. A phase-1B trial of humanized monoclonal antibody M195 (Anti-CD33) in myeloid leukemia — specific targeting without immunogenicity. *Blood* 1994; 83: 1760-1768.

24. Heider KH, Mulder JW, Ostermann E, Susani S, Patzelt E, Pals ST, Adolf GR. Splice variants of the cell surface glycoprotein CD44 associated with metastatic tumour cells are expressed in normal tissues of humans and cynomolgus monkeys. *Eur J Cancer* 1995; 31A: 2385-2391.

25. Himmler A, Maurer-Fogy I, Kronke M, Scheurich P, Pfizenmaier K, Lantz M, Olsson I, Hauptmann R, Stratowa C, Adolf GR. Molecular cloning and expression of human and rat tumor necrosis factor receptor chain (p60) and its soluble derivative, tumor necrosis factor-binding protein. *DNA Cell Biol* 1990; 9: 705-715.

26. Visser GWM, Gerretsen M, Herscheid JDM, Snow GB, van Dongen GAMS. Labeling of monoclonal antibodies with rhenium-186 using the MAG3 chelate for radioimmunotherapy of cancer: a technical protocol. *J Nucl Med* 1993; 34: 1953-1963.

27. Colnot DR, Roos JC, de Bree R, Wilhelm AJ, Kummer JA, Hanft G, Heider KH, Stehle G, Snow GB, van Dongen GAMS. Safety, biodistribution, pharmacokinetics, and immunogenicity of ^{99m}Tc-labeled humanized monoclonal antibody BIWA 4 (bivatuzumab) in patients with squamous cell carcinoma of the head and neck. *Cancer Immunol Immunother* 2003; 52: 576-582.

28. Shen S, DeNardo GL, Sgouros G, O'Donnell RT, DeNardo SJ. Practical determination of patient-specific marrow dose using radioactivity concentration in blood and body. *J Nucl Med* 1999; 40: 2102-2106.

29. Caron PC, Schwartz MA, Co MS, Queen C, Finn RD, Graham MC, Divgi CR, Larson SM, Scheinberg DA. Murine and humanized constructs of monoclonal antibody M195 (anti-CD33) for the therapy of acute myelogenous leukemia. *Cancer* 1994; 73: 1049-1056.

30. Kramer EL, Denardo SJ, Liebes L, Kroger LA, Noz ME, Mizrachi H, Salako QA, Furmanski P, Glenn SD, Denardo GL, Ceriani R. Radioimmunolocalization of metastatic breast-carcinoma using Indium-111-methyl benzyl DTPA BrE-3 monoclonal antibody: Phase I study. *J Nucl Med* 1993; 34: 1067-1074.

31. Denardo SJ, Kramer EL, ODonnell RT, Richman CM, Salako QA, Shen S, Noz M, Glenn SD, Ceriani RL, Denardo GL. Radioimmunotherapy for breast cancer using indium-111/yttrium-90 BrE-3: Results of a phase I clinical trial. *J Nucl Med* 1997; 38: 1180-1185.

32. Ritter G, Cohen LS, Williams C, Richards EC, Old LJ, Welt S. Serological analysis of human anti-human antibody responses in colon cancer patients treated with repeated doses of humanized monoclonal antibody A33. *Cancer Res* 2001; 61: 6851-6859.

33. Welt S, Divgi CR, Kemeny N, Finn RD, Scott AM, Graham M, Stgermain J, Richards EC, Larson SM, Oettgen HF, Old LJ. Phase I/II study of iodine 131-labeled monoclonal-antibody A33 in patients with advanced colon cancer. *J Clin Oncol* 1994; 12: 1561-1571.

34. de Bree R, Kuik DJ, Quak JJ, Roos JC, van den Brekel MWM, Castelijns JA, van Wagtendonk FW, Greuter H, Snow GB, van Dongen GAMS. The impact of tumour volume and other characteristics on uptake of radiolabelled monoclonal antibodies in tumour tissue of head and neck cancer patients. *Eur J Nucl Med* 1998; 25: 1562-1565.

Chapter 8

Dosimetric analysis of radioimmunotherapy with ^{186}Re-labeled bivatuzumab in patients with head and neck cancer

Ernst J. Postema
Pontus K.E. Borjesson
Wilhelmina C.A.M. Buijs
Jan C. Roos
Henri A.M. Marres
Otto C. Boerman
Remco de Bree
Margreet Lang
Gerd Munzert
Guus A.M.S. van Dongen
Wim J.G. Oyen

Journal of Nuclear Medicine 2003; 44: 1690-1699

Abstract

From December 1999 until July 2001, a phase I dose escalation study was performed with ^{186}Re-labeled bivatuzumab, a humanized monoclonal antibody against CD44v6, on patients with inoperable recurrent or metastatic head and neck cancer. The aim of the trial was to assess the safety and tolerability of intravenously administered ^{186}Re-bivatuzumab and to determine the maximum tolerated dose (MTD) of ^{186}Re-bivatuzumab. The data were also used for dosimetric analysis of the treated patients. Dosimetry is used to estimate the absorbed doses by nontarget organs, as well as by tumors. It can also help to explain toxicity that is observed and to predict organs at risk because of the therapy given.

Methods: Whole-body scintigraphy was used to draw regions around sites or organs of interest. Residence times in these organs and sites were calculated and entered into the MIRDOSE3 program, to obtain absorbed doses in all target organs except for red marrow. The red marrow dose was calculated using a blood-derived method. Twenty-one studies on 18 patients, 5 female and 16 male, were used for dosimetry.

Results: The mean red marrow doses were 0.49±0.03 mGy/MBq for men and 0.64 ± 0.03 mGy/MBq for women. The normal organ with the highest absorbed dose appeared to be the kidney (mean dose, 1.61±0.75 mGy/MBq in men and 2.15 ± 0.95 mGy/MBq in women; maximum kidney dose in all patients, 11 Gy), but the doses absorbed are not expected to lead to renal toxicity. Other organs with doses exceeding 0.5 mGy/MBq were the lungs, the spleen, the heart, the liver, the bones, and the testes. The doses delivered to the tumor, recalculated to the MTD level of 1.85 GBq/m^2, ranged from 3.8 to 76.4 Gy, with a median of 12.4 Gy. A good correlation was found between platelet and white blood cell counts and the administered amount of activity per kilogram of body weight ($r = -0.79$).

Conclusion: Dosimetric analysis of the data revealed that the range of doses to normal organs seems to be well within acceptable and safe limits. Tumor doses ranged from 4 to 76 Gy. Given the acceptable tumor doses, ^{186}Re-labeled bivatuzumab could be a good candidate for future adjuvant radioimmunotherapy in patients with minimal residual disease.

Introduction

Squamous cell carcinoma (SCC) is the predominant histologic type among tumors of the head and neck. They account for approximately 5% of all malignant neoplasms in Europe and the United States. Worldwide, more than 500,000 new cases were diagnosed in 2000 [1]. Patients with early

stages of disease (stage I or II) are usually treated with surgery or radiotherapy and have a good prognosis. Patients with stage III or IV disease usually undergo combined surgery and radiotherapy, but the failure rate is high: Locoregional disease recurs after conventional therapy in about 40% of these patients, and distant metastases develop in nearly 25%. The management of these advanced stages of disease especially leaves room for improvement. Development of an effective systemic adjuvant therapy for eradication of minimal residual disease is a major challenge. The use of radiolabeled monoclonal antibodies (mAbs) for this purpose may be a promising approach, since SCC of the head and neck (HNSCC) is a radiosensitive tumor type. The use of radiolabeled mAbs for the treatment of malignancies is called radioimmunotherapy (RIT). RIT appeared to be a successful treatment modality in patients with non-Hodgkin's lymphoma, a radiosensitive tumor type [2]. RIT is also used in studies for the treatment of solid tumors. For treatment of HNSCC, the CD44 antigen seems a suitable target. A particular CD44 isoform, containing the variant exon v6 (CD44v6), is expressed homogeneously in almost all tumors derived from squamous epithelium, whereas its expression on normal human tissues is highly restricted [3]. This expression is maintained in tumor metastases, as immunohistochemical evaluation showed homogeneous expression of CD44v6 in 94 of 95 lymph node metastases [3]. Antibodies directed against CD44v6 were already used in previous clinical RIT trials. In 1998, a phase I study using the ^{186}Re-labeled chimeric mAb U36 was performed for evaluation of the safety and efficacy of RIT [4]. In 5 of 12 patients treated with U36, human anti-chimeric antibodies developed. Therefore, a humanized mAb called bivatuzumab, which is also directed against CD44v6, was developed for further clinical trials.

In most RIT trials, the radionuclide ^{131}I or ^{90}Y is used. ^{131}I emits low-energy β-radiation and high-energy, high-abundance γ-radiation. Although, in most cases, treatment with ^{131}I-labeled mAbs can be given on an outpatient basis in the United States [5,6], the high-energy, high-abundance γ-radiation emitted by ^{131}I may, in some countries, require hospitalization of patients to protect relatives and the general public from radiation. ^{90}Y decays by high-energy β-emissions but lacks γ-radiation. Therefore, scintigraphy and dosimetry cannot be performed when only ^{90}Y-labeled mAbs are used — a limitation, especially when a new mAb is clinically evaluated in RIT for the first time. For this study, ^{186}Re was used because of its excellent physical properties. ^{186}Re decays by both β- and γ-emission. The mean energies of the β-emissions are 362 keV (71% of disintegrations) and 309 keV (22%). The low-energy (137 keV), low-abundance (10%) γ-radiation is ideal for scintigraphy, as shown in Figure 8.1, and permits treatment on

an outpatient basis even at high doses.

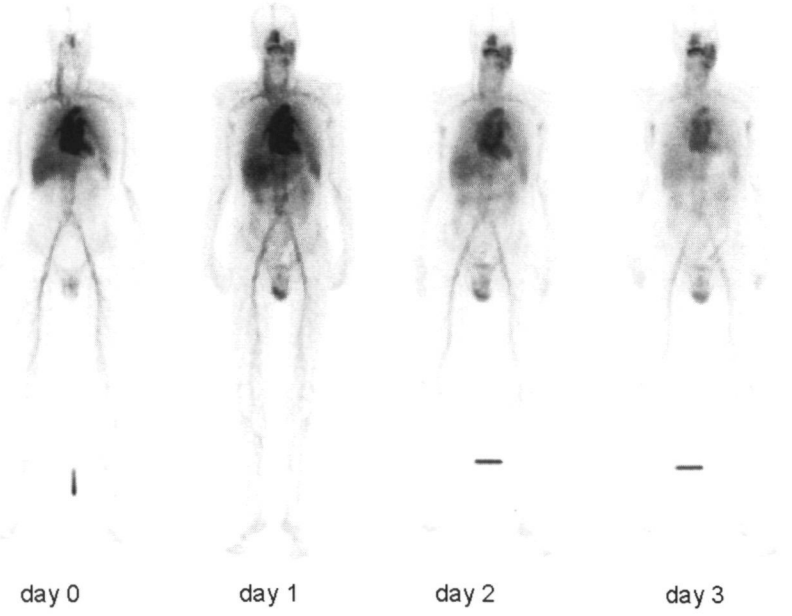

Figure 8.1: Biodistribution directly after and 1, 2, and 3 d after ^{186}Re-bivatuzumab RIT in patient #6, who had carcinoma in the left parotic region.

Given the encouraging RIT results with ^{186}Re-U36, the ideal physical properties of ^{186}Re, and the availability of a humanized mAb, this study was conducted to assess the safety and tolerability of intravenously administered ^{186}Re-bivatuzumab and to determine the maximum tolerated dose (MTD) of ^{186}Re-bivatuzumab. The data of this trial were also used for dosimetric analysis. Dosimetry can be used to give insight into the radiation doses absorbed by nontarget organs, as well as by tumors. It can also help to explain toxicity that is observed and to predict organs at risk because of the therapy given.

Materials and methods

Patient eligibility

Patients with a history of histologically confirmed HNSCC were candidates. At the time they entered the study, they had to have either distant metastases or local or regional recurrent disease for which curative treatment options were not available. The tumor had to be measurable clinically or radiologically. The patients had to be between 18 and 80 y old, give written informed consent, and have a life expectancy of at least 3 months and a Karnofsky performance status of over 60.

Patients with serious concomitant pathology, such as life-threatening infections, organ failure, or a recent myocardial infarction, were excluded. Other exclusion criteria were allergic diathesis, hematologic disorders, congestive heart failure, unstable angina pectoris, bronchial asthma, pregnancy, or the absence of acceptable means of birth control in fertile women.

The white blood cell (WBC) count had to be at least 3.0×10^9/l, the granulocyte count at least 1.5×10^9/l, and the platelet count at least 100×10^9/l. The last course of chemotherapy or radiotherapy had to have been at least 4 weeks before inclusion in the study.

Bivatuzumab

Bivatuzumab (also known as BIWA 4) is a humanized mAb of the IgG1 isotype. It was produced and supplied by Boehringer Ingelheim Pharma GmbH & Co KG. Bivatuzumab recognizes a transmembrane glycoprotein on the outer cell surface. After binding of the mAb to the antigen, an epitope encoded by CD44v6, it is slightly internalized (< 20%). This antigen is expressed by all primary head and neck tumors and by the majority of cells within these tumors. In addition, homogeneous expression has been observed in SCC of the lung, skin, esophagus, and cervix [3]. Heterogeneous expression was found in adenocarcinomas of the breast, lung, colon, pancreas, and stomach [3]. In normal tissues, expression has been found in epithelial tissues, such as skin, breast, prostate myoepithelium, and bronchial epithelium [3]. The reactivity of bivatuzumab is essentially restricted to squamous epithelia.

Bivatuzumab was labeled with ^{186}Re using *S*-benzoyl-mercaptoacetyltriglycine (MAG3) as a chelator by the method of Visser *et al.* [7]. The radiochemical purity of each ^{186}Re-bivatuzumab batch, as assessed by thin-layer chromatography or high-pressure liquid chromatography, always exceeded 95%. The immunoreactive fraction of each batch ranged

from 81% to 100%, with a mean of 90%. ^{186}Re and MAG3 were obtained from Mallinckrodt.

Study design

The present clinical trial was an uncontrolled dose escalation study. All patients underwent prestudy screening, consisting of a review of their history and physical examination, including examination by an experienced oncologic ear, nose, and throat surgeon; laboratory analysis; electrocardiography; CT of the thorax; and radiologic assessment of the tumor site by CT, MRI, or ultrasound.

Study treatment consisted of a single injection with 50 mg of bivatuzumab labeled with ^{186}Re in increasing doses, starting at 0.74 GBq/m^2 (20 mCi/m^2), with increments of 0.37 GBq/m^2 (10 mCi/m^2). Two patients were entered at the lowest dose level, at which toxicity did not exceed grade 1 according to the Common Toxicity Criteria, version 2.0, of the National Cancer Institute. At the higher dose levels, 3 patients were entered per level. If dose-limiting toxicity occurred (grade 3 non-hematologic or grade 4 hematologic toxicity), the group treated at that dose level had to be extended to a total of 6 patients. The MTD was defined as the dose level at which not more than 1 of 6 patients experienced dose-limiting toxicity.

Patients who responded to the first treatment with ^{186}Re-bivatuzumab were eligible for a second administration. They underwent the same visit schedule as for the first administration.

Pharmacokinetics

Blood samples for pharmacokinetic analysis were taken directly after injection, at 5 and 30 min after injection, and at 1, 2, 4, 16, 21, 48, 144, 240, and 336 h after injection. Both serum and blood samples were counted in a well-type γ-counter (Wizard 1470 [at the Amsterdam study center] or Wizard 1480 [at the Nijmegen study center]; Wallac) along with standards of the injection solution. The amount of activity in the samples was expressed as percentage injected dose per kilogram of blood or serum.

Scintigraphy

Whole-body scintigrams for visual assessment of biodistribution and for dosimetric analysis were made within 1 h after injection and at 21, 48, 72, and 144 h after injection. A known aliquot of the injected dose (gamma camera standard) was inserted in an acrylic block of 15-cm height and was

scanned at the same time for reference purposes. At the Nijmegen study center, images were acquired using a Siemens double-head gamma camera. The images were processed at ICON workstations using a locally developed dosimetry tool. This tool allows copying and transferring regions of interest (ROIs) between various whole-body studies. At the Amsterdam study center, the data were acquired with an ADAC double-head gamma camera. Data were transferred electronically in Interfile format and were converted without loss of information to ICON files. These data were analyzed using the same dosimetry tool.

ROIs were drawn around the gamma camera standard; the whole body; the heart and its background; the right lung and its background; the liver; the spleen and its background; the left kidney and its background; the testes, if applicable, and their background; and the tumor, if visible, and its background. All images were reviewed by one physician. The counts in each ROI were corrected for background using the ROIs drawn adjacent to each organ.

Dosimetry

Background correction

The activity in the body (C_{WB}) was determined as the geometric mean of the counts in the anterior image (CA_{WB}) minus the counts in the standard ROI on the anterior image (CA_{ST}), and the counts in the posterior image (CP_{WB}) minus the counts in the standard ROI on the posterior image (CP_{ST}). This is depicted in equation 8.1:

$$C_{WB} = \sqrt{(CA_{WB} - CA_{ST}) \cdot (CP_{WB} - CP_{ST})}. \tag{8.1}$$

The activity in the standard (C_{ST}) is determined as the geometric mean of the counts in the ROI on the anterior image (CA_{ST}) and the counts in the ROI on the posterior image (CP_{ST}):

$$C_{ST} = \sqrt{CA_{ST} \cdot CP_{ST}}. \tag{8.2}$$

The activity in the heart (C_H) was determined as the geometric mean of the counts in the anterior ROI (CA_H) and in the posterior ROI (CP_H) minus background (equation 8.3). The background in the anterior image ($CA_{H,BG}$) was calculated by multiplying the counts per pixel in the ROI for the background of the heart by the number of pixels in the ROI of the heart. Similarly, the background in the posterior image ($CP_{H,BG}$) was calculated. Partial background subtraction was used: Only a fraction of the counts in the background ROIs was subtracted [8]. This fraction (F) was calculated

by dividing abdomen thickness minus organ thickness by the abdomen thickness. For the heart, F equals 0.5 [8].

$$C_H = \sqrt{(CA_H - 0.5 \cdot CA_{H,BG}) \cdot (CP_H - 0.5 \cdot CP_{H,BG})}. \quad (8.3)$$

The activity in the lungs, spleen, and kidneys (C_{ORG}) was determined as the geometric mean of the counts in the anterior ROI (CA_{ORG}) and in the posterior ROI (CP_{ORG}), minus $F = 0.66$ times the background in the anterior image ($CA_{ORG,BG}$) and the posterior image ($CP_{ORG,BG}$), respectively (equation 8.4) [9]. The background for each organ was calculated similarly to the background for the heart. The activity in the lungs was assumed to be 2 times the activity in the right lung. The activity in the kidneys was assumed to be 2 times the activity in the left kidney.

$$C_{ORG} = \sqrt{(CA_{ORG} - 0.66 \cdot CA_{ORG,BG}) \cdot (CP_{ORG} - 0.66 \cdot CP_{ORG,BG})}. \quad (8.4)$$

The activity in the liver (C_{LI}) was determined as the geometric mean of the counts in the anterior ROI (CA_{LI}) and in the posterior ROI (CP_{LI}) (equation 8.5). No background correction was made, since the liver occupies almost the entire thickness of the patient's abdomen [8].

$$C_{LI} = \sqrt{CA_{LI} \cdot CP_{LI}}. \quad (8.5)$$

The activity in the testes (C_{TE}) was determined using the anterior image only (the geometric mean of the counts in the anterior ROI [CA_{TE}] and the background in the anterior image [$CA_{TE,BG}$]) (equation 8.6).

$$C_{TE} = CA_{TE} - CA_{TE,BG}. \quad (8.6)$$

The activity in the tumor (C_T) was determined using either the anterior image (the geometric mean of the counts in the anterior ROI [CA_T] and the background in the anterior image [$CA_{T,BG}$]) or the posterior image (the geometric mean of the counts in the posterior ROI [CP_T] and the background in the posterior image [$CP_{T,BG}$]), depending on the site of the tumor (equation 8.7).

$$C_T = CA_T - CA_{T,BG} \text{ or } C_T = CP_T - CP_{T,BG}. \quad (8.7)$$

Attenuation correction

The attenuation of the activity in the whole body and in the abdominal organs was considered to be caused by 11.25 cm of tissue between the center

of the patient and the skin. The attenuation of activity in the intrathoracic organs is less, because the lungs contain air, leading to less attenuation. Therefore, the residence times of these organs are multiplied by 0.85 to correct for the differences in attenuation in the abdomen and thorax.

The residence times of the testes and the tumor are multiplied by 0.25 and 0.58, respectively. The attenuation of the testes by an overlying layer of 1.5 cm of soft tissue can be defined using equation 8.8, in which μ equals $0.144\,cm^{-1}$ for 137-keV photons in tissue, and $x = 1.5$ cm of tissue. The attenuation of the abdomen can be defined using the same equation and $x = 11.25$ cm. By dividing $A_{11.25}$ by $A_{1.5}$, a correction factor of 0.25 is obtained.

$$A_x = A_0 \cdot e^{-\mu x}. \tag{8.8}$$

The distance between the center of the tumor and the skin is thought to be 7.5 cm, leading to a correction factor of 0.58, which is calculated using the same method as described for attenuation correction of the testes.

Residence times

Equations 8.1–8.7 were applied to each imaging time-point to yield time-activity curves for each organ. The activity in the whole body at each time-point was decay corrected. Time-activity curves for the whole body were obtained by assuming no biologic clearance of injected activity at the first imaging time-point. The decay-corrected counts were fit to a single-component exponential clearance expression, yielding the biologic half-life. Assuming that 100% of the injected dose was present at the first imaging time-point, the percentage of the injected dose for each succeeding scan was calculated by dividing counts of each succeeding scan by the counts of the first scan. These data were fit in a single-component exponential clearance expression, yielding the residence time value of the whole body.

Residence times in all organs were calculated using the trapezoidal method. First, a linear extrapolation was made between the assumed uptake fraction of 0 at the time of injection and the measured fractional uptake at the time of the first image. This extrapolation was not corrected for physical decay. From each time-point to the next, a line was drawn between the fractions of uptake. The areas under all these lines were summed. The remaining area under the curve from the end of data collection until infinity was determined by considering only physical decay of the radionuclide.

Absorbed doses

The absorbed dose to the organs was calculated using the MIRD schema. Tumor, heart (contents), lungs, liver, spleen, kidneys, red marrow, testes, urinary bladder, and the rest of the body (remainder) were considered source organs. The tumor as a source organ was considered to be located at the site of the thyroid gland. Because the organ anatomically nearest to the tumor is the thyroid gland, one cannot estimate the absorbed dose to it. The absorbed dose to the thyroid is expected to be (very) low, since no uptake in the thyroid (and the stomach) is seen, meaning that neither circulation of perrhenate ($^{186}ReO_4^-$) nor actual uptake of radiolabeled antibody occurs in the thyroid. For the bladder, the dynamic bladder model was used. A voiding interval of 4 h was assumed. Using the counts for the whole body, the biologic half-life was determined as described previously. Biologic half-life and voiding interval were entered into the dynamic bladder model, yielding the residence time in the urinary bladder. The calculated residence times as described in the previous section were entered into the MIRDOSE3 computer program, version 3.1 (Oak Ridge Associated Universities) [10], to compute the absorbed doses, using the reference adult software phantom for the men. For the women, the adult female phantom was used.

The absorbed doses in the tumors were calculated using the known fraction of activity in the tumor, divided by the weight of the tumor. To assess the volume of the tumor, its 3 dimensions — as assessed by CT scanning — were multiplied by $\pi/6$. The weight was estimated by multiplying the volume of the tumor by its density, being 1.0 g/cm^3. This calculated weight was entered into MIRDOSE3, in which a sphere represents the tumor. The dose rate in each tumor was estimated using iterative approximation.

The red marrow dose (D_{RM}) was estimated using the blood clearance data, as described by Shen *et al.* [11]. The absorbed dose in the red marrow (cGy/mCi) is calculated according to equation 8.9:

$$D_{RM} = \frac{0.5 \cdot 0.19 \cdot C_{blood}}{1 - Ht} + \frac{0.2128 \cdot \tilde{A}_{WB}}{W_{body}}. \qquad (8.9)$$

In equation 8.9, Ht represents the patient's hematocrit before infusion (l/l), C_{blood} is calculated using the residence times in blood (kBq · h · ml^{-1} · MBq^{-1}), $\tilde{A}_{WB}$ represents the whole-body residence time (h), and W_{body} represents the body weight of the patient (g).

Statistical analysis

Associations between myelotoxicity and doses were calculated with SPSS 10.0 software (SPSS Inc.) using the Pearson correlation test. Two-sided significance levels were calculated for all parameters, with $P < 0.05$ considered statistically significant.

Results

Twenty patients with locoregional recurrence or metastases of head and neck cancer, and for whom no curative options were available, were included in the trial and treated with ^{186}Re-bivatuzumab. Three of these patients received a second injection with 1.85 GBq/m^2 (50 mCi/m^2) ^{186}Re-bivatuzumab at least 12 weeks after the first injection. The specific clinical data of the patients treated and the trial outcome are described elsewhere [12]. For 2 patients treated, not enough data were available for adequate dosimetric analysis. Thus, the results of the dosimetry of 21 RIT procedures on 18 patients are presented.

Red marrow doses

The doses absorbed in the red marrow were estimated for all 21 patient studies, as presented in Table 8.1. The data of men and women are presented separately, since men and women have different mean blood volumes according to the standard phantom models (5.21 in men, 3.91 in women). Therefore, the weight of the bone marrow differs between the sexes, leading to differences in absorbed marrow doses. Table 8.2 shows the mean absorbed doses at the different dose levels.

Because pharmacokinetic data were used to estimate the red marrow doses, the small variance in absorbed doses suggests a consistency in the pharmacokinetics of these patients.

Absorbed doses in other organs

The calculated residence times in the source organs were entered into the MIRDOSE3 program. The results of the MIRDOSE3 analysis are listed in Tables 8.3 and 8.4. Since 2 different models were used (adult and female adult), the data for men and women are presented separately. As stated earlier, the thyroid dose could not be estimated. Although MIRDOSE3 lists both the effective dose and the effective dose equivalent, these values are not applicable to patients receiving radiation therapy. As an alternative,

Patient no.	Dose level (GBq/m^2)	Dose (GBq)	Red marrow dose (mGy/MBq)	Red marrow dose (Gy)
Men				
1	0.74	1.27	0.522	0.66
3	1.11	2.06	0.503	1.03
4	1.11	1.98	0.532	1.06
6	1.11	2.08	0.511	1.06
7	1.48	2.76	0.497	1.37
8	1.48	2.60	0.524	1.37
10	1.85	3.38	0.459	1.55
11.1	1.85	3.12	0.516	1.61
11.2	1.85	3.17	0.481	1.53
12.1	1.85	3.34	0.486	1.62
12.2	1.85	3.35	0.497	1.67
14.1	2.22	3.83	0.459	1.76
14.2	1.85	3.16	0.438	1.38
15	2.22	4.00	0.481	1.93
18	1.85	3.22	0.514	1.65
19	1.85	3.67	0.449	1.65
Mean ± SD			0.492 ± 0.029	
Women				
2	0.74	1.18	0.635	0.75
9	1.48	2.40	0.622	1.49
13	2.22	3.61	0.624	2.26
16	2.22	3.31	0.619	2.05
20	1.85	2.57	0.684	1.76
Mean ± SD			0.637 ± 0.027	

Table 8.1: Absorbed doses in red marrow

the absorbed total-body dose was calculated, considering the body as an organ.

Table 8.3 shows the mean absorbed doses, expressed as mGy/MBq and grouped by dose level, in all target organs of male patients. The mean dose actually absorbed by all organs was determined by MIRDOSE3 using the reference adult phantom and was calculated by multiplying the mGy/MBq values by the actual dose, in megabecquerels, that the patients received.

The data for the women were processed similarly, using the female adult phantom. The mean absorbed doses, expressed as mGy/MBq, are presented in Table 8.4. The absorbed doses in women appear to be higher than those in men because of the different reference body weight of the 2 models (female adult, 57 kg; adult, 70 kg). Because the data of only 5 women could be used for dosimetric analysis, no mean absorbed doses per dose level could be given, except for the highest dose level of 2.22 GBq/m^2 (60 mCi/m^2), at which 2 women were treated.

Patients treated (n)	Dose level (GBq/m^2)	Mean absorbed red marrow dose±SD (Gy)
Men		
1	0.74	0.66
3	1.11	1.05±0.02
2	1.48	1.37±0.00
8	1.85	1.58±0.09
2	2.22	1.85±0.12
Women		
1	0.74	0.75
1	1.48	1.49
1	1.85	1.76
2	2.22	2.15±0.15

Table 8.2: Mean absorbed doses

The organ that received the highest doses was the kidney (1.61 ± 0.75 mGy/MBq in men, 2.15 ± 0.95 mGy/MBq in women). Other organs receiving absorbed doses exceeding 0.5 mGy/MBq were the lungs (1.16 ± 0.29 mGy/MBq in men, 1.46 ± 0.22 mGy/MBq in women), the spleen (1.11 ± 0.39 mGy/MBq in men, 1.56 ± 0.53 mGy/MBq in women), the heart (0.83 ± 0.21 mGy/MBq in men, 1.27 ± 0.20 mGy/MBq in women), the liver (0.76 ± 0.17 mGy/MBq in men, 1.12 ± 0.26 mGy/MBq in women), the bones (0.92 ± 0.05 mGy/MBq in men, 0.92 ± 0.03 mGy/MBq in women), and the testes (0.73 ± 0.23 mGy/MBq).

Organ	Mean absorbed organ dose ± SD (mGy/MBq)	Mean absorbed organ dose for different dose levels ± SD (Gy)				
		0.74 GBq/m² (n = 1)	1.11 GBq/m² (n = 3)	1.48 GBq/m² (n = 2)	1.85 GBq/m² (n = 8)	2.22 GBq/m² (n = 2)
Adrenals	2.08E−01 ± 2.08E−02	0.27	0.44 ± 0.03	0.50 ± 0.09	0.68 ± 0.07	0.89 ± 0.09
Brain	2.01E−01 ± 2.14E−02	0.26	0.42 ± 0.04	0.48 ± 0.09	0.66 ± 0.07	0.86 ± 0.09
Gallbladder wall	2.08E−01 ± 2.11E−02	0.27	0.44 ± 0.04	0.49 ± 0.09	0.68 ± 0.07	0.88 ± 0.09
LLI wall	2.05E−01 ± 2.15E−02	0.27	0.43 ± 0.04	0.49 ± 0.09	0.67 ± 0.07	0.87 ± 0.09
Small intestine	2.05E−01 ± 2.15E−02	0.27	0.43 ± 0.04	0.49 ± 0.09	0.67 ± 0.07	0.88 ± 0.09
Stomach	2.04E−01 ± 2.13E−02	0.27	0.43 ± 0.04	0.49 ± 0.09	0.67 ± 0.07	0.87 ± 0.09
ULI wall	2.05E−01 ± 2.14E−02	0.27	0.43 ± 0.04	0.49 ± 0.09	0.67 ± 0.07	0.87 ± 0.09
Heart wall	8.35E−01 ± 2.12E−01	1.07	1.50 ± 0.10	2.53 ± 0.47	2.78 ± 0.82	3.21 ± 1.09
Kidneys	1.61E+00 ± 7.52E−01	1.80	2.54 ± 1.70	4.20 ± 0.03	6.14 ± 3.06	5.28 ± 2.45
Liver	7.62E−01 ± 1.72E−01	0.60	1.63 ± 0.28	2.39 ± 0.63	2.53 ± 0.48	2.75 ± 0.98
Lungs	1.16E+00 ± 2.89E−01	1.35	2.25 ± 0.77	3.29 ± 0.60	4.00 ± 0.84	3.89 ± 2.20
Muscle	2.02E−01 ± 2.13E−02	0.26	0.43 ± 0.04	0.48 ± 0.09	0.66 ± 0.07	0.86 ± 0.09
Pancreas	2.08E−01 ± 2.11E−02	0.27	0.44 ± 0.04	0.49 ± 0.09	0.68 ± 0.07	0.89 ± 0.09
Bone surfaces	9.22E−01 ± 4.65E−02	1.26	1.96 ± 0.08	2.53 ± 0.06	2.97 ± 0.14	3.51 ± 0.16
Skin	2.00E−01 ± 2.12E−02	0.26	0.42 ± 0.04	0.47 ± 0.09	0.65 ± 0.07	0.85 ± 0.09
Spleen	1.11E+00 ± 3.86E−01	1.97	1.65 ± 0.81	2.67 ± 0.27	3.78 ± 1.35	5.17 ± 0.75
Testes	7.31E−01 ± 2.28E−01	0.65	1.88 ± 0.32	1.77 ± 0.12	2.28 ± 0.81	2.89 ± 1.31
Urinary bladder wall	3.03E−01 ± 3.27E−02	0.37	0.60 ± 0.03	0.85 ± 0.28	1.01 ± 0.09	1.14 ± 0.15
Total Body	2.81E−01 ± 1.66E−02	0.36	0.58 ± 0.03	0.71 ± 0.10	0.92 ± 0.05	1.14 ± 0.02

LLI = lower large intestine; ULI = upper large intestine

Table 8.3: Absorbed organ doses in men

Organ	Mean absorbed organ dose ± SD (mGy/MBq)	Mean absorbed organ dose for different dose levels ± SD (Gy)			
		0.74 GBq/m^2 (n = 1)	1.48 GBq/m^2 (n = 1)	1.85 GBq/m^2 (n = 1)	2.22 GBq/m^2 (n = 2)
Adrenals	2.75E−01 ± 3.56E−02	0.37	0.60	0.63	1.00 ± 0.20
Brain	2.66E−01 ± 3.68E−02	0.36	0.57	0.60	0.98 ± 0.21
Breasts	2.66E−01 ± 3.63E−02	0.36	0.57	0.60	0.97 ± 0.20
Gallbladder wall	2.74E−01 ± 3.62E−02	0.37	0.59	0.62	1.00 ± 0.21
LLI wall	2.70E−01 ± 3.70E−02	0.36	0.58	0.61	0.99 ± 0.21
Small intestine	2.70E−01 ± 3.66E−02	0.36	0.58	0.61	0.99 ± 0.21
Stomach	2.71E−01 ± 3.63E−02	0.36	0.58	0.61	0.99 ± 0.21
ULI wall	2.71E−01 ± 3.69E−02	0.36	0.58	0.61	0.99 ± 0.21
Heart wall	1.27E+00 ± 1.97E−01	1.77	3.10	3.57	3.77 ± 0.28
Kidneys	2.15E+00 ± 9.51E−01	1.45	5.69	9.00	6.30 ± 2.58
Liver	1.12E+00 ± 2.59E−01	1.70	2.81	3.24	3.02 ± 0.34
Lungs	1.46E+00 ± 2.17E−01	1.76	3.86	4.37	4.34 ± 0.27
Muscle	2.67E−01 ± 3.66E−02	0.36	0.58	0.60	0.98 ± 0.21
Ovaries	2.70E−01 ± 3.66E−02	0.36	0.58	0.61	0.99 ± 0.21
Pancreas	2.75E−01 ± 3.63E−02	0.37	0.59	0.62	1.00 ± 0.21
Bone surfaces	9.18E−01 ± 2.56E−02	1.10	2.17	2.38	3.18 ± 0.32
Skin	2.64E−01 ± 3.61E−02	0.35	0.57	0.60	0.97 ± 0.20
Spleen	1.56E+00 ± 5.30E−01	1.99	2.09	5.45	5.35 ± 1.70
Urinary bladder wall	3.51E−01 ± 3.91E−02	0.34	0.90	0.92	1.29 ± 0.01
Uterus	2.69E−01 ± 3.66E−02	0.36	0.58	0.61	0.99 ± 0.21
Total Body	3.72E−01 ± 2.61E−02	0.48	0.84	0.93	1.30 ± 0.17

LLI = lower large intestine; ULI = upper large intestine

Table 8.4: Absorbed organ doses in women

Patient no.	Tumor volume (cm^3)	Tumor self-dose S-value (mGy $MBq^{-1} \cdot h^{-1}$)	Residence time (h)	Administered activity (GBq)	Actual tumor dose (Gy)	Tumor dose if treated at 1.85 GBq/m^2 (Gy)
1	285.9	7.38E−01	1.45	1.27	1.4	3.8
2	11.5	1.79E+01	1.19	1.18	25.2	65.1
3	19.2	1.02E+01	0.32	2.06	6.7	10.8
4	10.8	1.82E+01	0.22	1.98	7.9	13.5
6	11	1.79E+01	0.07	2.08	2.6	4.4
7	47.1	3.84E+00	0.54	2.76	5.7	7.4
8	8.1	2.37E+01	0.11	2.60	6.8	8.7
9	16.2	9.16E+00	0.44	2.40	9.7	12.4
10	5.1	4.14E+01	0.53	3.38	73.9	76.4
13	69.6	2.84E+00	2.65	3.61	27.1	22.8
14.1	32.5	5.97E+00	0.69	3.83	15.8	13.9
14.2	30.2	7.24E+00	0.94	3.16	21.5	22.3
15	56	3.54E+00	0.62	4.00	8.8	7.3
16	66	3.00E+00	1.84	3.36	18.5	15.5
19	6.7	2.86E+01	0.12	3.67	12.6	11.9
Median						

Table 8.5: Dose absorbed by tumor

Tumor dosimetry

If CT scanning before treatment with ^{186}Re-bivatuzumab showed a measurable tumor lesion, and if this lesion was visible on scintigraphy after RIT, dosimetry for the tumor was performed. In this study, 15 lesions could be evaluated and were analyzed.

The tumor sizes ranged from 5.1 to 285.9 cm^3. The tumor doses differed markedly: Doses ranged from 1.4 to 73.9 Gy. Because tumor doses in a dose-escalation study cannot easily be compared, tumor doses were calculated postulating that all patients were treated at MTD, being 1.85 GBq/m^2 (50 mCi/m^2). The recalculated tumor doses ranged from 3.8 to 76.4 Gy, with a median dose of 12.4 Gy. The tumor doses of all individual lesions are listed in Table 8.5.

In the patient studies used for tumor dosimetry, stable disease was observed in 2 cases. The actual absorbed doses in the tumors of these patients were 74 and 16 Gy, respectively.

Correlation between toxicity and absorbed doses

Because hematologic toxicity appeared to be dose-limiting, and because no other serious toxicity was observed, platelet and WBC nadir levels were compared with total injected activity, injected activity per square meter

of body surface area, injected activity per kilogram of body weight (all parameters listed in Table 8.6), whole-body absorbed dose (listed in Tables 8.3 and 8.4), and red marrow absorbed dose (as listed in Table 8.1). Correlation coefficients between nadir of platelets and WBCs, and the 5 parameters mentioned above, were plotted (Figure 8.2), calculated, and listed in Table 8.7. The injected activity per kilogram of body weight appeared to correlate best with hematologic toxicity, with a correlation coefficient of -0.79. Second-best correlations were found between whole-body dose and WBC nadir ($r = -0.75$) and between administered activity per square meter of body surface area and nadirs ($r = -0.73$).

Patient no.	Dose level (GBq/m^2)	Administered activity (GBq)	Weight (kg)	Administered activity (MBq/kg)	Platelet nadir ($\times 10^9$/l)	WBC nadir ($\times 10^9$/l)
1	0.74	1.27	70.0	18.1	199	10.1
2	0.74	1.18	56.0	21.1	321	7.5
3	1.11	2.06	59.0	34.9	52	1.8
4	1.11	1.98	64.0	30.9	183	7.4
6	1.11	2.08	71.0	29.3	143	5.2
7	1.48	2.76	73.0	37.8	277	10.6
8	1.48	2.68	60.0	44.7	89	3.0
9	1.48	2.40	61.5	39.0	202	4.9
10	1.85	3.38	72.0	47.0	89	3.4
11.1	1.85	3.12	64.0	48.7	122	4.5
12.1	1.85	3.34	65.0	51.5	117	2.3
13	2.22	3.61	59.0	61.1	25	0.7
14.1	2.22	3.82	79.0	48.4	78	2.7
15	2.22	4.00	61.0	65.6	47	2.0
16	2.22	3.36	50.0	67.3	18	1.2
17	2.22	3.61	60.0	60.2	12	0.4
18	1.85	3.22	58.0	55.4	8	0.9
19	1.85	3.67	70.0	52.4	94	2.3
20	1.85	2.57	43.5	59.1	65	2.9

Table 8.6: Administered doses and toxicity

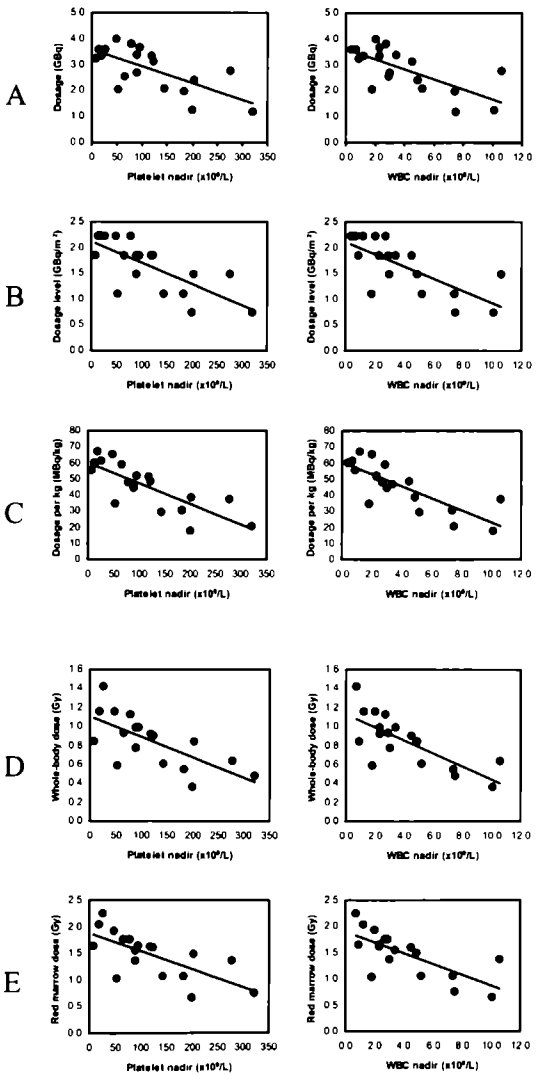

Figure 8.2: Correlation of platelet and WBC nadirs with total injected activity (A), injected activity per square meter of body surface area (B), injected activity per kilogram of body weight (C), whole-body absorbed dose (D), and red marrow absorbed dose (E).

Parameter	Platelet nadir	WBC nadir
Dose (GBq)	−0.69	−0.69
Dose level (GBq/m^2)	−0.73	−0.73
Dose per kg (MBq/kg)	−0.79	−0.79
Whole-body dose (Gy)	−0.69	−0.75
Red marrow dose (Gy)	−0.69	−0.72

Table 8.7: Correlation coefficients of hematologic toxicity *versus* dose

Discussion

Dosimetric analysis of patients treated with ^{186}Re-bivatuzumab did not reveal unexpectedly high absorbed doses in normal organs. The organ that received the highest dose is the kidney. Patients treated at MTD and 1 dose level higher (1.85 and 2.22 GBq/m^2, respectively) had absorbed doses in the kidneys of maximally 11 Gy, thus not exceeding 20–25 Gy, a dose that is thought to cause renal toxicity [13]. Other organs receiving relatively high absorbed doses are the lungs (maximally 5.4 Gy). Because lung toxicity is expected at doses of more than 27 Gy [14], the doses found in this trial were thought not to lead to pulmonary problems. For the spleen, the heart, the liver, and the bones, doses were considered to be within safe ranges as well. The absorbed dose in the testes appeared to be maximally 4 Gy, assuming that there was uptake in the testes only and not in the epididymides or scrotal skin. Some uptake in the scrotal skin could be expected, using a radiolabeled antibody that could target skin. In a particular patient, 2 separate testicles were seen, thus suggesting that not the scrotum was visualized, but the testes. Relatively high uptake of radiolabeled immunoglobulins in the testes is not unusual. It was also described for patients who received ^{111}In-labeled polyclonal IgG for infection detection [8]. Few data on the effects of radionuclides on fertility and deterministic effects have been published. Commentary 7 of the National Council on Radiation Protection and Measurements gives a threshold value of 3.5 Gy for external-beam radiation. Because the dose rate of radionuclide therapies is lower when compared with external-beam radiation, doses that can be tolerated by normal organs are higher than doses delivered by external-beam radiation. The effects of RIT on fertility have not been sufficiently established.

The absorbed dose to the red marrow was calculated using the pharmacokinetic data. Because pharmacokinetic data did not vary much between patients [12], the interindividual variation in red marrow doses per admin-

istered megabecquerel was small as well. There are some factors associated with stable clearance of the mAbs. The antibody is humanized, so aberrant clearance caused by neutralizing antibodies (human anti-murine or human anti-chimeric) is not to be expected. There is no antigenic sink in the bone marrow or other organs influencing clearance of the antibody. Because there is uptake neither in the bone marrow nor in the bone, the main contributor to the red marrow dose is activity in the blood. Therefore, we think it appropriate to use the blood-derived method of Shen *et al.* to estimate red marrow dose [11].

The absorbed red marrow dose correlated well with the blood cell nadirs ($r = -0.69$ for platelets, $r = -0.72$ for WBC). The whole-body dose even showed a slightly better correlation ($r = -0.69$ for platelets, $r = -0.75$ for WBC). Surprisingly, both dosimetry-independent parameters, the administered activity per kilogram of body weight ($r = -0.79$) and the administered activity per square meter of body surface area ($r = -0.73$), correlated well with the blood cell nadirs. The reason to correlate parameters such as dose/kg or absorbed whole-body dose with toxicity is that there are as many administration and dosing schemes as there are RIT trials. Most RIT trials concern the treatment of non-Hodgkin's lymphoma patients. Although trials on patients with this disease cannot be compared with trials on patients with head and neck cancer (differences in pretreatment, intrinsic activity of the mAbs used, localization of disease in the bone marrow, use of murine mAbs), the method of dosing the activity can be discussed. The 2 main dosing schemes are dosimetry based or weight based. The first method uses a tracer dose of ^{131}I-labeled mAb to determine the therapeutic dosage of radioiodinated anti-CD20 mAb tositumomab that would lead to a whole-body dose of 0.75 Gy [15]. The second method uses a body weight-derived dosing scheme for the ^{90}Y-labeled anti-CD20 mAb ibritumomab (15 MBq/kg) and does not analyze dosimetric data before treatment [16]. In retrospect, we can consider the suitability of these alternative methods of dosing if they had been applied in the present study. If a dose of 55 MBq/kg (the lowest dose at which grade 4 hematologic toxicity was observed) had been defined as MTD, only 3 patients would have appeared to tolerate a dose of more than 55 MBq/kg without having grade 4 hematologic toxicity (Table 8.6). Two of them had grade 3 toxicity. If a 0.84-Gy whole-body dose (the lowest whole-body dose at which grade 4 hematologic toxicity was observed) had been chosen as MTD, 9 patients would have been undertreated, since they appeared to tolerate higher whole-body doses. Our data suggest that to dose using the patient's weight can be safe and has the lowest chance of undertreating patients.

The absorbed doses in the tumors tend to vary enormously. These doses were similar to those achieved by treatment with the other anti-CD44v6 conjugate, ^{186}Re-U36 [4]. The absorbed dose is higher in small lesions than in larger tumors. Although it is to be expected that the smallest tumors will have the highest doses, the actual doses in these tumors could be lower: The statistical error could be significant, because the number of pixels in such a small ROI is low. In the estimation of tumor doses, the influence of necrosis within a tumor is not considered. Radiolabeled antibodies can reach only viable tumor cells, since there are no blood vessels in necrotic parts of the tumor. Moreover, intratumoral pressure plays a more important role in large lesions. The absorbed dose in the tumor could therefore be estimated more precisely by dividing the absorbed energy through the weight of viable tissue, leading to higher absorbed doses. The fact that high tumor doses can be achieved encourages the thought that ^{186}Re-bivatuzumab can be an effective systemic adjuvant treatment for patients with head and neck cancer with minimal residual disease.

Conclusion

Dosimetric analysis of the data on treatment of patients with ^{186}Re-bivatuzumab revealed that the range of doses to normal organs seems to be well within acceptable and safe limits. Attention should be paid to the absorbed dose in the testes. Hematologic toxicity was dose-limiting. The administered activity per kilogram of body weight correlated best with the extent of hematologic toxicity. Doses absorbed in tumors were quite similar to those achieved by treatment with the other anti-CD44v6 conjugate, ^{186}Re-U36. Given the acceptable tumor doses, ^{186}Re-labeled bivatuzumab could be a good candidate for future adjuvant RIT in patients with minimal residual disease.

Acknowledgments

The authors thank Michel de Groot for processing the scintigraphic data and helping with the dosimetric analysis. This study was sponsored by Boehringer Ingelheim BV.

References

1. Parkin DM, Bray F, Ferlay J, Pisani P. Estimating the world cancer burden: Globocan 2000. *Int J Cancer* 2001; 94: 153-156.

2. Postema EJ, Boerman OC, Oyen WJG, Raemaekers JMM, Corstens FHM. Radioimmunotherapy of B-cell non-Hodgkin's lymphoma. *Eur J Nucl Med* 2001; 28: 1725-1735.

3. Heider KH, Sproll M, Susani S, Patzelt E, Beaumier P, Ostermann E, Ahorn H, Adolf GR. Characterization of a high-affinity monoclonal antibody specific for CD44v6 as candidate for immunotherapy of squamous cell carcinomas. *Cancer Immunol Immunother* 1996; 43: 245-253.

4. Colnot DR, Quak JJ, Roos JC, van Lingen A, Wilhelm AJ, van Kamp GJ, Huijgens PC, Snow GB, van Dongen GAMS. Phase I therapy study of ^{186}Re-labeled chimeric monoclonal antibody U36 in patients with squamous cell carcinoma of the head and neck. *J Nucl Med* 2000; 41: 1999-2010.

5. Coover LR, Silberstein EB, Kuhn PJ, Graves MW. Therapeutic ^{131}I in outpatients: a simplified method conforming to the Code of Federal Regulations, title 10, part 35.75. *J Nucl Med* 2000; 41: 1868-1875.

6. Siegel JA, Kroll S, Regan D, Kaminski MS, Wahl RL. A practical methodology for patient release after tositumomab and ^{131}I-tositumomab therapy. *J Nucl Med* 2002; 43: 354-363.

7. Visser GWM, Gerretsen M, Herscheid JDM, Snow GB, van Dongen GAMS. Labeling of monoclonal antibodies with rhenium-186 using the MAG3 chelate for radioimmunotherapy of cancer: a technical protocol. *J Nucl Med* 1993; 34: 1953-1963.

8. Buijs WCAM, Oyen WJG, Dams ETM, Boerman OC, Siegel JA, Claessens RAMJ, van der Meer JWM, Corstens FHM. Dynamic distribution and dosimetric evaluation of human non-specific immunoglobulin G labelled with ^{111}In or ^{99m}Tc. *Nucl Med Commun* 1998; 19: 743-751.

9. Buijs WCAM, Siegel JA, Boerman OC, Corstens FHM. Absolute organ activity estimated by five different methods of background correction. *J Nucl Med* 1998; 39: 2167-2172.

10. Stabin MG. MIRDOSE: personal computer software for internal dose assessment in nuclear medicine. *J Nucl Med* 1996; 37: 538-546.

11. Shen S, DeNardo GL, Sgouros G, O'Donnell RT, DeNardo SJ. Practical determination of patient-specific marrow dose using radioactivity concentration in blood and body. *J Nucl Med* 1999; 40: 2102-2106.

12. Borjesson PKE, Postema EJ, Roos JC, Colnot DR, Marres HAM, van Schie MH, Stehle G, de Bree R, Snow GB, Oyen WJG, van Dongen GAMS. Phase I therapy study with ^{186}Re-labeled humanized monoclonal antibody BIWA 4 (bivatuzumab) in patients with head and neck squamous cell carcinoma. *Clin Cancer Res* 2003; 9: 3961s-3972s.

13. Paganelli G, Zoboli S, Cremonesi M, Bodei L, Ferrari M, Grana C, Bartolomei M, Orsi F, De Cicco C, Macke HR, Chinol M, de Braud F. Receptor-mediated radiotherapy with ^{90}Y-DOTA-D-Phe1-Tyr3-octreotide. *Eur J Nucl Med* 2001; 28: 426-434.

14. Press OW, Eary JF, Appelbaum FR, Martin PJ, Badger CC, Nelp WB, Glenn SD, Butchko G, Fisher D, Porter B, Matthews DC, Fisher LD, Bernstein ID. Radiolabeled-antibody therapy of B-cell lymphoma with autologous bone marrow support. *N Engl J Med* 1993; 329: 1219-1224.

15. Wahl RL, Kroll S, Zasadny KR. Patient-specific whole-body dosimetry: principles and a simplified method for clinical implementation. *J Nucl Med* 1998; 39: 14S-20S.

16. Wagner HN, Jr, Wiseman GA, Marcus CS, Nabi HA, Nagle CE, Fink-Bennett DM, Lamonica DM, Conti PS. Administration guidelines for radioimmunotherapy of non-Hodgkin's lymphoma with ^{90}Y-labeled anti-CD20 monoclonal antibody. *J Nucl Med* 2002; 43: 267-272.

Chapter 9

General discussion and future perspectives

Radioimmunotherapy (RIT) is a new treatment option for various tumors. Especially in the treatment of patients with non-Hodgkin's lymphoma (NHL) successes have been achieved. In this thesis, the results of preclinical RIT studies in a mouse lymphoma model and RIT studies of patients with NHL and of patients with squamous cell carcinoma of the head and neck (HNSCC) are described. In both studies, humanized monoclonal antibodies (mAbs) were used. Since human(ized) mAbs are less immunogenic than murine or chimeric mAbs, the chance to elicit human anti-murine antibodies (HAMAs) or human anti-chimeric antibodies (HACAs) are reduced. Therefore, retreatment with these mAbs is possible, as shown in Chapter 7.

The choice of an optimal radionuclide for RIT is essential as well. Ideally, a radionuclide for RIT should emit β-particles as well as low-energy, low-abundance γ-photons, the latter used for imaging. The half-life should be at least several days to ensure time for shipping and labeling of the mAb and to deliver enough dose to the tumor, since optimal uptake of radiolabeled mAbs is achieved after several days. Rhenium-186 (^{186}Re) meets these criteria. In the studies described in this thesis, ^{186}Re was used for RIT of patients. The combination of the radionuclide and the mAb should have an optimal biodistribution, meaning that the radiopharmaceutical should accumulate in and should be retained by the tumor, whereas there should be neither unwanted accumulation in normal organs, nor high doses absorbed by the normal organs. In this respect, ^{186}Re can compete with other radionuclides. Although in a mouse lymphoma model the uptake and retention of ^{186}Re-epratuzumab in the tumor were not as high as the tumor uptake and retention of ^{88}Y- and ^{177}Lu-epratuzumab, the accumulation of ^{186}Re in the bone is significantly less than that of ^{88}Y and ^{177}Lu (Chapter 3).

The clinical data presented in Chapters 4 and 7 confirm that RIT with both ^{186}Re-epratuzumab and ^{186}Re-bivatuzumab is well-tolerated. The dosimetric data described in Chapters 5 and 8 convincingly show that treatment with these ^{186}Re-labeled mAbs is safe with respect to absorbed doses to normal organs. In these two phase I trials objective responses were observed in one third of the patients with NHL, and in none of the patients with HNSCC.

Although the studies presented in this thesis give insight in optimal conditions for RIT, it does not answer which subpopulation of patients can be treated best on what time.

Two radiopharmaceuticals have been registered for clinical use in the USA so far, both for treatment of patients with NHL with a relapse after all conventional options have been tried. Chapter 4 describes the results of RIT in the same group of patients. In these patients, few therapies given

in a palliative setting show such encouraging results, with high remission rates. Therefore, it is likely that this non-myeloablative approach will be frequently used in relapsed or refractory lymphoma patients for whom no other options are left. Still, other approaches, like myeloablative RIT or first-line RIT, could possibly result in more and/or longer lasting remissions than conventional therapies, as described in Chapter 1. Future research should emphasize these approaches.

The future role of RIT of solid tumors seems to be hampered by the use of mAbs that lack intrinsic anti-tumor activity. Therefore, the radiation dose should be sufficiently high to induce anti-tumor effects and very radiosensitive tumors should be selected. As described in the Chapters 7 and 8, no objective responses in patients with inoperable and incurable HNSCC were achieved. Other RIT studies in patients with solid tumors for whom no curative options are available, showed similar results. Given the low tumor doses in macroscopic, irresectable tumors, whereas higher doses can be achieved in small and very small tumors, the most promising indication for RIT in the treatment of solid tumors is within an adjuvant setting after radical surgery, perhaps in combination with chemo- or radiotherapy. Hopefully, humanized mAbs like bivatuzumab will enter phase III trials to determine their role in the treatment of patients with cancer.

Summary

In this thesis, the potential of radioimmunotherapy (RIT) for two types of cancer is investigated. Treatment of non-Hodgkin's lymphoma (NHL) is described in the Chapters 1-5, whereas treatment of squamous cell carcimoma of the head and neck (HNSCC) is described in the Chapters 6-8. For RIT of both tumor types, humanized monoclonal antibodies (mAbs) against tumor-specific antigens are used. In the clinical studies, mAbs were labeled with ^{186}Re, an ideal radionuclide for therapy and imaging.

In *Chapter 1*, an overview is given of NHL, its treatment, and the role of mAbs in lymphoma management. Trials using unlabeled mAbs as well as trials using radiolabeled are discussed. Not only overall response rates and the additional value of radionuclides over unlabeled use of mAbs are described, but especially treatment strategies, dosing schedules, toxicity, and current status of these treatments are highlighted.

In *Chapter 2*, the development of a human lymphoma mouse model is described. Human lymphoma xenografts in general grow only poorly in mice. Even when immunocompromized, most mice will not develop tumors after inoculation with human lymphoma cells. Therefore, two pretreatment regimens of nude mice to improve the implantation and growth rate of lymphoma xenografts were compared. In non-pretreated mice, tumor induction after subcutaneous injections with Ramos cells was only 50%, whereas 80% of the mice pretreated with cyclophosphamide and 100% of the mice pretreated with whole-body irradiation developed subcutaneous tumors. Moreover, particularly in the group pretreated with whole-body irradiation, the tumors grew more synchronously. Pretreatment with cyclophosphamide or whole-body irradiation improved the tumor implantation rate of Ramos cells in nude mice, providing a workable animal model for further lymphoma studies.

In order to determine the optimal radionuclide for RIT of NHL, a biodistribution study was performed, as described in *Chapter 3*. The humanized anti-CD22 anti-lymphoma mAb epratuzumab (hLL2) was labeled with four different radionuclides, ^{131}I, ^{186}Re, ^{177}Lu, and ^{88}Y. After transplantation of Ramos cells in nude mice, that were pretreated with cyclophosphamide according to the animal model provided in the previous chapter, the mice were injected with radiolabeled epratuzumab, or with a control mAb labeled with ^{131}I or ^{88}Y. The biodistribution of the radiolabel was determined 1, 3, and 7 days after injection of the radiopharmaceutical. Radiolabeled epratuzumab had a higher tumor uptake than the control mAb at all time points, irrespective of the radionuclide used. Tumor accretion of ^{88}Y- and ^{177}Lu-labeled epratuzumab was higher than tumor uptake of ^{131}I- and ^{186}Re-epratuzumab. Not only tumor uptake, but also bone uptake was higher for the former two radiolabels than for the latter on day 7 after

injection. It was concluded that the residualizing radionuclides ^{88}Y and ^{177}Lu in combination with epratuzumab have a higher uptake and better retention in the tumor than the radiolabels ^{131}I and ^{186}Re, but the higher bone uptake of the former radionuclides could result in a higher radiation dose to the bone marrow, reducing the activity dose that can be tolerated without acceptable myleotoxicity.

In *Chapter 4*, the results of a phase I study using ^{186}Re-epratuzumab in patients with NHL were summarized. The aim of the study was to determine the maximum tolerated dose (MTD) and to get a first impression of the therapeutic potential of this novel radiopharmaceutical. Patients with relapsed or refractory CD22-positive NHL of diverse histopathology and prior treatments received ^{99m}Tc-labeled epratuzumab, followed by RIT with ^{186}Re-epratuzumab one week later. Dose escalation of RIT was started at 0.5 GBq/m^2. Three patients were entered per dose level. If no dose-limiting toxicity occurred, the dose was increased by 0.5 GBq/m^2; otherwise 3 additional patients were included on that dose level. A total of 18 patients received a diagnostic dose of ^{99m}Tc-epratuzumab. Fifteen patients were actually treated with ^{186}Re-epratuzumab at 4 different dose levels, 0.5, 1.0, 1.5, and 2.0 GBq/m^2. During or after infusion of ^{186}Re-epratuzumab, no serious adverse reactions were seen. In all patients a transient decrease of leukocyte and platelet levels was observed one month after treatment. At the 1.5-GBq/m^2 dose level, one grade 4 hematological toxicity was observed. At the highest dose level of 2.0 GBq/m^2, no grade 4 hematological toxicity was seen, but white blood cell and platelet counts of two of the three patients did not recover completely. One patient had a complete remission lasting 4 months. Four patients had a partial response, lasting 3, 3, 6, and 14 months, respectively. Four patients had stable disease for 3, 3, 7, and 9 months, respectively. Although no dose-limiting, grade 4 toxicity was observed, but given the slow recovery of peripheral blood counts in 2 of 3 patients treated at the dose level of 2.0 GBq/m^2, this dose level was defined as MTD. A single dose of ^{186}Re-epratuzumab led to objective responses in 5 of 15 treated patients.

Safety of treatment with ^{186}Re-epratuzumab with respect to absorbed radiation doses to normal organs, and possible relations of hematological toxicity with several parameters, were analyzed in *Chapter 5*. Thirteen (9 males, 4 females) of 15 patient studies could be used for dosimetric analysis. The absorbed dose in the spleen, an organ often involved in NHL, was highest with a mean of 1.89 ± 0.93 mGy/MBq for males and 2.33 ± 0.40 mGy/MBq for females. The mean bone marrow doses were 0.60 ± 0.19 mGy/MBq and 0.61 ± 0.14 mGy/MBq for males and females, respectively. All absorbed doses were within safe ranges. No correlation

could be found between toxicity observed and the absorbed doses.

In *Chapter 6*, an overview is given of current treatment of head and neck cancer, and the possibilities, requirements, and restrictions of RIT of HNSCC are discussed. Studies using mAbs against squamous cell carcinoma-associated antigens, such as CD44v6, are discussed in more detail. Finally, novel treatment strategies are anticipated.

One of the limitations of previous RIT studies using mAbs against CD44v6 appeared to be the immunogenicity of the chimeric mAbs. *Chapter 7* summarizes the results a phase I study using the humanized mAb bivatuzumab, labeled with ^{186}Re. In this study, the safety, MTD, immunogenicity, and therapeutic potential of this radiolabeled antibody preparation were determined in patients with HNSCC. Twenty patients with inoperable recurrent and/or metastatic HNSCC received a single dose of ^{186}Re-bivatuzumab in radiation dose-escalation steps of 0.74, 1.11, 1.48, 1.85, and 2.22 GBq/m^2. Three patients received a second dose of 1.85 GBq/m^2 at least 3 months after the initial dose. First and second administrations were all well tolerated and targeting of tumor lesions proved to be excellent. The only significant manifestations of toxicity were dose-limiting myelotoxicity consisting of thrombo- and leukocytopenia, and, to a lesser extent, oral mucositis (grade 2). Grade 4 myelotoxicity was seen in 2 patients treated at a dose level of 2.22 GBq/m^2. The MTD was established at 1.85 GBq/m^2, at which level dose-limiting myelotoxicity was seen in 1 out of 6 patients. Stable disease, varying between 6 and 21 weeks, was observed in 3 of 6 patients treated at MTD-level. Two patients experienced a HAHA response. It was concluded that ^{186}Re-bivatuzumab can be safely administered, also when given twice.

The data of the previous study were also used for dosimetric analysis, as described in *Chapter 8*. Whole body scintigraphy was used to draw regions around sites or organs of interest. Residence times in these organs and sites were calculated and entered into the MIRDOSE3 program, to obtain absorbed doses in all target organs except for red marrow. The red marrow dose was calculated using a blood-derived method. Twenty-one studies in 18 patients were used for dosimetry, five of them in females, 16 in males. The mean red marrow dose was 0.49 ± 0.03 mGy/MBq for males, and 0.64 ± 0.03 mGy/MBq for females. The normal organ with the highest absorbed dose appeared to be the kidney (mean dose in males 1.61 ± 0.75 mGy/MBq, in females 2.15 ± 0.95 mGy/MBq, maximum kidney dose in all patients 11 Gy), which is not expected to lead to renal toxicity. The doses delivered to the tumor, recalculated to the MTD level of 1.85 GBq/m^2, ranged from 3.8–76.4 Gy, with a median of 12.4 Gy. A good correlation was found between platelet and white blood cell nadirs and the

administered amount of activity per kg body weight ($r = -0.79$). Since the range of the doses to normal organs was well within acceptable and safe limits, and given the acceptable tumor doses, ^{186}Re-labeled bivatuzumab could be a good candidate for future adjuvant radioimmunotherapy in patients with minimal residual disease.

In *Chapter 9*, general aspects of the studies described in this thesis are discussed and future perspectives are identified.

Samenvatting

In dit proefschrift worden de mogelijkheden voor radioimmunotherapie (RIT) van twee typen maligniteiten onderzocht. De behandeling van non-Hodgkin lymfoom (NHL) wordt beschreven in de Hoofdstukken 1-5, de behandeling van plaveiselcelcarcinoom van het hoofd-hals gebied (PC-CHH) in de Hoofdstukken 1-6. Voor RIT van beide maligniteiten wordt gebruik gemaakt van gehumaniseerde monoklonale antilichamen (mAbs), gericht tegen tumorspecifieke antigenen. In de klinische studies worden de mAbs gelabeld met rhenium-186 (^{186}Re), een ideaal radionuclide voor therapie en scintigrafie.

In *Hoofdstuk 1* wordt een overzicht gegeven van NHL, de behandeling ervan en de rol van mAbs bij die behandeling. Studies waarbij gebruik gemaakt werd van zowel mAbs zonder radionuclide als mAbs voorzien van een radionuclide worden beschreven. Niet alleen responspercentages en de toegevoegde waarde van radionucliden in vergelijking met het ongelabeld gebruik van mAbs, maar vooral behandelingsstrategieen, doseringswijzen, toxiciteit en de huidige stand van zaken worden toegelicht.

In *Hoofdstuk 2* wordt de ontwikkeling van een humaan lymfoommodel in muizen beschreven. Xenografts van humane lymfoomcellijnen groeien over het algemeen slecht in muizen. Zelfs bij de meeste immunodeficiente muizen ontstaan geen tumoren na inoculatie met humane lymfoomcellen. Derhalve werden twee verschillende voorbehandelingen van naakte muizen met elkaar vergeleken, teneinde de implantatie en de groeisnelheid van de xenografts te verbeteren. In niet-voorbehandelde muizen bleek de tumorinductie na subcutane injectie met Ramos-cellen slechts 50% te bedragen, terwijl 80% van de muizen voorbehandeld met cyclofosfamide en 100% van de muizen voorbehandeld met hele-lichaamsbestraling een subcutane tumor ontwikkelden. Vooral in de groep die bestraald werd, bleken de tumoren synchroner te groeien. Voorbehandeling met cyclofosfamide of hele-lichaamsbestraling verbeterde de tumorimplantatie van Ramos-cellen in naakte muizen, waardoor een acceptabel diermodel voor vervolgstudies naar lymfomen beschikbaar kwam.

Vervolgens werd een biodistributiestudie verricht teneinde het geschiktste radionuclide voor RIT van NHL te bepalen, zoals beschreven in *Hoofdstuk 3*. Het gehumaniseerde anti-CD22 antilymfoom mAb epratuzumab (hLL2) werd gelabeld met vier verschillende radionucliden, te weten jodium-131 (^{131}I), ^{186}Re, lutetium-177 (^{177}Lu) en yttrium-88 (^{88}Y). Na inoculatie met Ramos-cellen werden naakte muizen, die voorbehandeld waren met cyclofosfamide zoals beschreven in het voorgaande hoofdstuk, geïnjecteerd met gelabeld epratuzumab of met een controle-mAb, dat gelabeld was met ^{131}I of ^{88}Y. De biodistributie van het radionuclide werd 1, 3 en 7 dagen na injectie van het radiofarmacon bepaald. Gelabeld

epratuzumab had een hogere opname in de tumor dan het controle-mAb op alle tijdstippen, onafhankelijk van het gebruikte radionuclide. De opname in de tumor van met ^{88}Y en ^{177}Lu gelabeld epratuzumab was hoger dan die van epratuzumab gelabeld met ^{131}I en ^{186}Re. Zeven dagen na injectie was niet alleen de opname in de tumor, maar ook de opname in bot van de eerstgenoemde radionucliden hoger dan die van jodium en rhenium. Geconcludeerd werd dat het gebruik van de radionucliden ^{88}Y en ^{177}Lu in combinatie met epratuzumab een hogere opname en betere tumorretentie gaf dan epratuzumab gelabeld met ^{131}I en ^{186}Re, maar de hogere botopname van yttrium en lutetium zou kunnen leiden tot een hogere beenmergdosis.

In *Hoofdstuk 4* worden de resultaten van een fase I-studie met ^{186}Re-epratuzumab bij NHL-patiënten samengevat. Het doel van de studie was het vaststellen van de maximaal tolereerbare dosis (MTD) en het krijgen van een eerste indruk van de therapeutische mogelijkheden van dit nieuwe radiofarmacon. Patiënten met een recidief of persisterend CD22-positief NHL, met uiteenlopende histopathologie en voorbehandelingen, kregen ^{99m}Tc-epratuzumab i.v. toegediend, een week later gevolgd door RIT met ^{186}Re-epratuzumab. De dosisescalatie van deze RIT-studie werd gestart op een dosering van 0,5 GBq/m^2. Per dosisniveau werden drie patiënten geïncludeerd. Indien geen dosislimiterende toxiciteit optrad, werd de dosering voor het volgende dosisniveau verhoogd met 0,5 GBq/m^2. Indien wel dosislimiterende toxiciteit optrad, werden nog eens 3 patiënten geïncludeerd op dat dosisniveau. In totaal ontvingen 18 patiënten een diagnostische dosis ^{99m}Tc-epratuzumab. Vijftien patiënten werden daadwerkelijk behandeld met ^{186}Re-epratuzumab op 4 verschillende dosisniveaux, te weten 0,5, 1,0, 1,5 en 2,0 GBq/m^2. Tijdens of na de infusie van ^{186}Re-epratuzumab werden geen ernstige bijwerkingen waargenomen. Bij alle patiënten trad een maand na behandeling een voorbijgaande afname van leuco- en trombocytengetallen op. Op het dosisniveau van 2,0 GBq/m^2 werd in één geval graad 4 haematologische toxiciteit waargenomen. Op het hoogste dosisniveau van 2,0 GBq/m^2 werd geen graad 4 haematologische toxiciteit gezien, maar de leuco- en trombocytengetallen van twee van de drie patiënten kwamen niet op het uitgangsniveau terug. Eén patiënt was gedurende 4 maanden in complete remissie. Bij vier patiënten trad gedurende resp. 3, 3, 6 en 14 maanden een partiële respons op. Gedurende resp. 3, 3, 7 en 9 maanden hadden vier patiënten stabiele ziekte. Hoewel geen dosislimiterende, graad 4 toxiciteit werd gezien, werd het dosisniveau van 2,0 GBq/m^2 beschouwd als MTD, gegeven het langzame herstel van trombo- en leucocytengetal bij 2 van de 3 patiënten behandeld met deze dosering. Een enkelvoudige toe-

diening van ^{186}Re-epratuzumab leidde tot objectieve responsen bij 5 van de 15 behandelde patienten.

Geabsorbeerde stralingsdoses in normale organen na behandeling met ^{186}Re-epratuzumab werden geanalyseerd in *Hoofdstuk 5*, teneinde vast te stellen of een behandeling veilig was en of er een relatie bestond tussen de waargenomen haematologische toxiciteit en enkele parameters. Dertien (9 mannen, 4 vrouwen) van de 15 patiëntenstudies waren geschikt voor dosimetrische analyse. De geabsorbeerde dosis in de milt, een orgaan dat vaak aangedaan is bij NHL, was het hoogst, namelijk gemiddeld $1,89 \pm 0,93$ mGy/MBq bij mannen en $2,33 \pm 0,40$ mGy/MBq bij vrouwen. De gemiddelde beenmergdosis was $0,60 \pm 0,19$ mGy/MBq and $0,61 \pm 0,14$ mGy/MBq voor resp. mannen en vrouwen. Alle geabsorbeerde doses bleven binnen veilige grenzen. Er werd geen correlatie gevonden tussen toxiciteit en de geabsorbeerde doses.

In *Hoofdstuk 6* wordt een overzicht gegeven van de huidige behandeling van hoofd-halskanker, waarbij de mogelijkheden, vereisten en beperkingen van RIT bij PCCHH worden besproken. In meer detail wordt ingegaan op studies die mAbs tegen plaveiselcelcarcinoom-geassocieerde antigenen, zoals CD44v6, beschrijven. Tenslotte worden nieuwe behandelstrategieën toegelicht.

Eén van de beperkingen van eerdere RIT-studies met mAbs tegen CD44v6 bleek de immunogeniciteit van dit chimere mAb te zijn. *Hoofdstuk 7* vat de resultaten van een fase I studie samen, waarbij gebruik gemaakt werd van het gehumaniseerde mAb bivatuzumab, gelabeld met ^{186}Re. In deze studie werden de veiligheid, MTD, immunogeniciteit en de therapeutische mogelijkheden van dit radiofarmacon bepaald bij patiënten met PCCHH. Twintig patienten met een inoperabel recidief en/of metastasen van een PCCHH ontvingen een enkele toediening ^{186}Re-bivatuzumab in een stralingsdosis-escalatieschema van 0,74, 1,11, 1,48, 1,85 en 2,22 GBq/m^2. Drie patiënten kregen een tweede dosering van 1,85 GBq/m^2 tenminste 3 maanden na de eerste RIT. Eerste en tweede toediening werden goed verdragen en er bleek uitstekende targeting van de tumoren te zijn. De enige wezenlijke vorm van toxiciteit bleek dosislimiterende thrombo- and leucopenie te zijn, en in mindere mate graad 2 orale mucositis. Graad 4 myelotoxiciteit trad op bij 2 patiënten, die behandeld waren op een dosisniveau van 2,22 GBq/m^2. De MTD werd vastgesteld op 1,85 GBq/m^2, het dosisniveau waarop dosislimiterende myelotoxiciteit optrad bij 1 van de 6 patienten. Stabiele ziekte, varierend van 6-21 weken, werd geconstateerd bij 3 van de 6 patiënten behandeld op MTD-niveau. Bij twee patienten werd een HAHA-respons gemeten. De conclusie luidde dat ^{186}Re-bivatuzumab veilig toegediend kan worden, ook voor een tweede

keer.

De data van de voorgaande studie werden tevens gebruikt voor dosimetrische analyse, zoals beschreven in *Hoofdstuk 8*. Hele-lichaamsscintigrafie werd gebruikt om de hoeveelheid activiteit in bepaalde gebieden of organen vast te stellen. Verblijfstijden in die gebieden of organen werden berekend en ingevoerd in het MIRDOSE3-programma, teneinde geabsorbeerde doses te berekenen voor alle doelorganen met uitzondering van het beenmerg. De beenmergdosis werd berekend met een op de verblijfstijd in het bloed gebaseerde methode. Eenentwintig studies van 18 patiënten (vijf mannen, zestien mannen) werden gebruikt voor dosimetrie. De gemiddelde beenmergdosis bedroeg $0,49 \pm 0,03$ mGy/MBq bij mannen en $0,64 \pm 0,03$ mGy/MBq bij vrouwen. Het normale orgaan met de hoogste geabsorbeerde dosis bleek de nier te zijn. De gemiddelde nierdosis bij mannen bedroeg $1,61 \pm 0,75$ mGy/MBq en bij vrouwen was deze $2,15 \pm 0,95$ mGy/MBq, met een maximale nierdosis in de totale patiëntengroep van 11 Gy, hetgeen naar men aanneemt niet tot niertoxiciteit leidt. De tumordoses, herberekend naar het MTD-niveau van 1,85 GBq/m^2, bedroeg 3,8–76,4 Gy, met een mediane dosis van 12,4 Gy. Er werd een goede correlatie gevonden tussen thrombo- en leucocytennadir en de toegediende hoeveelheid activiteit per kg lichaamsgewicht ($r = -0,79$). Aangezien de geabsorbeerde doses in normale organen binnen acceptabele en veilige grenzen lagen, en gegeven de acceptabele tumordoses, zou ^{186}Re-bivatuzumab een goede kandidaat zijn voor toekomstige adjuvante RIT van patienten met minimale residuele ziekte.

In *Hoofdstuk 9* tenslotte worden algemene aspecten van de in dit proefschrift beschreven studies besproken en worden toekomstperspectieven geschetst.

Dankwoord

Allereerst zou ik hierbij mijn promotores, prof.dr. F.H.M. Corstens en prof.dr. W.J.G. Oyen, en copromotores, dr. O.C. Boerman en dr. J.M.M. Raemaekers, willen bedanken. Beste Frans, de afgelopen zeseneenhalf jaar was je zowel opleider als promotor. Dank voor je begeleiding en adviezen. Maar ook voor je onconventionele personeelsbeleid: toen ik je voor het eerst belde voor informatie over een opleidingsplaats, zei ik eerlijk dat ik geen enkele ervaring had op het gebied van nucleaire geneeskunde. Jouw antwoord was simpel en helder: "Dat leren we je hier wel, daar is een opleiding voor. Wat kan je zoal wèl?" Door zo'n open mind zie je mogelijkheden die anderen niet zien.

Beste Wim, als directe begeleider en supervisor van de radioimmunotherapieprojecten had ik veel steun aan je. Overleg was altijd plezierig en constructief. Vooral qua visie hoe de projecten verder moesten, zaten wij op een lijn, en overleg leidde altijd tot een positief plan. De reisjes en reizen waren gezellig en onvergetelijk. Vooral de trip naar Portugal is er één om nog vaak met een brede lach op terug te kijken. Dank bovenal voor de wijze waarop je me het vak hebt bijgebracht.

Beste Otto, vanaf het begin van het promotie-onderzoek was je steevast enthousiast en zag je altijd nieuwe mogelijkheden. Met heel veel humor wist je me door elk onderzoeksdal te krijgen. Je snelheid waarmee je manuscripten van zeer bruikbaar commentaar voorziet, is niet te evenaren. Ik roem je manier waarop je bij elke beslissing rekening houdt met de consequenties voor de mens die het betreft.

Beste John, dank voor je begeleiding en steun binnen het AGIKO-project, maar ook voor de manier waarop je me bij alle andere gezamenlijke projecten en klinische vragen vanuit de haematologie betrok. Ondanks perioden waarin weinig patienten binnen de studie behandeld werden, zag je altijd mogelijkheden om verder te gaan met het promotie-onderzoek, zoals door het opzetten van een PET-studie bij lymfoompatienten. Ik waardeer onze gesprekken en je adviezen zeer.

Daarnaast bedank ik alle co-auteurs Hun bijdrage was onmisbaar Drie van hen wil ik hier extra aandacht geven, te weten dr. C.M.P.W. Mandigers, prof dr. A.A.M S. van Dongen en drs P.K.E. Borjesson. Beste Caroline, wat hebben wij vaak samen overlegd over de behandeling van patienten, over onze promotie-onderzoeken, over de werkkring. Dank voor al je moeite. Ook na je vertrek naar het CWZ bleef je enthousiast over het behandelen van lymfoompatienten met radioimmunotherapie, en stak je me een hart onder de riem.

Beste Guus, je was niet alleen de initiator van de hoofd-halsstudie, maar je was ook vanaf het begin zeer intensief betrokken bij de lymfoomstudie Dankzij jouw expertise werden alle rheniumlabelingen op jouw afdeling uitgevoerd Je was altijd zeer betrokken bij alle projecten. Ik vond het stimulerend geregeld met je te overleggen, zowel telefonisch als tijdens veelvuldige bezoeken aan de VU Ik denk met zeer veel plezier terug aan het weekend in New York.

Baste Pontus, utan dig hade den andra delen i denna avhandling inte forverkligats på ett så angenamt satt. Varje kontakt har varit optimal anda från borjan Mina svenskakunskaper lamnar fortfarande en hel del kvar att onska, i synnerhet nar jag forsåg en man med ett kvinnonamn. Vår trevliga resa till Princeton var en hojdpunkt. Tack for din kollegialitet och vanskap.

De in dit proefschrift beschreven studies waren niet mogelijk geweest zonder de hulp en ondersteuning van collegae en medewerkers van het UMC St Radboud en de afdeling KNO van het VUmc Hen dank ik hiervoor Bovenal wil ik hier alle medewerkers van de afdeling nucleaire geneeskunde van ons ziekenhuis en de radionuclidenunit van het CDL bedanken voor hun hulp, hartelijkheid en steun. Van al die mensen wil ik er hier graag drie met name noemen. Cathelijne Frielink, als analiste was jij vanaf het begin betrokken bij al het preklinisch werk van dit proefschrift Dank voor al je hulp en inzet. Emile Koenders, elke labeling moest jouw toets der kritiek doorstaan en voldeed aan alle kwaliteitseisen Dank je voor al die bereidingen, berekeningen en je hulp bij de toediening. Michel de Groot, jou ben ik dank verschuldigd voor al je ondersteuning rond imaging en dosimetrie Ik waardeer je inzet bijzonder.

Dit is ook de plaats waar ik alle vrienden en familieleden heel hartelijk wil bedanken voor hun steun. Een aantal van hen verdient een extra toelichting

Beste Jeroen en Siert, de leden van het opleidingstrio "Voor elkaar" sloegen na de registratie elk hun eigen weg in We deelden lief en leed, en we hadden vooral heel veel lol, op de werkvloer en erbuiten Ook in moeilijker tijden is het heel fijn zulke collegae en vrienden te hebben Na jullie

vertrek bleef het nog lang onrustig in Nijmegen...

Beste Mark, hoewel ik dit dankwoord voor jou als Zweeds staatsburger ook in het Zweeds had moeten schrijven, lukt me dat niet na al twee decennia uitsluitend Nederlands met je gepraat te hebben. Een vriendschap die zo lang over een afstand van vele kilometers stand houdt, is een heel bijzondere, zoals jij het ook memoreerde in jouw proefschrift. Ik vind het geweldig dat je ook nu weer de overtocht wilt maken om hier aanwezig te zijn.

Paranimfen, Ronald en Hans, jullie zijn niet alleen deze dag steun en toeverlaat, dit zijn jullie al jaren. Beste Hans, dankzij Yvonne leerden wij elkaar kennen. Yvonne en jij hebben een heel belangrijke bijdrage geleverd aan de keuzes die ik afgelopen jaren maakte. Ik bewonder jullie durf om zo nu en dan af te wijken van de gebaande paden. Ik dank jullie voor je vriendschap.

Beste Ronald, ook voor jou geldt dat een zo lang bestaande vriendschap iets heel bijzonders is. Postzegels, wiskunde, Limburg, trefwoorden genoeg om terug te kijken op heel veel jaar plezier en vriendschap. Na 15 jaar kom ik overigens een belofte na: ik ga ook naar Eindhoven. Dank voor al jouw en Antjes hartelijkheid en steun.

Dr. H.J. Postema, dr. F.J.A. Jagtenberg, pappa en Fred, ik begrijp nu pas wat een enorme prestatie jullie hebben neergezet door te promoveren tussen de bedrijven van een voltijdsbaan en een druk gezinsleven door. Hulde.

Lieve Fred en Frederiek, fijnere schoonouders kan een mens zich niet wensen. Lieve Rik, naast een geweldige zwager en oom van Tobias, ben je een zeer begaafd kunstenaar. Niet voor niets siert jouw ontwerp dit boek.

Lieve pappa en mamma, door en dankzij jullie ben ik wie ik ben. Dank jullie wel. Ik draag hierbij dit proefschrift aan jullie op.

Lieve Michiel en Nicole, lieve Rolf en Pamela, vorig jaar tijdens jullie huwelijksvoltrekking vertelde ik al hoe belangrijk jullie voor mij zijn. Ik dank jullie voor alles. $M^{I}C_{H}I\varepsilon L$, de lay-out is fantastisch.

Liefste Sjaanke, het boek is uit, we sluiten weer een periode af. Voor ons ligt weer een nieuwe weg. Samen met Tobias gaan we heel erg genieten van de komende maanden, voor en na 31 mei. Ik houd van jou.

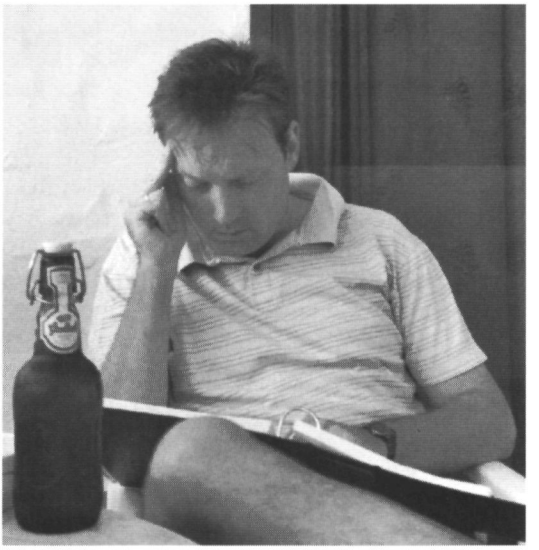

Correctie der drukproeven op Fuerteventura

Curriculum Vitæ

Ernst Postema werd op 13 augustus 1971 geboren te Blokzijl. Hij groeide op in Nunspeet. Van 1983 tot 1989 doorliep hij de gymnasiumafdeling van het Chr. College Nassau-Veluwe te Harderwijk Vanaf 1989 studeerde hij geneeskunde aan de Erasmus Universiteit Rotterdam, alwaar hij in 1996 het artsexamen aflegde Na AGNIO chirurgie geweest te zijn in ziekenhuis sint Antoniushove te Leidschendam, was hij sinds 1 september 1997 werkzaam op de afdeling nucleaire geneeskunde van het UMC St Radboud, waar hij bij opleider en promotor prof.dr. F.H.M. Corstens opleiding en onderzoek als AGIKO combineerde. Het stagejaar interne geneeskunde doorliep hij in het Slingeland ziekenhuis te Doetinchem bij opleider dr. F. de Vries. Sinds zijn registratie per 1 augustus 2003 bleef hij als nucleair geneeskundige werkzaam op de afdeling nucleaire geneeskunde van het UMC St Radboud. Per 1 april 2004 zal hij zijn loopbaan vervolgen in het Catharina-ziekenhuis te Eindhoven.

Stellingen

behorend bij het proefschrift

"Radioimmunotherapy using ^{186}Re-labeled humanized monoclonal antibodies"

1. De gehumaniseerde antilichamen epratuzumab en bivatuzumab zijn dusdanig weinig immunogeen dat herhaalde toediening mogelijk is.

   dit proefschrift

2. Gezien de relatief lage tumordosis in grote tumoren, maar de uitstekende targeting van plaveiselcelcarcinoomcellen zou radioimmunotherapie bij voorkeur in adjuvante setting bij minimale residuale ziekte gegeven moeten worden.

   dit proefschrift

3. Het gebruik van een radionuclide gekoppeld aan een werkzaam monoklonaal antilichaam heeft bij de behandeling van non-Hodgkin lymfoom toegevoegde waarde.

   dit proefschrift

4. De keuze voor een radionuclide voor radioimmunotherapie op klinisch-practische gronden leidt niet tot slechtere klinische resultaten dan een keuze gebaseerd op theoretische of dierexperimentele argumenten.

   dit proefschrift

5. Dosimetrie is slechts de getalsmatige onderbouwing van klinisch reeds waargenomen feiten.

6. Bij radioimmunotherapie is de nucleair geneeskundige niet een nucleair adviseur, maar primair geneeskundige.

   Postema *et al., J Nucl Med* 2003; 44: 853

7. In tegenstelling tot wat in de literatuur gesuggereerd wordt, is er geen toegevoegde waarde van FDG-PET bij de stadiëring van de hals bij hoofd-halscarcinoom.

   Postema *et al., Eur J Nucl Med Mol Imaging* 2003; 30: S159

8. Aangezien direct contact tussen oog en genitaal weinig waarschijnlijk is, is de hand de meest waarschijnlijke vector bij het ontstaan van een chlamydia conjunctivitis op volwassen leeftijd.

   Postema *et al., Genitourin Med* 1996; 72: 203-205

9. Door de invoering van de euro hoeft er niet meer zo vaak geld gewisseld te worden. Dit geringe persoonlijke voordeel valt in het niet bij de structurele prijsverhogingen die bij de invoering van de euro hebben plaatsgevonden. De Zweden hebben derhalve gelijk.

10. Zelfklevende postzegels zijn zeer gebruiksvriendelijk, maar het einde voor de filatelist.

E.J. Postema
Nijmegen, 23 maart 2004

ISBN 90-9017813-9